


2014

Protein 14-3-3 (YWHA) isoforms and their roles in regulating mouse oocyte maturation

Santanu De

Kent State University - Kent Campus, sde@nova.edu

Follow this and additional works at: https://nsuworks.nova.edu/cnso_bio_facbooks

 Part of the [Animal Sciences Commons](#), [Biology Commons](#), [Cell Biology Commons](#), [Developmental Biology Commons](#), and the [Physiology Commons](#)

NSUWorks Citation

De, Santanu. 2014. "Protein 14-3-3 (YWHA) isoforms and their roles in regulating mouse oocyte maturation." *Protein 14-3-3 (YWHA) isoforms and their roles in regulating mouse oocyte maturation* : , 2014. https://nsuworks.nova.edu/cnso_bio_facbooks/22

This Dissertation is brought to you for free and open access by the Department of Biological Sciences at NSUWorks. It has been accepted for inclusion in Biology Faculty Books and Book Chapters by an authorized administrator of NSUWorks. For more information, please contact nsuworks@nova.edu.

**Protein 14-3-3 (YWHA) isoforms and their roles
in regulating mouse oocyte maturation**

A dissertation submitted to Kent State University
in partial fulfillment of the requirements for
the degree of Doctor of Philosophy

By

Santanu De

August, 2014

Dissertation written by

Santanu De

B.S., Presidency College, University of Calcutta, Kolkata, India, 2005

M.S., University of Calcutta, Kolkata, India, 2007

Ph.D., Kent State University, Kent, Ohio, U.S.A, 2014

Approved by

_____, Chair, Doctoral Dissertation Committee
Dr. Douglas W. Kline

_____, Member, Doctoral Dissertation Committee
Dr. Derek Damron

_____, Member, Doctoral Dissertation Committee
Dr. Colleen M. Novak

_____, Member, Doctoral Dissertation Committee
Dr. Werner J. Geldenhuys

_____, Graduate Faculty Representative
Dr. Nicola E. Brasch

Accepted by

_____, Acting Chair, Department of Biological Sciences
Dr. Laura G. Leff

_____, Associate Dean, College of Arts and Sciences
Dr. Janis Crowther

TABLE OF CONTENTS

List of Figures.....	v
List of Tables.....	ix
Dedication.....	x
Acknowledgements.....	xi
<u>CHAPTER 1:</u>	1
Introduction.....	2
Bibliography.....	8
<u>CHAPTER 2: Identification and distribution of 14-3-3 (YWHA) protein isoforms in mouse oocytes, eggs and ovarian follicular development.....</u>	11
Background.....	12
Results and Discussion.....	14
Materials and Methods.....	38
Conclusions.....	46
Bibliography.....	47
<u>CHAPTER 3: Investigation of isoform-specific interactions of 14-3-3 (YWHA) proteins with CDC25B phosphatase in regulating mouse oocyte maturation.....</u>	52
Background.....	53
Results and Discussion.....	60
Materials and Methods.....	87
Conclusions.....	100

Bibliography.....	101
<u>CHAPTER 4: Determination of the requirement of 14-3-3η (YWHAH) in</u>	
meiotic spindle assembly during mouse oocyte maturation.....	109
Background.....	110
Results and Discussion.....	114
Materials and Methods.....	138
Conclusions.....	145
Bibliography.....	146
<u>CHAPTER 5:</u>	156
Summary and Significance.....	157
Appendix of Abbreviations.....	161

LIST OF FIGURES

CHAPTER 1

Figure 1. Schematic representation of the process of mouse oocyte maturation.....3

Figure 2. Morphology of oocytes and eggs of the adult mouse.....4

CHAPTER 2

Figure 1. Immunoblots identifying 14-3-3 isoforms in extracts from mouse oocytes, eggs and ovaries.....15

Figure 2. Comparison of the relative abundance of individual 14-3-3 isoforms in immature oocytes and mature eggs.....17

Figure 3. Representative immunofluorescence images of 14-3-3 isoforms in oocytes and eggs isolated from adult mice.....20

Figure 4. Representative immunohistochemistry images of 14-3-3 β in the different stages of follicular development in ovarian sections.....25

Figure 5. Representative immunohistochemistry images of 14-3-3 γ in the different stages of follicular development in ovarian sections.....26

Figure 6. Representative immunohistochemistry images of 14-3-3 ϵ in the different stages of follicular development in ovarian sections.....27

Figure 7. Representative immunohistochemistry images of 14-3-3 ζ in the different stages of follicular development in ovarian sections.....28

Figure 8. Representative immunohistochemistry images of 14-3-3 η in the different stages of follicular development in ovarian sections.....29

Figure 9. Representative immunohistochemistry images of 14-3-3 τ in the different

stages of follicular development in ovarian sections.....	30
Figure 10. Representative immunohistochemistry images of 14-3-3 σ in the different stages of follicular development in ovarian sections.....	31
Figure 11. Representative immunohistochemistry images of 14-3-3 protein isoforms in atretic follicles of adult mouse ovaries.....	32
Figure 12. Representative control immunohistochemistry images for different 14-3-3 protein isoforms in tissue sections.....	33
Figure 13. Representative immunocytochemistry images of 14-3-3 protein isoforms along and in the <i>zonae pellucidae</i> of cumulus-free oocytes isolated from ovaries of adult mice.....	36
 <u>CHAPTER 3</u>	
Figure 1. Simplified diagram of the key proteins involved in oocyte arrest at prophase I (left) and the release from meiotic arrest (right).....	55
Figure 2. Schematic representation of the process of <i>in situ</i> Proximity Ligation Assay to detect interaction between two proteins.....	58
Figure 3. Representative indirect immunofluorescence images showing intracellular distribution of CDC25B during mouse oocyte maturation.....	61
Figure 4. Representative oocytes and eggs showing PLA reaction spots for interaction of 14-3-3 β with CDC25B, compared to controls.....	65
Figure 5. Representative oocytes and eggs showing PLA reaction spots for interaction of CDC25B with 14-3-3 γ , 14-3-3 ϵ , 14-3-3 ζ , 14-3-3 η , 14-3-3 τ and 14-3-3 σ ...	67

Figure 6. Per cent PLA sites of interaction of seven mammalian 14-3-3 isoforms with CDC25B in mouse eggs compared to oocytes.....	69
Figure 7. Co-immunoprecipitation of 14-3-3 isoforms with CDC25B phosphatase.....	72
Figure 8. Western blot detecting CDC25B phosphorylation in oocytes versus eggs by λ -phosphatase treatment.....	75
Figure 9. CDC25B is phosphorylated at Ser149 in oocytes, and the phosphorylation is reduced in eggs.....	78
Figure 10. The 14-3-3 proteins, specifically 14-3-3 η , is required for maintaining prophase I arrest of oocytes.....	83
Figure 11. Representative mouse oocytes showing maturation-promoting effect of 14-3-3-inhibitory peptide R18, compared to controls.....	84
Figure 12. Representative mouse oocytes showing maturation-promoting effect of antisense morpholino against 14-3-3 η , compared to control.....	85
Figure 13. Schematic experimental approach to detect phosphorylation of CDC25B at Ser-149 by <i>in situ</i> Proximity Ligation Assay.....	96
Figure 14. Schematic experimental approach of inhibition of interactions of 14-3-3 proteins with CDC25B by intracytoplasmic microinjection of R18 into mouse oocytes.....	98

CHAPTER 4

Figure 1. The 14-3-3 η protein accumulates at the metaphase II spindle of the mouse egg matured <i>in vitro</i>	116
Figure 2. The 14-3-3 η protein accumulates and co-localizes with α -tubulin in MI and	

MII meiotic spindles during oocyte maturation.....	119
Figure 3. The 14-3-3 η protein interacts directly with α -tubulin.....	123
Figure 4. Summary of experimental results on meiotic spindle structure following injection of the 14-3-3 η morpholino and control conditions.....	127
Figure 5. Microinjection of a morpholino against 14-3-3 η causes absence or deformation of meiotic spindles in cells matured <i>in vitro</i>	128
Figure 6. Representative control eggs matured <i>in vitro</i> from injected oocytes, showing normal, bipolar meiotic spindles.....	132

LIST OF TABLES

CHAPTER 2

Table 1. Characteristic differences in expression of 14-3-3 protein isoforms in the different stages of follicular development as observed by immunohistochemical staining of adult mouse ovarian sections.....	35
--	----

Dedicated to
My Parents

ACKNOWLEDGEMENTS

First and foremost, I would like to express my sincere gratitude and appreciation towards my adviser, Dr. Douglas Kline for his incredible support and patient guidance over the past many years. From the bottom of my heart I thank him for enabling me to develop, pursue, present and publish in-depth research projects, along with providing valuable directions to troubleshoot experimental problems. I will forever be grateful to him for pointing out my mistakes from time to time and encouraging me to improve upon my weaknesses. Under his mentorship I learnt to try facing challenges in life with a smile.

I am sincerely grateful to Dr. Derek Damron, Dr. Colleen Novak, Dr. Werner Geldenhuys, Dr. Nicola Brasch and Dr. Jennifer Marcinkiewicz for their kind service in my dissertation committee. I thank Dr. Srinivasan Vijayaraghavan, Dr. Jenny, Dr. Brent Bruot, Dr. Yijing Chen and Dr. Dean Dluzen for sharing their expertise and suggestions with experiments, and Dr. Michael Model for imaging assistance. I wish to acknowledge the research funding provided by the National Institutes of Health Grants #HD061869 to Dr. Kline and #HD038520 to Dr. Vijayaraghavan, and the Graduate Student Senate, Kent State University. My humble thanks to Dr. Laura Leff, Dr. Helen Piontkivska, Dr. Sean Veney, Dr. Kline, Dr. Jenny, Dr. Damron, Dr. Heather Caldwell, Mrs. Allison Grampa and Mrs. Sarah Vash for considering me to teach diverse courses in the department and gain significant pedagogical experience alongside my research performances.

I wish to express my gratitude to all previous and present lab-mates including Ariana, Alaa, Trisha, Isabella, Shawn, Sourabh, Tariq, Angela, Benjamin, Daniel, Cyrus, Leslie, Debra, Ryan, Sam, Garrett, Nicholas, Adam, David, Kevin, Ken, Erica and Michele as well as to all other colleagues, faculties, students, and staff of our departmental office, stockroom, animal care and computer facility for their continued assistance. It is my privilege to thank the numerous people in the USA and India who directly or indirectly made my doctoral journey memorable, enriching and rewarding.

I thank the Almighty for everything in life. Words will not be enough to express my gratitude towards my father, Uday Kumar De and my mother, Indrani De – whatever I am today is because of their selfless sacrifices, faith and motivation for years, even from thousands of miles away. I must thank my beloved sister Subhalaxmi Niyogi, brother-in-law Soumyajit Niyogi and my little nephew Shomshubhro Niyogi for giving me the strength to fight through tough times. My thankfulness also goes towards all my dear relatives, especially my uncle, Arun Kumar De who has been an exemplary inspiration, as well as to Rajlakshmi Ghosh, Amiya Ghosh, Sudeshna Mitra, Somnath Ghosh, Prabal Kanti Ghosh, Tamal Kanti Ghosh and Mridul Ghosh for sharing the times of high and low. I am deeply grateful to my aunts – Sharmila Mitra, Jyotsna De, Shyamali Ghosh and Rama Ghose who have prayed for me and wished me success. At the same time, I respectfully thank those well-wishers who are no more – Lt. Dipika Dutta, Lt. Asoke Ghose and many others, whose blessings will always remain alive in me. There is no limit to my indebtedness towards Gita Mitra and all the maids and care-takers who brought me up with unconditional love and concern.

I should also thank all my past teachers and tutors including Tripti Chatterjee, Rajat Chatterjee, all members of Edxcare International and the United States-India Educational Foundation (USIEF, Kolkata) and Sashibhushan Betal for their profound contributions in shaping my academic career. My heart-felt thanks to every friend of mine including Soutik, Dipak, Aritri, Swarupa, Arghya, Nilam, Sayantani, Sreeramakrishna, Sabyasachi, Rahul, Pritam, Tejasvi, Sony, Sewwandi, Orthis, Tariq, Krishna, Jyotiska, David, Jillian, Deb, JJ, Bob, Seth and many more – for years of unswerving support, laughter and love.

Last but not the least, I will forever remain grateful to my late grandparents Samarendra Nath De, Sushama De, Arun Krishna Biswas and Chameli Biswas for the moral values and principles they inculcated in me during my childhood, which will help me to try and grow as a good human being.

CHAPTER 1

Introduction

Introduction

In female mammals, meiosis is initiated prenatally and oocytes (immature germ cells) remain arrested for long periods at prophase of the first meiotic division within the ovary, by signals from the surrounding granulosa cells. With the onset of puberty, the arrest is released as a result of the pre-ovulatory surge in luteinizing hormone (Figure 1) mediated by granulosa cells surrounding the oocyte, activating the maturation promoting factor (MPF) within the oocyte. The arrest of oocytes at meiosis I can be mimicked *in vitro* by dibutyryl cAMP, represented in Figure 1. MPF triggers the resumption and completion of meiosis I by forming a first polar body, leading to a mature, haploid egg [1-4] that remains arrested at metaphase of meiosis II until fertilized by a haploid sperm to produce the diploid zygote, along with extrusion of second polar body.

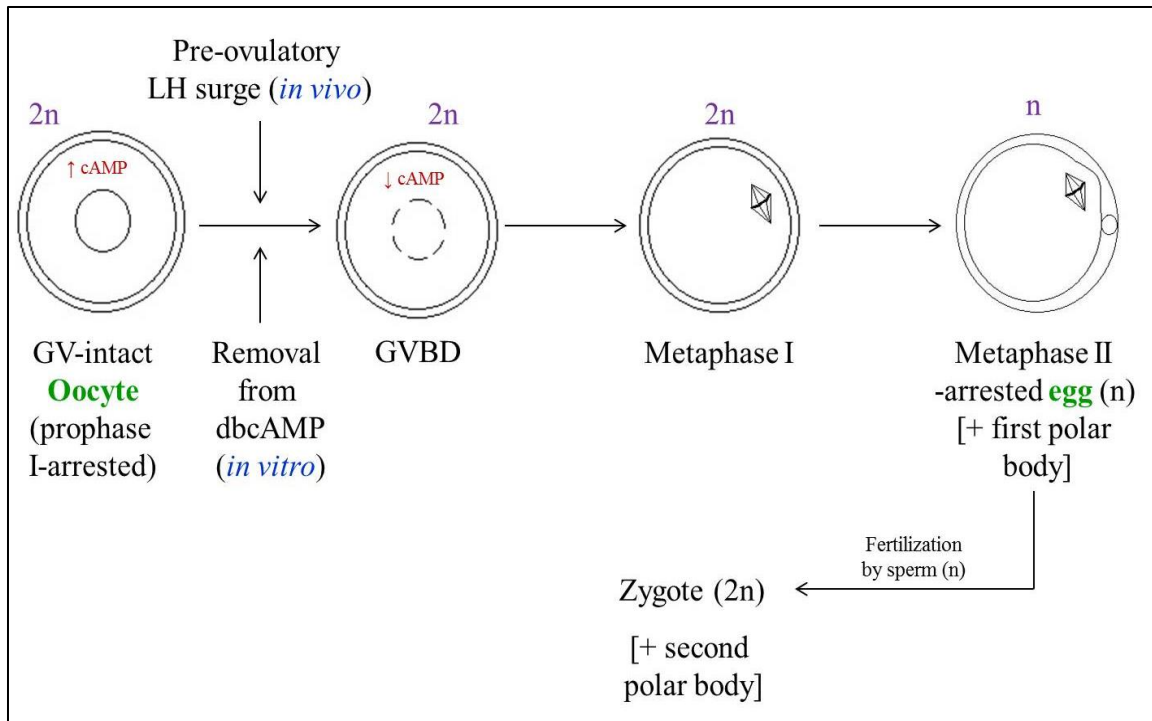


Figure 1. Schematic representation of the process of mouse oocyte maturation.

GV: Germinal Vesicle; GVBD: Germinal Vesicle Break Down; LH: Luteinizing Hormone; dbcAMP: dibutyryl cAMP.

Figure 2 shows a normal mouse oocyte with an intact germinal vesicle (GV; oocyte nucleus) and a typical, metaphase II-arrested mouse egg matured from an oocyte following germinal vesicle breakdown (GVBD). Both oocytes and eggs are surrounded by a protective, membranous covering – the zona pellucida (Figure 2), known to contain sperm-binding proteins critical to the process of fertilization. Failure of oocyte maturation has been documented in animal models and must be considered when human female infertility is examined [5].

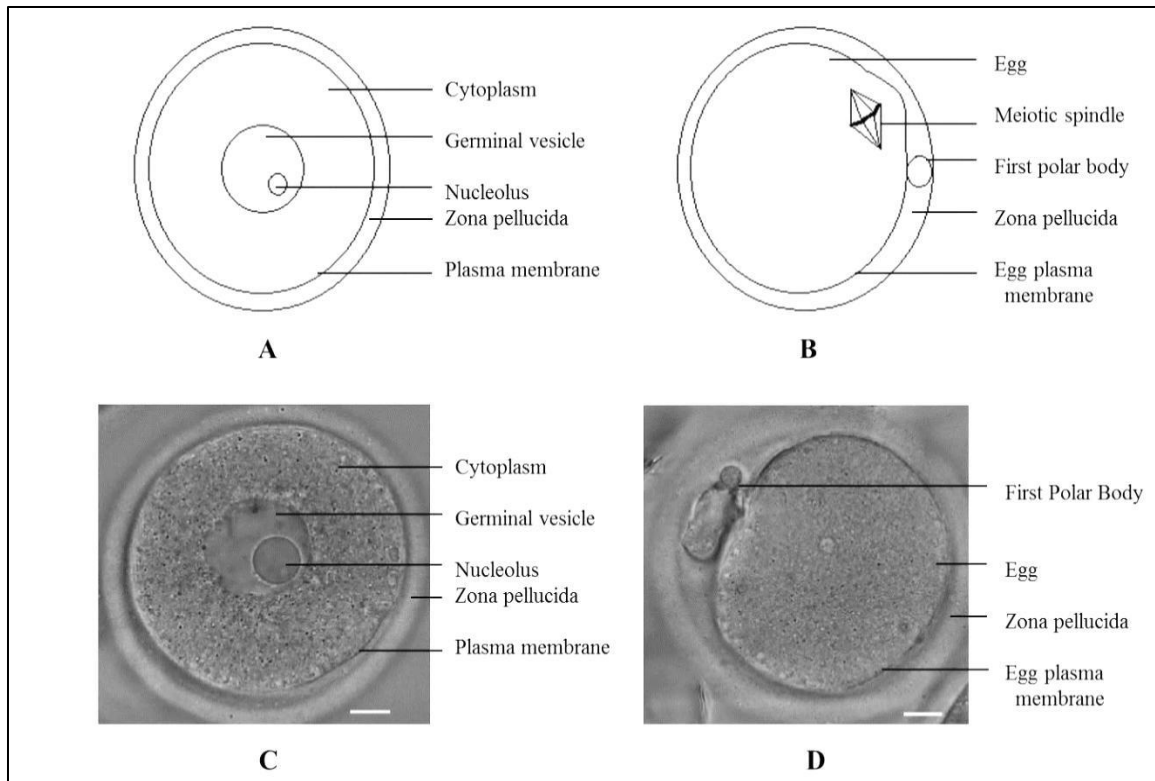


Figure 2. Morphology of oocytes and eggs of the adult mouse.

A: Schematic structure of an oocyte. B: Schematic structure of an egg. C: Bright field, equatorial image of an oocyte. D: Bright field, equatorial image of an egg associated with a first polar body.

The 14-3-3 proteins (YWHA or Tyrosine 3-Monooxygenase/Tryptophan 5-Monooxygenase Activation proteins) are a highly conserved family of acidic proteins expressed abundantly and ubiquitously in a wide variety of eukaryotic cells and organisms ranging from plants to mammals [6]. They were first identified during a systematic classification of brain proteins [7]. The name ‘14-3-3’ was used to denote the elution fraction comprising these proteins after DEAE-cellulose chromatography and

their migration position after subsequent starch gel electrophoresis. These proteins are known regulators in important physiological and cellular events including metabolism, transcription, signal transduction, cell cycle control, apoptosis, protein trafficking, stress responses, malignant transformation and embryonic development. Over 200 proteins that may interact with 14-3-3 have been detected by proteomic and biochemical methods [8-11]. This broad range of partners suggests a role of 14-3-3 as a general biochemical regulator. They are key regulatory proteins that may alter the activity of bound proteins, change the associations or interactions of the bound proteins with other proteins, protect protein phosphorylation, promote protein stability and/or alter the intracellular localization or destination of the bound protein. The role of 14-3-3 proteins in mammalian reproduction has not yet been completely known. My dissertation focused upon the isoform-specific expression, distribution and roles of 14-3-3 proteins during mouse oocyte maturation.

The 14-3-3 proteins are a family of homologous proteins encoded by separate genes. To date, seven mammalian isoforms of 14-3-3 have been discovered and were named after their respective elution positions on HPLC [12]. The phosphorylated forms of 14-3-3 β and 14-3-3 γ were initially described as 14-3-3 α and 14-3-3 δ respectively [13].

Protein 14-3-3 exists mainly as homo- or hetero-dimers with a monomeric molecular mass of approximately 30 kDa [8]. It is known that different 14-3-3 isoforms can interact with the same ligand and so are somewhat interchangeable; however, although isoforms of 14-3-3 often bind the same protein, there are some indications that homodimers of different types or even heterodimers of 14-3-3 may have different roles in the regulation

or sequestering of proteins [14, 15]. Dimerization of 14-3-3s is important, because point mutations that disrupt 14-3-3 dimers can impair regulatory functions of 14-3-3s [16, 17].

The 14-3-3 proteins have been shown to bind to various signaling molecules by phosphorylation-dependent mechanisms. They have been found to complement or supplement intracellular events involving phosphorylation-dependent switching or protein-protein interaction [10, 18]. The 14-3-3s bind to proteins containing phosphoserine and phosphothreonine residues with RSXpSXP and X(Y/F)XpSXP motifs [19, 20]. Most of the binding partners of 14-3-3 are phosphorylated, however, phosphorylation-dependent sites that differ significantly from these motifs have been reported [14], and some interactions of 14-3-3 do exist independent of phosphorylation. The effect of 14-3-3 binding has diverse cellular effect(s) depending on the nature of the ligand. Changes in phosphorylation status of the 14-3-3 binding motif on target proteins may result in changes in binding patterns. For instance, dephosphorylation of certain serine residues on target proteins may release the interaction with 14-3-3; likewise, serine phosphorylation may lead to 14-3-3-target interactions. Members of the 14-3-3 family of proteins play a central role in mitosis in mammalian cells and meiosis in amphibians, but their role in mammalian meiosis has not been entirely defined.

This dissertation aimed at unraveling the differential expressions of 14-3-3 protein isoforms and their roles in the regulation of mouse oocyte maturation, involving three major projects:

I. Identification and distribution of 14-3-3 (YWHA) protein isoforms in mouse oocytes, eggs and ovarian follicular development

Hypothesis: One or more isoforms of 14-3-3 proteins are expressed in mouse oocytes, eggs and in various stages of ovarian folliculogenesis.

II. Investigation of isoform-specific interactions of 14-3-3 (YWHA) proteins with CDC25B phosphatase in mouse oocyte maturation

Hypothesis: One or more isoforms of 14-3-3 proteins interact with CDC25B phosphatase to regulate mouse oocyte maturation.

III. Determination of the requirement of 14-3-3 η (YWHAH) in meiotic spindle assembly during mouse oocyte maturation

Hypothesis: Protein 14-3-3 η is essential for meiotic spindle formation by interacting with α -tubulin to regulate the assembly of microtubules.

Bibliography

1. Jones K: Turning it on and off: M-phase promoting factor during meiotic maturation and fertilization. *Mol Hum Reprod* 2004, 10(1):1-5.
2. Mehlmann LM: Stops and starts in mammalian oocytes: recent advances in understanding the regulation of meiotic arrest and oocyte maturation. *Reproduction* 2005, 130(6):791-799.
3. Von Stetina JR, Orr-Weaver TL: Developmental control of oocyte maturation and egg activation in metazoan models. *Cold Spring Harbor Perspect Biol* 2011, 3(10):a005553.
4. Conti M, Hsieh M, Zamah AM, Oh JS: Novel signaling mechanisms in the ovary during oocyte maturation and ovulation. *Mol Cell Endocrinol* 2012, 356(1–2):65-73.
5. Beall S, Brenner C, Segars J: Oocyte maturation failure: a syndrome of bad eggs. *Fertil Steril* 2010, 94(7):2507-2513.
6. Yaffe M.B. How do 14-3-3 proteins work? – Gatekeeper phosphorylation and the molecular anvil hypothesis. *FEBS Lett* 2002; 513: 53-57.
7. Moore, B. W. and Perez, V. J. (1967). *Specific Acid Proteins in the Nervous System*. Englewood Cliffs, New Jersey: Prentice-Hall.
8. Aitken, A., 2006. 14-3-3 Proteins: A Historic Overview. *Seminars in Cancer Biology* 16, 162-172.

9. Conti, M., Andersen, C. B., Richard, F., Mehats, C., Chun, S. Y., Horner, K., Jin, C., and Tsafri, A. (2002). Role of cyclic nucleotide signaling in oocyte maturation. *Molecular and Cellular Endocrinology* 187, 153-159.
10. Mackintosh, C. (2004). Dynamic interactions between 14-3-3 proteins and phosphoproteins regulate diverse cellular processes. *Biochemical Journal* 381, 329-342.
11. Meek, S. E. M., Lane, W. S., and Piwnica-Worms, H. (2004). Comprehensive proteomic analysis of interphase and mitotic 14-3-3-binding proteins. *Journal of Biological Chemistry* 279, 32046-32054.
12. Ichimura T, Isobe T, Okuyama T, Takahashi N, Araki K, Kuwano R, Takahashi Y. Molecular cloning of cDNA coding for brain-specific 14-3-3 protein, a protein kinase-dependent activator of tyrosine and tryptophan hydroxylases, 1988. *Proc Natl Acad Sci U S A.* 85:19; 7084-7088.
13. Aitken, A., Howell, S., Jones, D., Madrazo, J. and Patel, Y. (1995). 14-3-3 alpha and delta are the phosphorylated forms of raf-activating 14-3-3 beta and zeta. *In vivo stoichiometric phosphorylation in brain at a Ser-Pro-Glu-Lys MOTIF.* *J. Biol. Chem.* 270, 5706-5709.
14. Aitken, A., 2002. Functional Specificity in 14-3-3 Isoform Interactions through Dimer Formation and Phosphorylation. *Chromosome Location of Mammalian Isoforms and Variants.* *Plant Mol Biol* 50, 993-1010.

15. Benzinger, A., Muster, N., Koch, H.B., Yates, J.R., Hermeking, H., 2005. Targeted Proteomic Analysis of 14-3-3 Sigma, a p53 Effector Commonly Silenced in Cancer. *Molecular and Cellular Proteomics* 4, 785-795.
16. Cahill, C. M., Tzivion, G., Nasrin, N., Ogg, S., Dore, J., Ruvkun, G. and Alexander-Bridges, M. (2001) Phosphatidylinositol 3-kinase signaling inhibits DAF-16 DNA binding and function via 14-3-3-dependent and 14-3-3-independent pathways. *J. Biol. Chem.* 276, 13402–13410.
17. Tzivion, G., Luo, Z. and Avruch, J. (1998) A dimeric 14-3-3 protein is an essential cofactor for Raf kinase activity. *Nature (London)* 394, 88–92.
18. Dougherty, M. K., and Morrison, D. K. (2004). Unlocking the code of 14-3-3. *Journal of Cell Science* 117, 1875-1884.
19. Rittinger K, Budman J, Xu J, Volinia S, Cantley LC, Smerdon SJ, Gamblin SJ, Yaffe MB, 1999. Structural analysis of 14-3-3 phosphopeptide complexes identifies a dual role for the nuclear export signal of 14-3-3 in ligand binding. *Mol Cell*: 4; 153–166.
20. Yaffe MB, Rittinger K, Volinia S, Caron PR, Aitken A, Leffers H, Gamblin SJ, Smerdon SJ, Cantley LC, 1997. The structural basis for 14-3-3: phosphopeptide binding specificity. *Cell*: 91; 961–971.

CHAPTER 2

**Identification and distribution of 14-3-3
(YWHA) protein isoforms in mouse oocytes,
eggs and ovarian follicular development**

Background

Members of the 14-3-3 family are key proteins in a number of intracellular events, particularly those involving phosphorylation-dependent switching. The proteins bind to a diverse set of target proteins and alter cellular function by binding to and causing conformational changes in target proteins or modifying target protein interactions with other proteins. Of particular interest, 14-3-3 appears to be central to several aspects of vertebrate development and cell cycle regulation, including meiosis in amphibians [1,2]; however, the functions of 14-3-3 in mammalian reproductive organs and in gametes have not been completely elucidated. There is also interest in understanding the role of 14-3-3 proteins in the regulation of oogenesis and the cell cycle during oocyte maturation and in early development. In addition, 14-3-3 proteins, by their participation in the regulation of the cell cycle, apoptosis, and tumor suppression, are important in normal growth and development as well as in cancer [3].

The 14-3-3 proteins are a family of highly conserved, homologous proteins encoded by separate genes. The name for the protein family is tyrosine 3-monooxygenase/tryptophan 5-monooxygenase activation protein family (YWHA). The 14-3-3 name is still commonly used. There are seven mammalian isoforms of 14-3-3 encoded by seven different genes: β (Ywhab), γ (Ywhag), ϵ (Ywhae), ζ (Ywhaz), η (Ywhah), τ (Ywhaq) and σ (Sfn) [4]. The 14-3-3 proteins exist as homo- or hetero-dimers [5,6]. It is known that different 14-3-3 isoforms can interact with the same ligand and so are somewhat interchangeable. Although different isoforms of 14-3-3 may bind the same

protein, there are some indications that homodimers of different types or even heterodimers of 14-3-3 may have different roles in the regulation or sequestering of proteins [7-9].

The roles of 14-3-3 proteins in the ovary may parallel function in other tissues. For example, 14-3-3 σ is expressed at lower levels in cancerous cells in a number of tissues including adenocarcinomas of the ovary [3, 10]. However, specific descriptions of the roles of 14-3-3 proteins in the ovary are few. In female mammals, meiosis is initiated prenatally and oocytes remain arrested in an immature state at late prophase of the first meiotic division for long periods of time. This arrest is released as a result of the pre-ovulatory surge in luteinizing hormone and oocytes resume the first meiotic division cycle and arrest at metaphase II of meiosis to form the mature egg. It has been suggested that, in mammalian oocytes, 14-3-3 binds to and regulates the cell cycle control protein CDC25B phosphatase (cell division cycle 25 homolog B), as it does in amphibian oocytes, to hold the cell in prophase arrest [11]. In another case, our lab showed that 14-3-3 interacts with phosphorylated PADI6, a key maternal effect protein, in mature eggs, but not with unphosphorylated PADI6 in immature oocytes [12]. While such interactions have been examined in part, more information about specific isoforms is needed. It is also clear that many more cellular processes in the ovary and in the female gametes might be regulated by 14-3-3. As a pre-requisite for understanding the role(s) of 14-3-3 in mammalian female reproductive development and oocyte maturation, we must understand which cell types express which individual isoforms. The present study explores the various isoforms of this protein and the characteristic patterns of expression

in immature oocytes, mature eggs and in the various developmental stages of ovarian follicles in the adult mouse.

Results and Discussion

The 14-3-3 proteins in oocytes and eggs

Immature, prophase I-arrested mouse oocytes and mature, metaphase II-arrested eggs appear to express all seven 14-3-3 isoforms. Three approaches were used to determine if these cells contained each of the isoforms of 14-3-3. The proteins in oocyte and egg extracts were examined by Western blotting after polyacrylamide gel electrophoresis; cells were fixed and viewed by indirect immunofluorescence, and also by immunohistochemical staining of cells within ovarian sections. All three approaches relied on a panel of antibodies that has been shown to be specific for the various 14-3-3 isoforms. Martin and his colleagues [13, 14] described the generation of the panel of antibodies and used them to detect the major brain isoforms of 14-3-3. They confirmed, by several methods, the high specificity of each of these antibodies, which is due to the fact that the epitope for each antibody is mainly in the N-acetylated amino terminus of the different peptide immunogens. The panel of 14-3-3 isoform-specific antibodies was also used to identify the isoforms of 14-3-3 proteins expressed in human dermal and epidermal layers [15] and in adrenal chromaffin cells [16].

Presence and relative abundance of 14-3-3 isoforms in oocytes and eggs determined by Western blotting

Western blots of extracts from 200 oocytes or 200 eggs indicate the presence of six of the seven isoforms (Figure 1). These six isoforms of 14-3-3 were also detected in ovarian protein extracts by Western blotting. Protein 14-3-3 σ could not be detected by Western blotting; however, it was identified in oocytes and eggs by immunocytochemistry and in ovarian follicle cells, including oocytes, by immunohistochemical staining. The inability to detect 14-3-3 σ in Western blots may be due to the unsuitability of this antibody in recognizing a denatured antigen by Western blotting procedure.

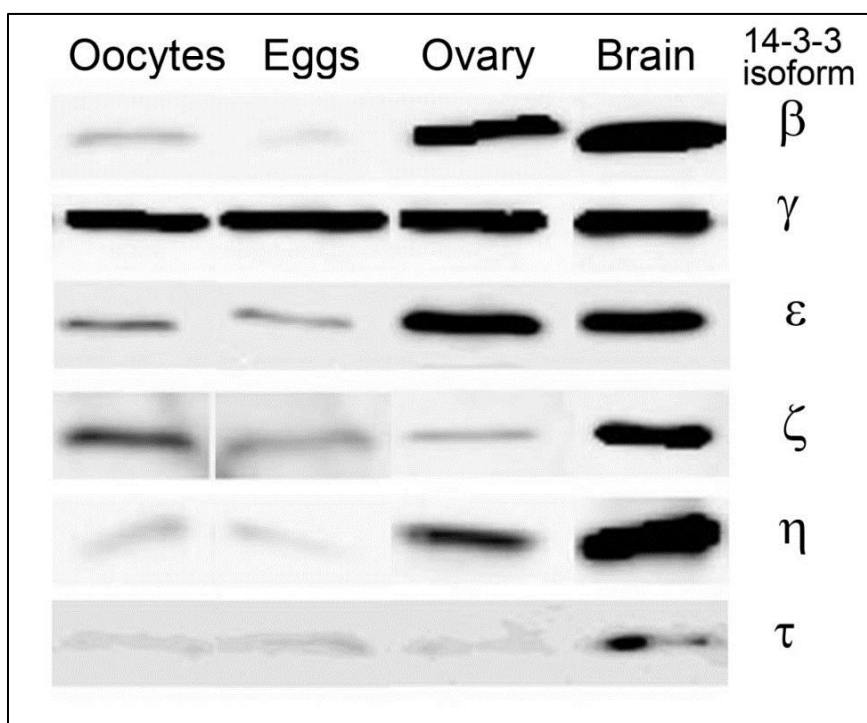


Figure 1. Immunoblots identifying 14-3-3 isoforms in extracts from mouse oocytes, eggs and ovaries. Proteins from cell lysates were separated by electrophoresis under

reducing conditions, transferred to membranes and probed with antibodies directed against the 14-3-3 isoforms indicated. Each isoform shown was detected in lysates of 200 oocytes or 200 eggs. Protein extracts of ovaries and brain from adult mice are included for comparison. The 14-3-3 protein is approximately 30 kDa.

It is interesting to determine the relative amounts of the 14-3-3 isoforms in immature oocytes and in mature eggs. Quantitative changes in total amount of specific 14-3-3 isoforms could provide insights into the regulation of oocyte maturation or other aspects of development. Such a comparison is possible as each experiment examines proteins from the same number of oocytes or eggs (200 cells) loaded onto two lanes of gel and the proteins are simultaneously transferred to a membrane and probed with the same antibody and Western blotting reagents. The qualitative comparison of one such experiment is shown in Figure 1. This experiment was repeated two additional times and a relative comparison was drawn for each isoform (Figure 2). The proteins 14-3-3 β , 14-3-3 ϵ , 14-3-3 η , and 14-3-3 ζ appear in lesser amounts in mature eggs than in immature oocytes. For example, a marked decrease in the 14-3-3 β isoform after maturation of oocytes into eggs is observed. On the contrary, amounts of 14-3-3 γ and 14-3-3 τ were found to increase following oocyte maturation. It should be noted that, in these experiments, it is only possible to make quantitative comparisons for a single isoform and not between different isoforms as the isoform-specific antibodies may have different affinities and therefore different intensities on a Western blot.

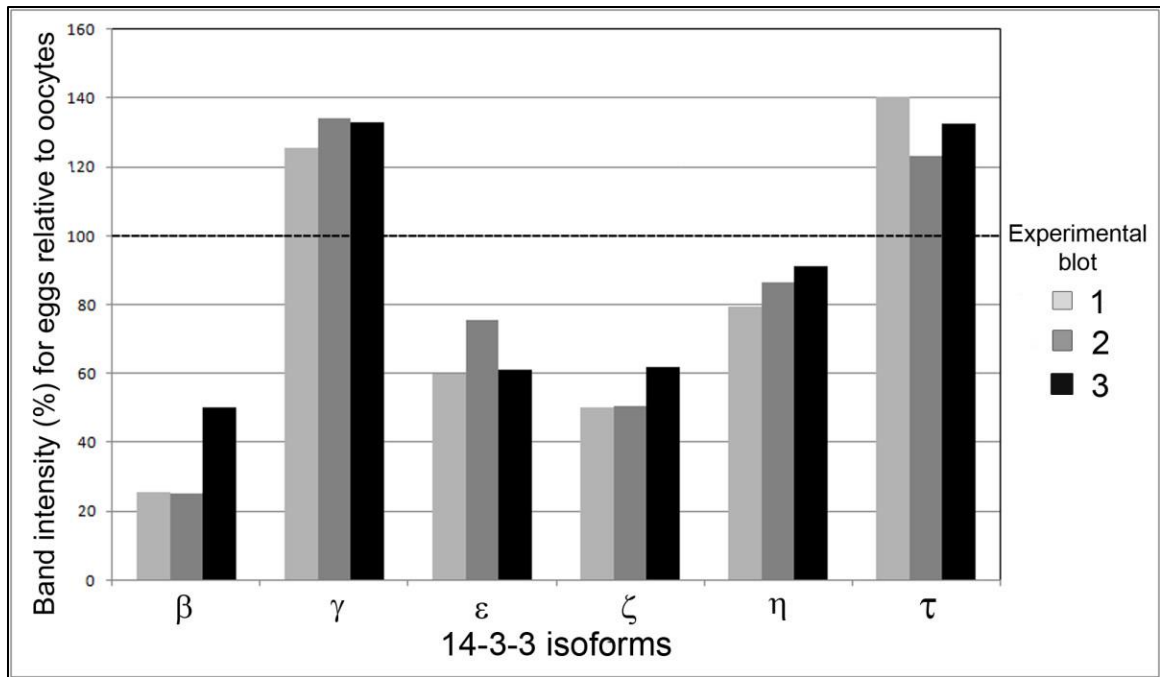


Figure 2. Comparison of the relative abundance of individual 14-3-3 isoforms in immature oocytes and mature eggs. The relative abundance of each individual isoform is based on the integrated densities of bands obtained from immunoblots (see Methods). Three experimental immunoblots were prepared for each of the six isoforms shown. In each experiment, for one of the isoforms, protein extracts from 200 oocytes and 200 eggs was analyzed after electrophoresis and immunoblotting on the same blot. For every blot, the density of the band for oocyte extracts was normalized to 100% and the density of the band for eggs is given as a percent with regards to the normalized oocyte value.

Expression of 14-3-3 isoforms in oocytes and eggs determined by immunofluorescence

Immunofluorescence microscopy confirms the presence of all seven 14-3-3 isoforms in oocytes and eggs (Figure 3). Oocytes and eggs were fixed in paraformaldehyde, permeabilized with detergent and incubated with isoform-specific antibodies for 14-3-3, followed by application of a fluorescently-labeled secondary antibody and viewed by scanning confocal microscopy. The subcellular distributions of the isoforms were found to vary from one isoform to another. For example, 14-3-3 ϵ is expressed uniformly throughout the oocyte with some peripheral accumulation, and absent in the interior of the egg cytoplasm (Figure 3E-F). Protein 14-3-3 τ is distributed uniformly in oocytes and eggs, but is particularly absent along the inner nuclear membrane of all oocytes examined (Figure 3I-J). Isoforms 14-3-3 β , 14-3-3 γ and 14-3-3 ζ exhibit a notable peripheral accumulation in oocytes, with a uniform distribution in eggs (Figure 3A-B, 3C-D and 3G-H respectively). Protein 14-3-3 σ is found to be expressed in higher levels in nuclei of all oocytes studied, as compared to their cytoplasm, where it is uniformly dispersed with some accumulation selectively along one half of the cell (Figure 3K); however, the 14-3-3 σ isoform shows a uniform distribution in eggs (Figure 3L). Protein 14-3-3 η is diffusely dispersed in oocyte with lesser distribution in the germinal vesicle than in the cytoplasm, but attains a uniform punctuate distribution with prominent accumulation in the region of the meiotic spindle in all eggs observed (Figure 3M-N).

Control oocytes and eggs incubated in secondary antibody alone displayed little background fluorescence at the same laser intensities and confocal imaging settings used

for each immunofluorescence experiment (Figure 3O-P). No attempt was made to compare the relative fluorescence intensity of a particular isoform in oocytes or eggs with that of a different isoform, since the antibodies detecting the isoforms were all different.

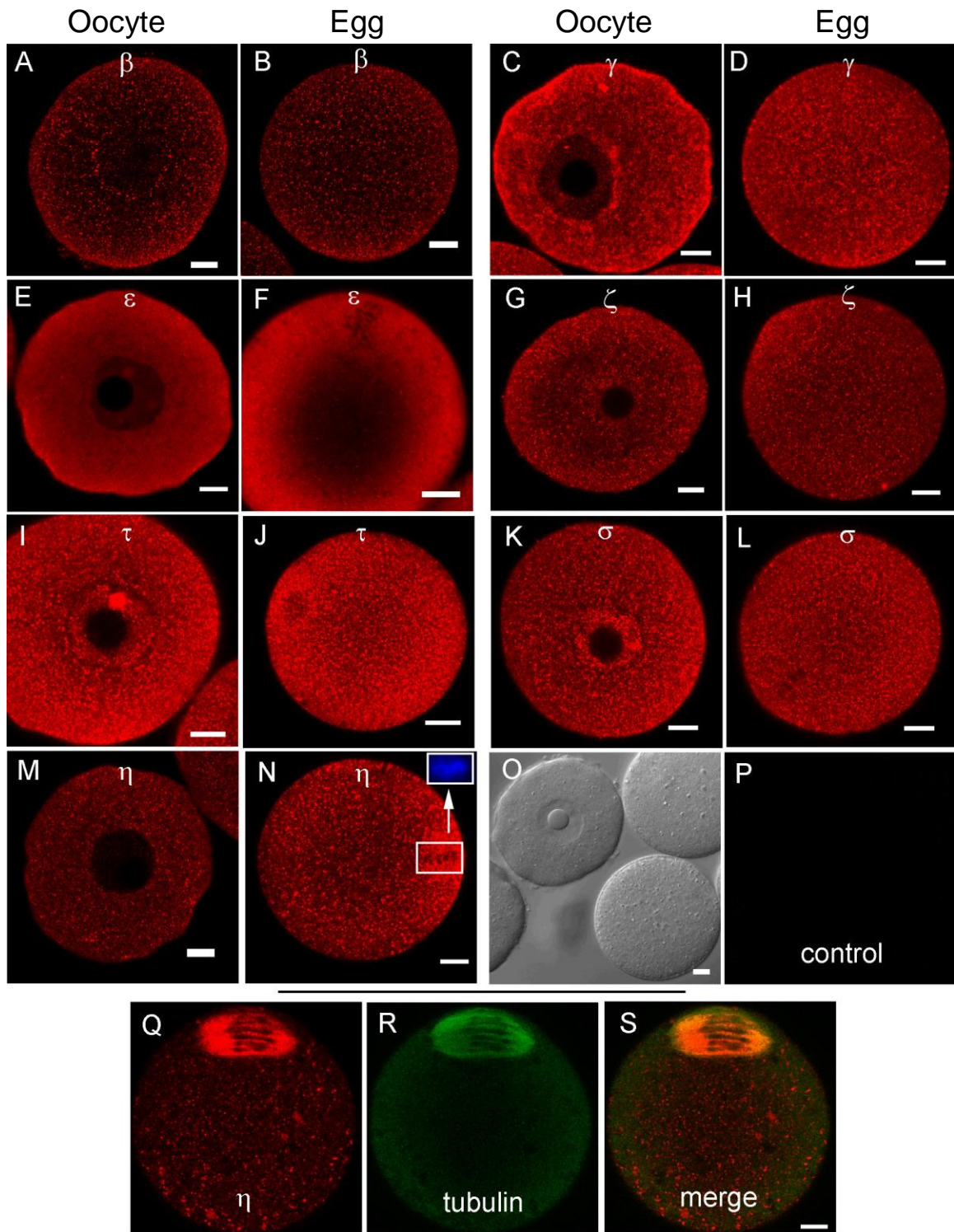


Figure 3. Representative immunofluorescence images of 14-3-3 isoforms in oocytes and eggs isolated from adult mice. (A, B) 14-3-3 β . (C, D) 14-3-3 γ . (E, F) 14-3-3 ϵ . (G, H) 14-3-3 ζ . (I, J) 14-3-3 τ . (K, L) 14-3-3 σ . (M, N) 14-3-3 η . Confocal sections with regions of red fluorescence indicating the corresponding isoforms studied (see Methods). The inset in N shows the same egg labeled blue with Hoechst DNA stain (non-confocal image) and confirms that the darker areas in this region of the larger image are condensed metaphase II chromosomes. Control cells were included for each isoform experiment and were imaged using the same confocal settings. Representative control oocytes and eggs are shown in bright-field (O) and fluorescence (P). 14-3-3 η accumulates, in part, in the meiotic spindle in eggs as shown by simultaneous labeling with 14-3-3 η (Q) and tubulin (R) antibodies. These sequential scans are merged (14-3-3 η + tubulin) in (S). The scale bars represent 10 μm for all images.

These experiments are the first to examine all of the 14-3-3 proteins in mouse oocytes and eggs. Previous work suggested that multiple isoforms could be present, for example an examination of the maternal component of the zygotic polysomal mRNA population in mouse eggs and one-cell embryos revealed an increase in maternal mRNAs for 14-3-3 β , 14-3-3 γ , 14-3-3 ζ , 14-3-3 η and 14-3-3 τ . The other isoform mRNAs were not examined in this paper [17].

It has been suggested that, in mammalian oocytes, 14-3-3 binds to and regulates the cell cycle control protein CDC25B phosphatase [11]. There is good evidence from studies of frog oocytes that 14-3-3 protein may act to hold the oocyte in prophase I arrest

by binding to and localizing phosphorylated CDC25B in the cytoplasm [18]. Following the induction of oocyte maturation, CDC25B is thought to be dephosphorylated and released from 14-3-3, allowing it to participate in the activation of MPF which leads to germinal vesicle breakdown and the resumption of meiosis. It is not known which of the seven isoforms in the mammalian oocyte might be interacting with CDC25B; it is shown here that all are present in oocytes. The interaction of 14-3-3 with the cell cycle control protein CDC25B has been examined in mammalian somatic cells. There is strong evidence to indicate that 14-3-3 β , 14-3-3 ϵ , and 14-3-3 σ bind to CDC25B and that 14-3-3 β is responsible for sequestering CDC25B in the cytoplasm [11, 19]. Future experiments (chapter 3) determined if the other 14-3-3 isoforms, which have now been found to be present as well in mouse oocytes, also interact with CDC25B and whether they are involved in the regulation of oocyte maturation.

Prominent localization of 14-3-3 σ in the nuclei of oocytes (Figure 3I) is consistent with the observations that 14-3-3 proteins can shuttle through the nuclear membrane, but is in contrast with some observations in somatic cells in which it was noted that 14-3-3 σ is more abundant in the cytoplasm than in the nucleus, while 14-3-3 ζ is more abundant in the nucleus as compared to the cytoplasm [20].

Localization of 14-3-3 η in the meiotic spindle (Figure 3N, Q, R and S) suggests a role for 14-3-3 in spindle assembly or cell cycle control. This is the first evidence for the localization of a specific 14-3-3 isoform in the metaphase II spindle of mouse eggs. It has been reported that 14-3-3 ϵ and 14-3-3 γ localize in the centrosome and mitotic spindle of some mouse somatic cells lines [21]. As detailed in chapter 4, additional functional

studies were performed to determine if 14-3-3 η plays a role in the formation or regulation of the meiotic spindle or chromosome separation in mammalian oocytes.

Expression of 14-3-3 isoforms in ovarian cells determined by immunohistochemistry

As work on the role of 14-3-3 in ovarian development, oogenesis and cancer proceeds, it will be valuable to know which 14-3-3 isoforms are present and/or abundant in both the somatic cells and the germ cells within the ovary. Mouse ovarian follicular sections were examined by immunohistochemical staining using isoform-specific antibodies and the Avidin: Biotinylated enzyme Complex (ABC) technique. The sections contained ovarian follicles at all stages of development. The ABC method relies on the high affinity of avidin for biotin and the method is known to produce minimal background staining in the absence of primary antibody [22, 23]. Regions stained brown indicate presence of the 14-3-3 isoforms in contrast with regions counterstained blue. Again it is not possible to determine the relative amounts of distribution of a particular isoform in cells compared to other isoforms as the antibodies are different; nevertheless for a given isoform, variations in the intensities of staining indicate differences in relative amounts of expression among different cells in follicles and surrounding tissue.

All seven isoforms of 14-3-3 protein were detected by immunohistochemistry, in cells of the ovary. Follicles at various stages of development exhibit some common features of expression of the isoforms. All isoforms of 14-3-3 were detected, to varying extents, in the oocyte and cumulus cells surrounding the oocyte, mural granulosa cells, theca interna and theca externa of all follicular stages examined, as well as in cells of the

corpus luteum (Figures 4, 5, 6, 7, 8, 9 and 10). In each of the follicular stages studied, all the isoforms appear to be expressed in the cytoplasm of the oocytes and to some extent in the corresponding germinal vesicles (Figures 4, 5, 6, 7, 8, 9 and 10). For all isoforms, staining appeared more intense in the cytoplasm than in the nuclei of somatic cells in granulosa and theca layers as well as in cells of corpora lutea (Figures 4, 5, 6, 7, 8, 9 and 10). Cells within corpora lutea were also found to have relatively higher amounts of expression of all of the isoforms as compared to surrounding interstitial cells F in (F in Figures 4, 5, 6, 7, 8, 9 and 10). The isoform 14-3-3 τ appears to be expressed at lower levels in somatic cells when compared to oocytes (Figure 9A-E). Atretic follicles, characterized by intensely stained pyknotic (apoptotic) and/or lytic cells, exhibit prominent accumulation of all isoforms of 14-3-3 (Figure 11A-G). Brain tissue sections were used as positive control for all isoforms of 14-3-3 except 14-3-3 σ for which skin tissue was used as positive control as shown in Figure 13 (see methods).

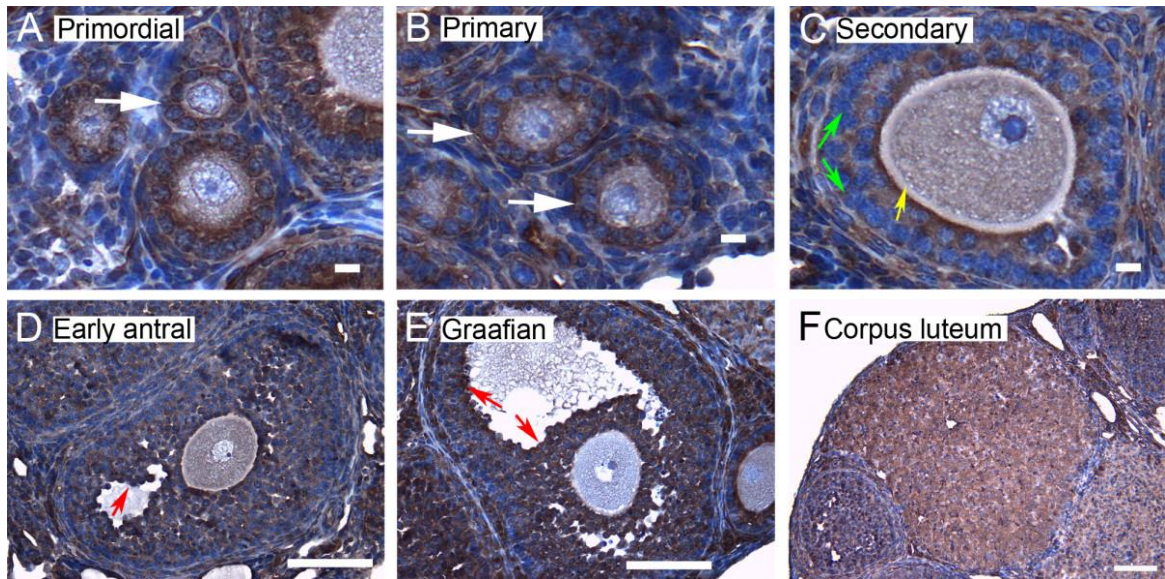


Figure 4. Representative immunohistochemistry images of 14-3-3 β in the different stages of follicular development in ovarian sections. Brown staining represents 14-3-3 β against regions counterstained blue with hematoxylin. (A) Primordial follicle. (B) Primary follicle. (C) Secondary follicle. (D) Early antral follicle. (E) Graafian (advanced antral) follicle. (F) Corpus luteum. White arrows indicate the primordial or primary follicles in (A and B). Note the weaker staining in mural granulosa cells in secondary follicles (C, green arrows), the more intense stain along the zona pellucida of the oocyte (C, yellow arrow), and the more intense staining in cells lining the antral cavity (D and E, red arrows). The scale bars represent 10 μm (A-C) or 100 μm (D-F).

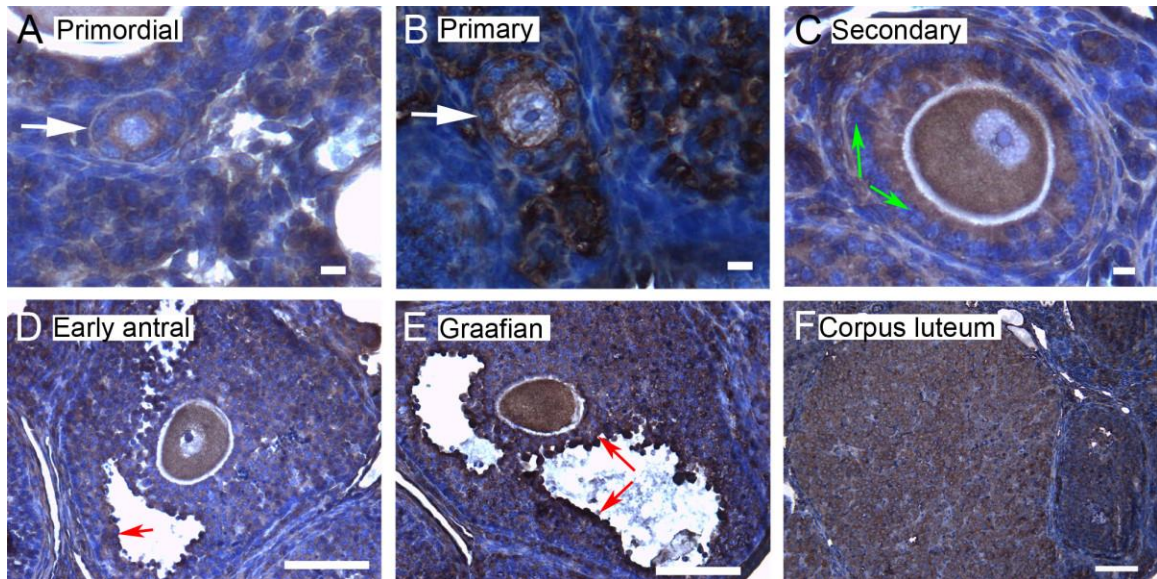


Figure 5. Representative immunohistochemistry images of 14-3-3 γ in the different stages of follicular development in ovarian sections. (A) Primordial follicle. (B) Primary follicle. (C) Secondary follicle. (D) Early antral follicle. (E) Graafian (advanced antral) follicle. (F) Corpus luteum. White arrows indicate the primordial or primary follicles in (A and B). Note the weaker staining in mural granulosa cells in secondary follicles (C, green arrows) and the more intense staining in cells lining the antral cavity (D and E, red arrows). The scale bars represent 10 μm (A-C) or 100 μm (D-F).

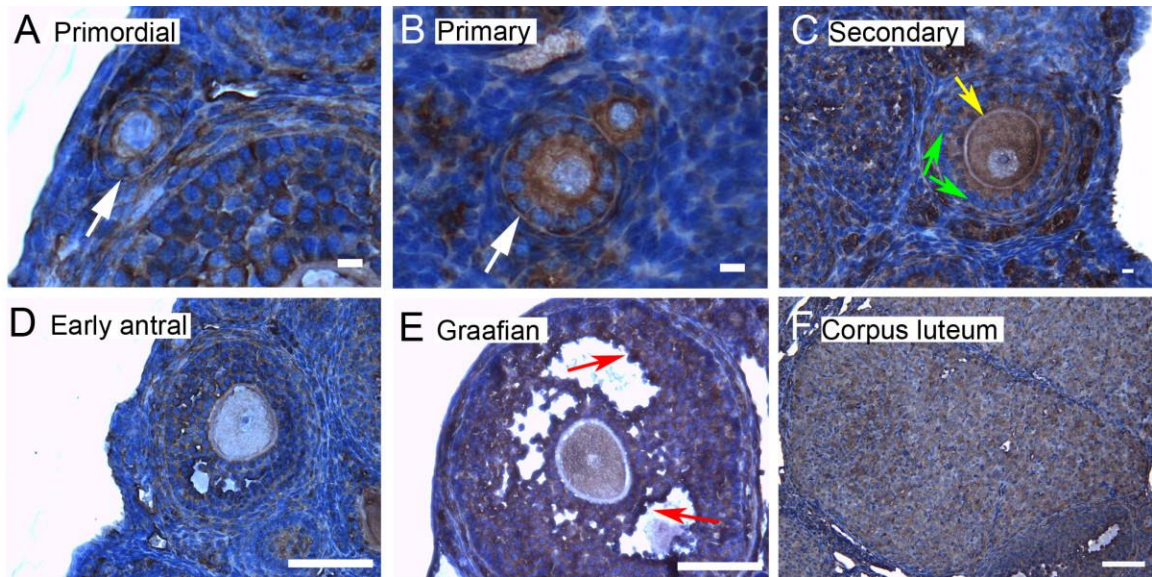


Figure 6. Representative immunohistochemistry images of 14-3-3 ϵ in the different stages of follicular development in ovarian sections. (A) Primordial follicle. (B) Primary follicle. (C) Secondary follicle. (D) Early antral follicle. (E) Graafian (advanced antral) follicle. (F) Corpus luteum. White arrows indicate the primordial or primary follicles in (A and B). Note the weaker staining in mural granulosa cells in secondary follicles (C, green arrows), the more intense stain along the zona pellucida of the oocyte (C, yellow arrow), and the more intense staining in cells lining the antral cavity (E, red arrows). The scale bars represent 10 μm (A-C) or 100 μm (D-F).

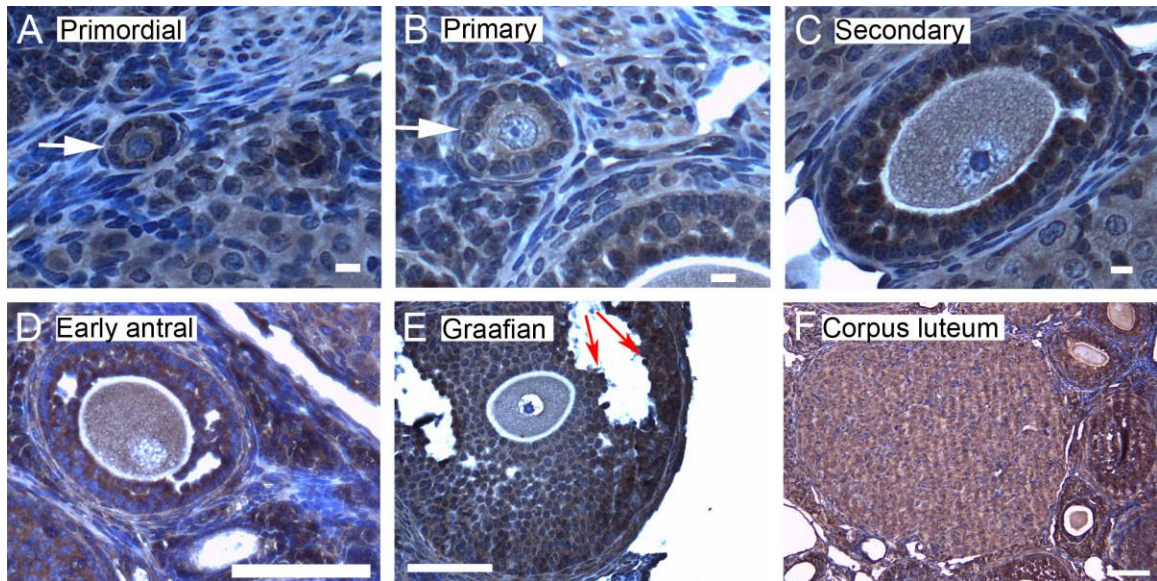


Figure 7. Representative immunohistochemistry images of 14-3-3 ζ in the different stages of follicular development in ovarian sections. (A) Primordial follicle. (B) Primary follicle. (C) Secondary follicle. (D) Early antral follicle. (E) Graafian (advanced antral) follicle. (F) Corpus luteum. White arrows indicate the primordial or primary follicles in (A and B). Note the more intense staining in cells lining the antral cavity (E, red arrows). The scale bars represent 10 μm (A-C) or 100 μm (D-F).

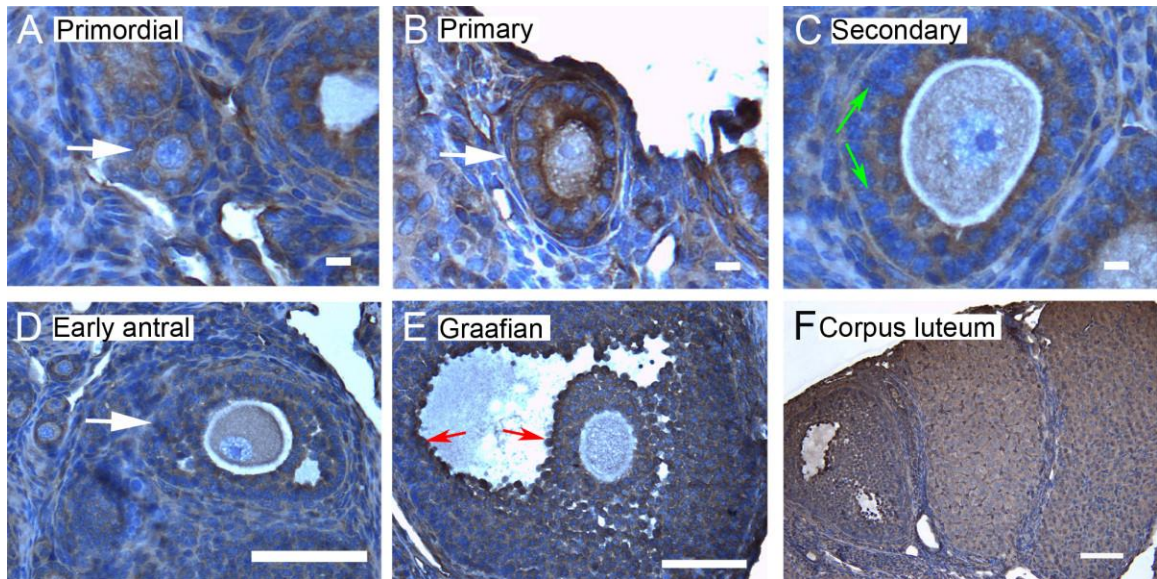


Figure 8. Representative immunohistochemistry images of 14-3-3 η in the different stages of follicular development in ovarian sections. (A) Primordial follicle. (B) Primary follicle. (C) Secondary follicle. (D) Early antral follicle. (E) Graafian (advanced antral) follicle. (F) Corpus luteum. White arrows indicate the primordial or primary follicles in (A and B). Note the weaker staining in mural granulosa cells in secondary follicles (C, green arrows) and the more intense staining in cells lining the antral cavity (E, red arrows). The scale bars represent 10 μm (A-C) or 100 μm (D-F).

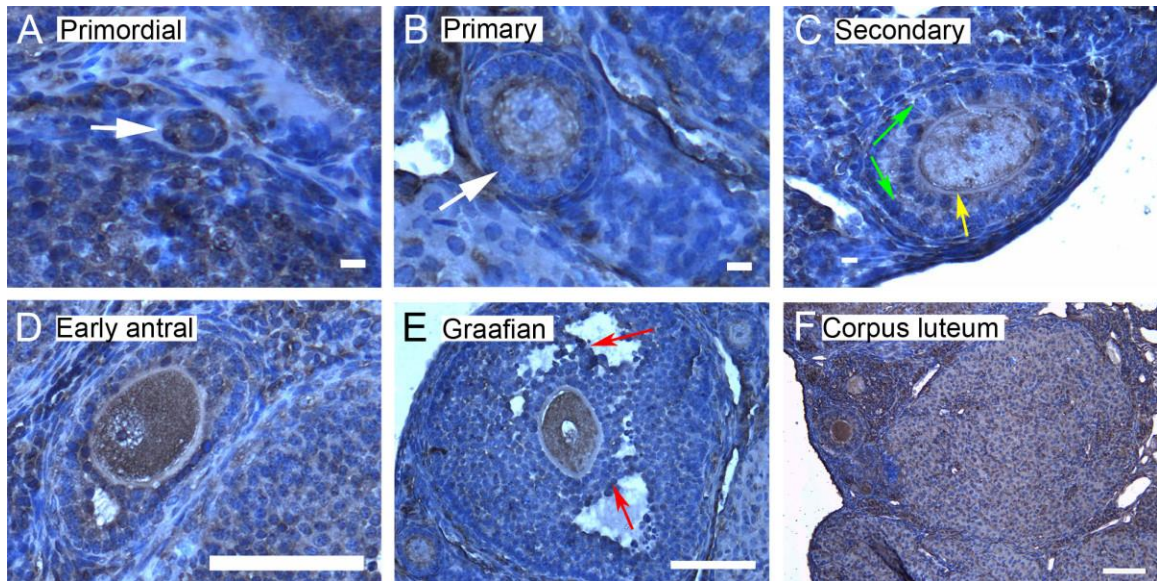


Figure 9. Representative immunohistochemistry images of 14-3-3 τ in the different stages of follicular development in ovarian sections. (A) Primordial follicle. (B) Primary follicle. (C) Secondary follicle. (D) Early antral follicle. (E) Graafian (advanced antral) follicle. (F) Corpus luteum. White arrows indicate the primordial or primary follicles in (A and B). Note the weaker staining in mural granulosa cells in secondary follicles (C, green arrows), the more intense stain along the zona pellucida of the oocyte (C, yellow arrow), and the more intense staining in cells lining the antral cavity (E, red arrows). The scale bars represent 10 μm (A-C) or 100 μm (D-F).

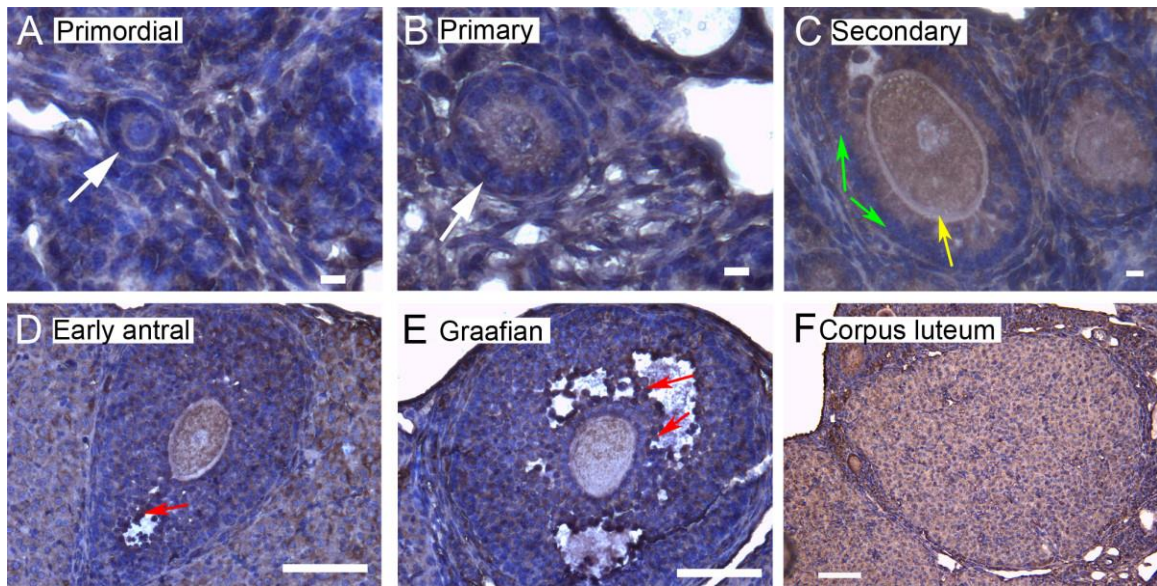


Figure 10. Representative immunohistochemistry images of 14-3-3 σ in the different stages of follicular development in ovarian sections. (A) Primordial follicle. (B) Primary follicle. (C) Secondary follicle. (D) Early antral follicle. (E) Graafian (advanced antral) follicle. (F) Corpus luteum. White arrows indicate the primordial or primary follicles in (A and B). Note the weaker staining in mural granulosa cells in secondary follicles (C, green arrows), the more intense stain along the zona pellucida of the oocyte (C, yellow arrow), and the more intense staining in cells lining the antral cavity (D and E, red arrows). The scale bars represent 10 μm (A-C) or 100 μm (D-F).

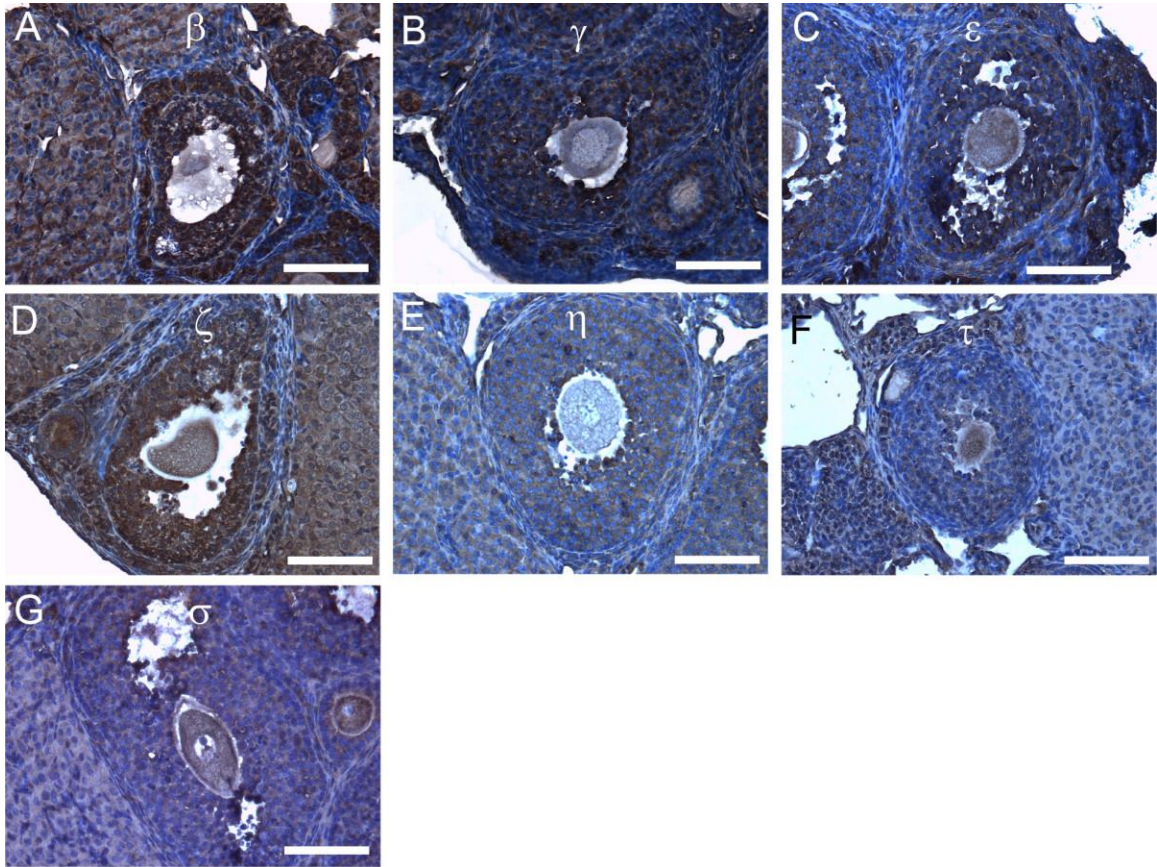


Figure 11. Representative immunohistochemistry images of 14-3-3 protein isoforms in atretic follicles of adult mouse ovaries. (A) 14-3-3 β . (B) 14-3-3 γ . (C) 14-3-3 ϵ . (D) 14-3-3 ζ . (E) 14-3-3 η . (F) 14-3-3 τ . (G) 14-3-3 σ . All scale bars indicate 100 μm .

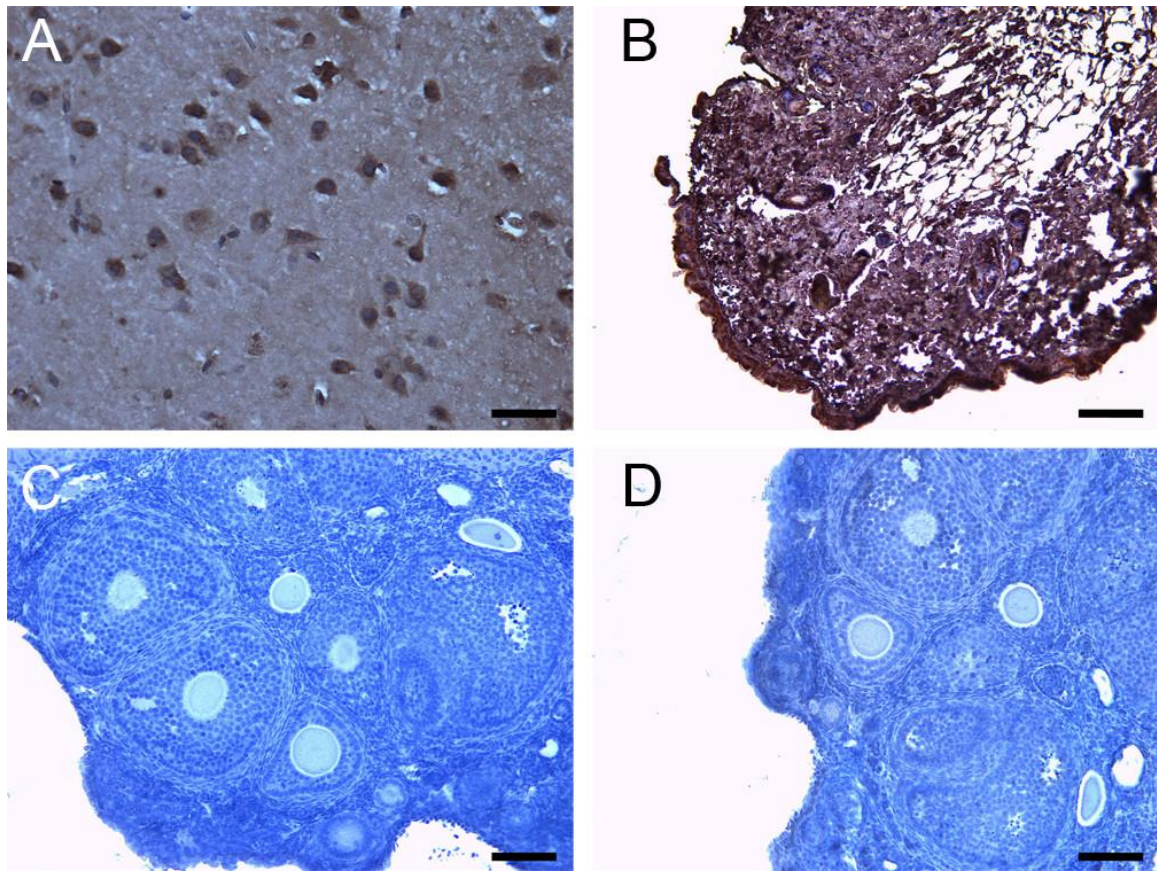


Figure 12. Representative control immunohistochemistry images for the different 14-3-3 protein isoforms in tissue sections. (A) Example of a positive control brain section obtained for all 14-3-3 isoforms except for 14-3-3 σ . (B) Skin positive control for 14-3-3 σ . (C) Example of a negative control section with no primary antibody obtained for all isoforms. (D) Example of a negative control with rabbit serum in place of primary antibody obtained for all isoforms. All scale bars indicate 100 μm .

While the specific activities of 14-3-3 proteins in ovarian function are largely unknown, these proteins could play a significant role. For example, 14-3-3 τ , shown to be present in human granulosa cells, has been shown to bind to the human follitropin

(follicle stimulating hormone, FSH) receptor suggesting a role for 14-3-3 proteins in follicle stimulating hormone signaling in granulosa cells [24, 25]. The reason for intense 14-3-3 staining in apoptotic cells is not known. 14-3-3 is generally associated with anti-apoptotic functions [26]. The 14-3-3 proteins appear to be involved in several ways in promoting cell survival; for example, 14-3-3 has been found to enhance the activity of proteins with proliferative or survival roles, such as members of the Raf family, while antagonizing the activity of proteins that promote cell death [3, 27]. There is some suggestion that 14-3-3 σ is associated with the survival of granulosa cells and inhibition of 14-3-3 interaction with target proteins, without regard to isoform, promotes apoptosis in these cells [28, 29].

Several characteristic differences in expression of 14-3-3 protein isoforms in different stages of follicular development were observed by immunohistochemical staining. Detection of 14-3-3 β , 14-3-3 γ , 14-3-3 ϵ , 14-3-3 τ and 14-3-3 σ in zonae pellucidae of oocytes by immunohistochemical staining indicates secretion of some 14-3-3 proteins into the zonae and perivitelline space (Table 1; C in Figures 4, 6, 9 and 10). To examine this by another method, zona-intact oocytes were isolated and viewed by immunofluorescence. Such immunocytochemical staining detected the same isoforms along the membranes of the isolated oocytes and within or along the zonae pellucidae of oocytes (Figure 12B, D, F, L and N), indicating secretion of those 14-3-3 isoforms by the oocyte or associated follicle cells. Control oocytes processed for fluorescence microscopy without the addition of primary antibody showed minimal or no background fluorescence (Figure 12O-P).

Table 1 Characteristic differences in expression of 14-3-3 protein isoforms in the different stages of follicular development as observed by immunohistochemical staining of adult mouse ovarian sections				
Feature	Isoform	Stage of Ovarian Follicle		
		Secondary	Early Antral	Graafian
Expression in <i>zona pellucida</i> around oocytes	14-3-3 β	++	++	++
	14-3-3 γ	+	+	+
	14-3-3 ϵ	++	++	++
	14-3-3 ζ	+	+	-
	14-3-3 η	-	-	-
	14-3-3 τ	++	++	++
	14-3-3 σ	++	++	++
Prominent lack of expression in peripheral mural granulosa cells	14-3-3 β	Yes	Yes	Yes
	14-3-3 γ	Yes	No	Yes
	14-3-3 ϵ	Yes	No	Yes
	14-3-3 ζ	No	No	No
	14-3-3 η	Yes	No	No
	14-3-3 τ	Yes	No	Yes
Marked accumulation in granulosa cells surrounding the antrum	14-3-3 β		Yes	Yes
	14-3-3 γ		Yes	Yes
	14-3-3 ϵ		No	Yes
	14-3-3 ζ		No	Yes
	14-3-3 η		No	Yes
	14-3-3 τ		No	Yes
14-3-3 σ		Yes	Yes	

'++' = Considerable expression; '+' = Some expression;
'-' = Non-detectable expression; 'Yes' = Presence of the feature; 'No' = Feature not detectable

Table 1. Characteristic differences in expression of 14-3-3 protein isoforms in the different stages of follicular development as observed by immunohistochemical staining of adult mouse ovarian sections.

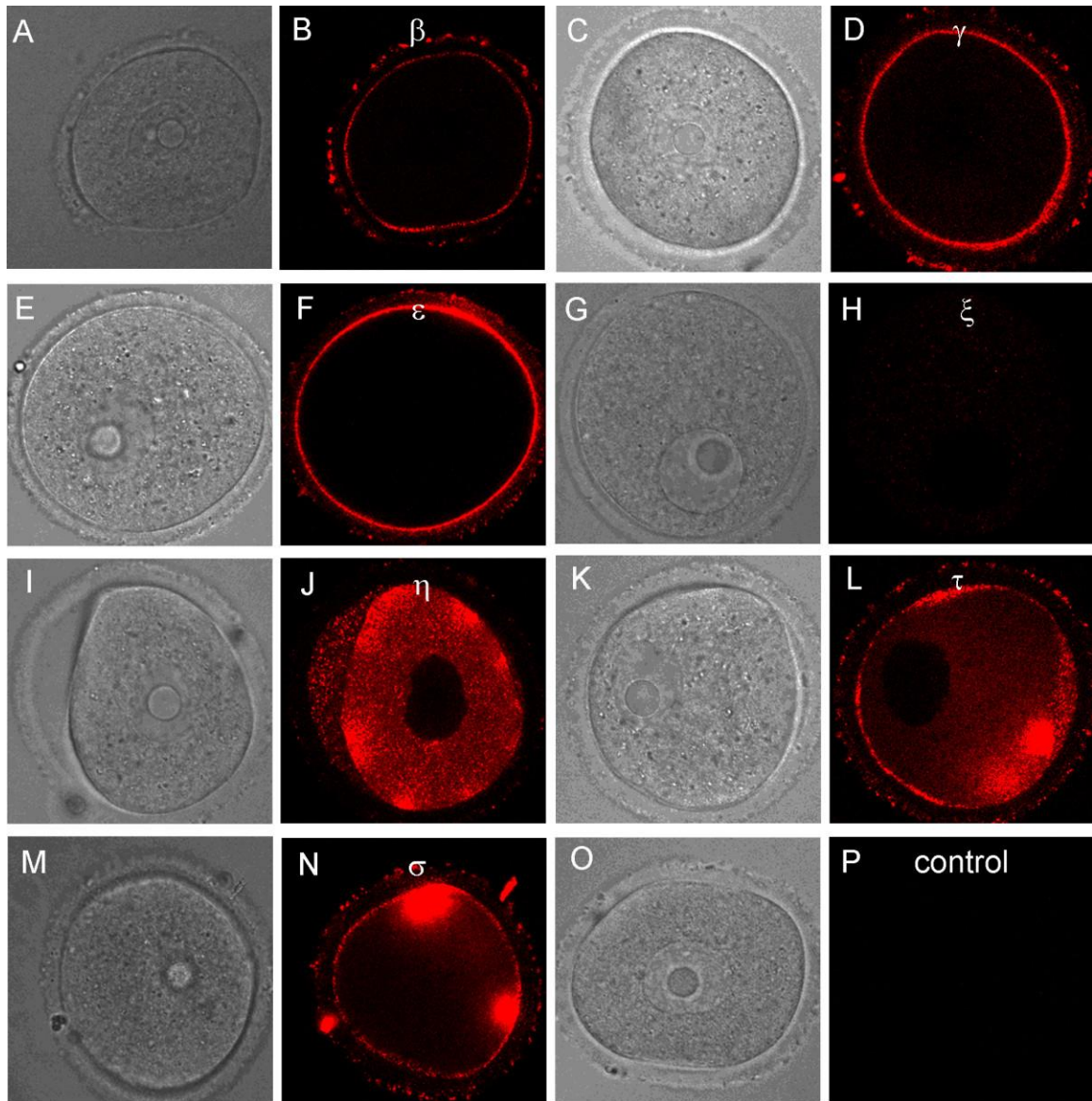


Figure 13. Representative immunocytochemistry images of 14-3-3 protein isoforms along and in the *zonae pellucidae* of cumulus-free oocytes isolated from ovaries of adult mice. The zona-intact cells were fixed in paraformaldehyde but not treated with detergent (see Methods). Paired images of an oocyte (left image is brightfield and right is immunofluorescence) indicate staining along the zona and/or the cell membrane for all isoforms except 14-3-3 ζ . Note: the intent of this part of the study was not to examine the

intracellular distribution of the isoforms (see Figure 3 for those experiments) since the cells were not permeabilized to permit complete antibody penetration; however, cells may be partially permeabilized by fixation accounting for the detection of intracellular proteins in some cells. (A, B) 14-3-3 β . (C, D) 14-3-3 γ . (E, F) 14-3-3 ϵ . (G, H) 14-3-3 ζ . (I, J) 14-3-3 η . (K, L) 14-3-3 τ . (M, N) 14-3-3 σ . (O, P) Control image without primary antibody addition.

The function, if any, of extracellular 14-3-3 surrounding the oocyte is not yet known. This was not believed to be an artifact of fixation since the appearance of the extracellular 14-3-3 was found by two different methods and the absence of staining for some isoforms argues against nonspecific artifacts. No extracellular 14-3-3 proteins were found to be associated with mature, ovulated eggs, which also suggests that this is not an artifact (data not shown). While the 14-3-3 proteins are generally known as intracellular proteins, some 14-3-3 proteins are known to be secreted by somatic cells; for example, it has been known for some time that 14-3-3 proteins are found in the cerebrospinal fluid [30] where they may serve as markers for Creutzfeldt-Jakob disease. Keratinocytes secrete 14-3-3 σ which induces expression of matrix metalloproteinase 1 (MMP1 or collagenase) in fibroblasts [31]. Three isoforms, 14-3-3 σ , 14-3-3 γ and 14-3-3 ζ , are secreted by corneal epithelial cells and ocular cell lines [32]. The 14-3-3 ζ protein is secreted by certain tumor-associated inflammatory cells [33].

Another notable difference in the distribution of 14-3-3 isoforms in ovarian folliculogenesis is prominent lack of expression 14-3-3 β , 14-3-3 γ , 14-3-3 ϵ , 14-3-3 τ , 14-3-

3 η and 14-3-3 σ in the peripheral mural granulosa cells, as compared to other cells of secondary, early antral and/or Graafian follicles (Table 1; C in Figures 4, 5 and 6 and 8, 9 and 10). At early antral stages, intense staining was noted for 14-3-3 β , 14-3-3 γ and 14-3-3 σ in granulosa cells surrounding the antrum (Table 1; D in Figures 1, 2 and 10). At the Graafian stage, all isoforms appear to accumulate in these cells (Table 1; E in Figures 4, 5, 6, 7, 8, 9 and 10).

Materials and Methods

Collection of Oocytes and Eggs and Preparation of Ovarian Tissue Extracts

All mice used in the present experiments were housed and used at Kent State University under an approved Institutional Animal Care and Use Committee protocol following the National Research Council's publication Guide for the Care and Use of Laboratory Animals. Oocytes and eggs were collected as previously described [12]. CD1 mice (2.5 months old) were injected with 7.5 IU eCG and, 44-48 hours later, the ovaries were removed and repeatedly punctured with a 26-gauge needle to rupture follicles. Cumulus cell-enclosed oocytes were isolated and the cumulus cells were removed by repeated pipetting through a small-bore pipette. Fully-grown oocytes with intact nuclei (germinal vesicles) were cultured in MEM containing 0.1 mg/ml dibutyryl cAMP to prevent spontaneous oocyte maturation. Mature, metaphase II-arrested eggs were obtained from mice 13-14 h following superovulation by injection of 7.5 IU hCG which

was preceded by a priming injection of 7.5 IU eCG injection 48 h earlier. The cumulus cells were removed with 0.3 mg/ml hyaluronidase. Zonae pellucidae from oocytes and eggs thus collected were removed by a brief treatment in acid Tyrode's solution (0.14 M NaCl, 3 mM KCl, 1.6 mM CaCl₂·2H₂O, 0.5 mM MgCl₂·6H₂O, 5.5 mM glucose, and 0.1% PVA, pH 2.5). Cells were rinsed in MEM and prepared for use in Western blot or immunocytochemistry as described below.

Ovaries from unprimed adult mice (2.5 months old), along with brain tissues, were homogenized in a buffer containing (10 mM Tris pH 7.0, 1 mM EDTA, 1 mM EGTA, 0.16% benzamidine hydrochloride, 14 mM beta-mercaptoethanol, 1 mM PMSF and 0.1 mM TPCK) pH 7.2, using a mechanical homogenizer. The homogenized cell lysates were then centrifuged at 16,000 g for 30 minutes and the supernatants containing the total soluble protein extracts were used for SDS-PAGE and Western blotting.

SDS-PAGE, Western Blotting and Protein Analysis

The 14-3-3 isoforms were identified through multiple Western blots (using standard Western blotting procedures), each testing for one of the seven isoforms in protein extracts. Oocytes and eggs were rinsed in MEM, counted, and transferred to Tris-buffered saline (TBS; 25 mM Tris-HCl [pH 7.5] and 150 mM NaCl) containing 0.1% PVA. Cells were removed from the TBS, lysing buffer was added, and the cell lysates were quick-frozen in ethanol/dry ice and stored at -70°C until use. The lysis buffer contained 10 mM Tris-HCl [pH 7.2], 1 mM EDTA, 1 mM EGTA, 0.1% (v/v) b-mercaptoethanol, 1% (v/v) Triton X-100, protease inhibitors (1 mM PMSF, 0.1 mM

TPCK, 10 μ M leupeptin, 1 μ M pepstatin A, and 75 nM aprotinin), and phosphatase inhibitors (1 mM Na_3VO_4 , 100 nM calyculin A, 10 mM beta-glycerophosphate, and 5 mM sodium pyrophosphate).

Proteins from the lysates of 200 oocytes or 200 eggs were separated by SDS-PAGE using a 4% stacking, 12% resolving polyacrylamide gel and electrophoretically transferred to Immobilon-P PVDF membrane (Millipore Corp.). The membranes were incubated in blocking buffer (5% milk in TBS, 0.1% Tween-20) and then with primary antibodies overnight at 4°C, washed and incubated with secondary antibody and imaged by chemiluminescence with an enhanced chemiluminescence kit according to the manufacturer's instructions (GE Healthcare Life Sciences) using the Fujifilm LAS-3000 luminescent image analyzer. Protein extracts of ovaries from adult mice were included for comparison among immunoblots for all 14-3-3 isoforms. Brain extract was used as a positive control for detecting all isoforms of 14-3-3 except 14-3-3 σ for which skin extract was used as positive control. This is because all isoforms of 14-3-3 have been identified in brain except 14-3-3 σ which has been detected in skin [15].

The commercial rabbit anti-14-3-3 isoform panel (PAN017) from AbD Serotec was used for Western blotting as well as immunocytochemical and immunohistochemical staining (see below) of the different 14-3-3 isoforms in mouse ovaries, oocytes and eggs. The immunogens, against which the antibodies were raised, were synthetic peptides corresponding to acetylated N-terminal sequences of sheep 14-3-3 proteins. They are raised against synthetic peptides corresponding to the following acetylated N-terminal sequences of sheep 14-3-3 isoforms: 14-3-3 β , TMDKSELVC; 14-3-3 γ ,

VDREQLVQKAC; 14-3-3 ϵ , MDDREDLVYQAKC; 14-3-3 ζ : MDKNELVQKAC; 14-3-3 η , GDREQLLQRARC; 14-3-3 τ , MEKTELIQKAC; 14-3-3 σ , MERASLIQKAC.

Two additional antibodies to 14-3-3 β and 14-3-3 ζ were also used to confirm the presence of these isoforms (rabbit anti-14-3-3 β , sc-628 and rabbit anti-14-3-3 ζ sc-1019, Santa Cruz Biotechnology). All antibodies were used at a dilution of 1:1,000 in blocking buffer (5% milk in 1X TBS, 0.1% Tween-20). The secondary antibody for all experiments was HRP-conjugated goat anti-rabbit (Genscript; 1 mg/ml stock) used at a dilution of 1:2,000 in the blocking buffer.

The relative abundance of each 14-3-3 isoform in oocytes and eggs was determined in a semi-quantitative manner. Proteins from 200 oocytes and 200 eggs were separated by electrophoresis on the same gel, transferred to membrane at the same time and immunoblotted together under the same conditions using one of the six 14-3-3 antibodies. This procedure was repeated two additional times with the same antibody. There will be inherent differences in the intensities of bands for each immunoblot processed, but for a given blot the intensity of the egg band can be compared to the intensity of the oocyte band. To summarize the three experiments for each of the six isoforms, the band intensities for oocyte and egg lanes in a given blot were analyzed using NIH image and compared to each other. The intensity of the oocyte band was normalized to 100% for each blot and the egg intensity (reflecting the relative protein amount) was then expressed as a percentage of the oocyte intensity for each of the three blots analyzed for each isoform. Note that no comparison should be drawn for the band

intensities among the isoforms since the antibodies detecting the isoforms were different from each other, with possible differences in their affinities.

Immunocytochemistry of oocytes and eggs

Oocytes and eggs were fixed in freshly prepared 3.7% paraformaldehyde for 30-60 min, washed in PBS-PVA (PBS containing 1% PVA), permeabilized with 1% Triton X-100 to promote antibody penetration, washed in PBS-PVA, then treated with blocking buffer (5% normal goat serum in PBS-PVA), and incubated overnight with each of the primary antibodies for 14-3-3 isoforms (rabbit anti-14-3-3 isoform panel PAN017, AbD Serotec; diluted 1:200 in 1% goat serum blocking buffer). Following washing, the cells were incubated with Cy3-conjugated goat anti-rabbit secondary antibody (Jackson ImmunoResearch Laboratories) diluted 1:200 in blocking buffer for several hours, washed again and transferred to an anti-fade solution (SlowFade; Invitrogen). All cells were imaged with the Olympus Fluoview FV500 confocal microscopy system using a 60× oil immersion lens and various confocal zooms; the scale bars on the images indicate the final magnification. Images were captured and examined at multiple confocal planes. The representative images shown here are primarily images at the plane of the optical equator. For each isoform experiment, 5-7 oocytes and 5-7 eggs were examined at the same time under the same staining and imaging conditions. The experiment was repeated twice for each isoform.

In oocytes, the nucleus is readily discernible in fluorescence images or the corresponding bright field images. In eggs, the location of the condensed metaphase II

chromosomes can sometimes be determined by a bulge at one pole of the egg or by the absence of fluorescence causing an outline of the unlabeled chromosomes. In an additional experiment using the 14-3-3 η antibody, condensed meiotic chromosomes in eggs were identified by staining with the DNA-staining Hoechst dye (0.001 mg/ml) and imaged with conventional epifluorescence microscopy (Figure 3N, inset). In several experiments, eggs were simultaneously incubated in both the 14-3-3 η isoform antibody and an antibody to α -tubulin to identify the meiotic spindle microtubules (rat anti- α -tubulin; sc-69970; 200 μ g/ml diluted 1:200 in 1% blocking buffer; Santa Cruz Biotechnology). The secondary antibody was FITC-conjugated goat anti-rat from (Jackson Laboratories) (diluted 1:200 in blocking buffer). In all cases, control oocytes and eggs were incubated in secondary antibody alone and imaged using the same confocal settings as used for experimental, antibody-labeled cells. Background fluorescence was minimal.

An additional set of immunofluorescence experiments was performed to examine the presence of extracellular 14-3-3 isoforms associated with isolated oocytes. The immunofluorescence method was used as described above, but with several changes. In this case, the *zonae* were not removed before fixation in 3.7% paraformaldehyde and the cells were not treated Triton X-100 to permeabilize the cell membranes following fixation. All other staining procedures were the same. I wanted to look at the possibility of secreted proteins in oocytes. This experiment was not intended to examine the intracellular distribution of isoforms (see above methods and Figure 3 for that experiment); however, it is known for many years that mouse oocytes and eggs

sometimes are partially permeabilized on fixation alone (no detergent added). Therefore some staining within the oocytes may occur, but is not be a complete representation since the permeability of cells may vary from cell to cell and is not uniform within a cell.

Immunohistochemistry of tissue sections

Ovaries, brain and skin tissues were collected from unprimed adult mice (2.5 months old) and fixed in 4% paraformaldehyde in PBS overnight. They were then dehydrated through a graded series of ethanol followed by two changes of CitriSolv and embedded in paraffin. Multiple microtome tissue sections of 6 μm thickness were transferred to slides pre-coated with poly-L-lysine. Following removal of paraffin and rehydration, antigens were recovered by boiling the sections for 1 min, three times in Antigen Retrieval Citra solution (#HK086-5K, Biogenex) with intermittent cooling. Tissue sections were then cooled at room temperature for 30 min and then washed in deionised water for 5 min. Endogenous peroxidase was blocked by incubation of tissue sections in 0.3% hydrogen peroxide for 30 min. Tissues were then incubated for 20 min in PBS blocking buffer with 0.15% normal goat serum (VectaStain Elite ABC Kit, #PK-6101, Vector Laboratories). Tissues sections were incubated overnight at 4°C in a humidified chamber with each of the different primary antibodies (14-3-3 isoform panel PAN017, AbD Serotec, see above) diluted in blocking buffer at dilutions recommended by the manufacturer and a prior study [34]: 14-3-3 β 1:600, 14-3-3 γ 1:800, 14-3-3 ϵ 1:400, 14-3-3 ζ 1:400, 14-3-3 η 1:3,200, 14-3-3 τ 1:60, and 14-3-3 σ 1:100. The same dilutions were used for positive control sections. The rabbit serum used in matching negative

control sections, were immunostained at a dilution identical to that used in corresponding sample sections for the isoforms.

Following antibody incubation, slides containing tissue sections were washed in buffer (PBS, pH 7.5) for 5 min, incubated for 30 min in biotinylated secondary antibody (VectaStain Elite ABC Kit, Vector Laboratories) diluted in blocking buffer and washed again in buffer for 5 minutes. This was followed by incubation of the tissues for 30 min in VectaStain Elite ABC Reagent (prepared according to the manufacturer's instructions; Vector Laboratories). DAB substrate was prepared using Vector Laboratories DAB peroxidase substrate Kit (SK-4100) according to instructions specified in kit. Tissues were treated with DAB substrate for 3-4 minutes until development of optimum brown color, rinsed with tap water and counter-stained with Hematoxylin.

The ABC-immunostaining method produces minimal background staining. To examine the background staining, two sets of negative controls were used. One set of tissue sections was processed without the addition of primary antibodies. Since the primary antibodies were rabbit polyclonals, the other control set utilized tissue sections incubated in normal rabbit serum (Jackson ImmunoResearch) prior to incubation with the secondary antibodies. In both cases, control sections did not show brown staining, confirming specific localization by this method. Brain tissue sections were used as positive control for all isoforms of 14-3-3 except 14-3-3 σ for which skin tissue was used as positive control (see Figure 13). This is because all isoforms of 14-3-3 have been identified in brain with the exception of 14-3-3 σ [13]. Skin sections were used as positive control for 14-3-3 σ since 14-3-3 σ is known to be found in epidermis [15] (see Figure 13).

For each isoform, dilutions of primary antibodies or rabbit serum for positive and negative controls were kept identical. Each 14-3-3 isoform was studied individually in a set of three separately stained ovarian tissue sections, along with simultaneous staining of appropriate positive and negative controls. In addition the studies were repeated on sections obtained from the ovary of a different unprimed adult mouse of the same age. The characteristic features for all 14-3-3 isoforms, as identified by immunohistochemical staining, were examined and tabulated (Table 1) independently by three individuals with agreement on the observations.

Conclusions

The work shows, for the first time, the expression of all seven mammalian isoforms of the protein 14-3-3 in the female mouse germ cells and in cells of mouse ovarian follicles at various stages of development. There are characteristic differences in the relative amount and distribution of 14-3-3 proteins in oocytes and eggs. Protein 14-3-3 η , for example localizes, in part, to the meiotic spindle in eggs. A number of isoforms appear to be extracellular and associated with the *zona pellucidae* in ovarian oocytes. The distribution of some 14-3-3 isoforms within cells of the ovary differs, for example with peripheral mural granulosa cells expressing some isoforms and not others. All 14-3-3 isoforms appear to be present in relatively greater amounts in cells lining the antral cavity of Graafian follicles and in granulosa cells of atretic follicles. These results will enable further research investigating 14-3-3 interactions with other key proteins involved in ovarian development and gamete function.

Bibliography

1. Lau JMC, Wu CL, Muslin AJ: Differential role of 14-3-3 family members in *Xenopus* development. *Dev Dyn* 2006, 235(7):1761-1776.
2. Margolis S, Perry J, Weitzel D, Freel C, Yoshida M, Haystead T, Kornbluth S: A role for PP1 in the Cdc2/Cyclin B-mediated positive feedback activation of Cdc25. *Mol Biol Cell* 2006, 17(4):1779-1789.
3. Morrison DK: The 14-3-3 proteins: integrators of diverse signaling cues that impact cell fate and cancer development. *Trends Cell Biol* 2009, 19(1):16-23.
4. Aitken A: 14-3-3 proteins: a historic overview. *Semin Cancer Biol* 2006, 16(3):162-172.
5. Jones DH, Ley S, Aitken A: Isoforms of 14-3-3-protein can form homodimers and heterodimers in-vivo and in-vitro - implications for function as adapter proteins. *FEBS Lett* 1995, 368(1):55-58.
6. Chaudhri M, Scarabel M, Aitken A: Mammalian and yeast 14-3-3 isoforms form distinct patterns of dimers in vivo. *Biochem Biophys Res Commun* 2003, 300(3):679-685.
7. Aitken A: Functional specificity in 14-3-3 isoform interactions through dimer formation and phosphorylation. Chromosome location of mammalian isoforms and variants. *Plant Mol Biol* 2002, 50(6):993-1010.
8. Benzinger A, Muster N, Koch HB, Yates JR, Hermeking H: Targeted proteomic analysis of 14-3-3 sigma, a p53 effector commonly silenced in cancer. *Mol Cell Proteomics* 2005, 4(6):785-795.

9. Mackintosh C: Dynamic interactions between 14-3-3 proteins and phosphoproteins regulate diverse cellular processes. *Biochem J* 2004, 381:329-342.
10. Mhaweche-Fauceglia P, Herrmann FR, Andrews C, South S, Beck A, Lele S, Odunsi K: 14-3-3 sigma expression and prognostic value in patients with epithelial ovarian carcinoma: a high throughput tissue microarray analysis. *Ejso* 2009, 35(7):763-767.
11. Pirino G, Wescott MP, Donovan PJ: Protein kinase a regulates resumption of meiosis by phosphorylation of Cdc25B in mammalian oocytes. *Cell Cycle* 2009, 8(4):665-670.
12. Snow AJ, Puri P, Acker-Palmer A, Bouwmeester T, Vijayaraghavan S, Kline D: Phosphorylation-dependent interaction of tyrosine 3-monooxygenase/tryptophan 5-monooxygenase activation protein (YWHA) with PAD16 following oocyte maturation in mice. *Biol Reprod* 2008, 79(2):337-347.
13. Martin H, Rostas J, Patel Y, Aitken A: Subcellular-localization of 14-3-3-isoforms in rat-brain using specific antibodies. *J Neurochem* 1994, 63(6):2259-2265.
14. Martin H, Patel Y, Jones D, Howell S, Robinson K, Aitken A: Antibodies against the major brain isoforms of 14-3-3-protein-an antibody specific for the N-acetylated amino-terminus of a protein. *FEBS Lett* 1993, 331(3):296-303.
15. Kilani RT, Medina A, Aitken A, Jalili RB, Carr M, Ghahary A: Identification of different isoforms of 14-3-3 protein family in human dermal and epidermal layers. *Mol Cell Biochem* 2008, 314(1-2):161-169.

16. Roth D, Morgan A, Martin H, Jones D, Martens G, Aitken A, Burgoyne R:
Characterization of 14-3-3 proteins in adrenal chromaffin cells and demonstration of isoform-specific phospholipid binding. *Biochem J* 1994, 301:305-310.
17. Potireddy S, Vassena R, Patel BG, Latham KE: Analysis of polysomal mRNA populations of mouse oocytes and zygotes: dynamic changes in maternal mRNA utilization and function. *Dev Biol* 2006, 298(1):155-166.
18. Margolis SS, Walsh S, Weiser DC, Yoshida M, Shenolikar S, Kornbluth S: PP1 control of M phase entry exerted through 14-3-3-regulated Cdc25 dephosphorylation. *EMBO J* 2003, 22(21):5734-5745.
19. Uchida S, Kuma A, Ohtsubo M, Shimura M, Hirata M, Nakagama H, Matsunaga T, Ishizaka Y, Yamashita K: Binding of 14-3-3 beta but not 14-3-3 sigma controls the cytoplasmic localization of CDC25B: binding site preferences of 14-3-3 subtypes and the subcellular localization of CDC25B. *J Cell Sci* 2004, 117(14):3011-3020.
20. van Hemert M, Niemantsverdriet M, Schmidt T, Backendorf C, Spaik H: Isoform-specific differences in rapid nucleocytoplasmic shuttling cause distinct subcellular distributions of 14 3 3 σ and 14 3 3 ζ . *J Cell Sci* 2004, 117(8):1411-1420.
21. Pietromonaco S, Seluja G, Aitken A, Elias L: Association of 14-3-3 proteins with centrosomes. *Blood Cells Mol Dis* 1996, 22(19):225-237.
22. Hsu SM, Raine L, Fanger H: A comparative-study of the peroxidaseantiperoxidase method and an avidin-biotin complex method for studying polypeptide hormones with radioimmunoassay antibodies. *Am J Clin Pathol* 1981, 75(5):734-738.

23. Hsu SM, Raine L, Fanger H: Use of avidin-biotin-peroxidase complex (abc) in immunoperoxidase techniques-a comparison between Abc and unlabeled antibody (Pap) procedures. *J Histochem Cytochem* 1981, 29(4):577-580.
24. Cohen B, Nechamen C, Dias J: Human follitropin receptor (FSHR) interacts with the adapter protein 14-3-3 tau. *Mol Cell Endocrinol* 2004, 220(1-2):1-7.
25. Dias JA, Mahale SD, Nechamen CA, Davydenko O, Thomas RM, Ulloa-Aguirre A: Emerging roles for the FSH receptor adapter protein APPL1 and overlap of a putative 14-3-3 tau interaction domain with a canonical G-protein interaction site. *Mol Cell Endocrinol* 2010, 329(1-2):17-25.
26. Rosenquist M: 14-3-3 Proteins in Apoptosis. *Braz J Med Biol Res* 2003, 36(4):403-408.
27. Porter G, Khuri F, Fu H: Dynamic 14-3-3/client protein interactions integrate survival and apoptotic pathways. *Semin Cancer Biol* 2006, 16(3):193-202.
28. Peluso JJ, Pappalardo A: Progesterone regulates granulosa cell viability through a protein kinase G-dependent mechanism that may involve 14-3-3 sigma. *Biol Reprod* 2004, 71(6):1870-1878.
29. Peluso JJ, Liu X, Romak J: Progesterone maintains basal intracellular adenosine triphosphate levels and viability of spontaneously immortalized granulosa cells by promoting an interaction between 14-3-3 sigma and ATP synthase beta/precursor through a protein kinase G-dependent mechanism. *Endocrinology* 2007, 148(5):2037-2044.

30. Wiltfang J, Otto M, Baxter H, Bodemer M, Steinacker P, Bahn E, Zerr I, Kornhuber J, Kretzschmar H, Poser S, Ruther E, Aitken A: Isoform pattern of 14-3-3 proteins in the cerebrospinal fluid of patients with CreutzfeldtJakob disease. *J Neurochem* 1999, 73(6):2485-2490.
31. Ghaffari A, Li Y, Karami A, Ghaffari M, Tredget E, Ghahary A: Fibroblast extracellular matrix gene expression in response to keratinocytereleasable stratifin. *J Cell Biochem* 2006, 98(2):383-393.
32. Shankardas J, Senchyna M, Dimitrijevic SD: Presence and distribution of 14-3-3 proteins in human ocular surface tissues. *Mol Vis* 2008, 14:2604-2615.
33. Kobayashi R, Deavers M, Patenia R, Rice-Stitt T, Halbe J, Gallardo S, Freedman RS: 14-3-3 zeta protein secreted by tumor associated monocytes/macrophages from ascites of epithelial ovarian cancer patients. *Cancer Immunol Immunother* 2009, 58(2):247-258.
34. Baxter H, Liu W, Forster J, Aitken A, Fraser J: Immunolocalisation of 14-3-3 isoforms in normal and scrapie-infected murine brain. *Neuroscience* 2002, 109(1):5-14.

CHAPTER 3

**Investigation of isoform-specific interactions
of 14-3-3 (YWHA) proteins
with CDC25B phosphatase
in regulating mouse oocyte maturation**

Background

Within the mammalian ovary, the oocyte is held in first meiotic prophase. At puberty, oocytes in pre-ovulatory follicles resume meiosis in response to luteinizing hormone (LH). Release from meiotic arrest and production of a mature, fertilizable egg is dependent on the activation of maturation promoting factor (MPF; outlined in Figure 1), a complex of cyclin-dependent kinase 1 (CDK1) and the regulatory cyclin B1 (CCNB1) reviewed in [1]. MPF is well characterized, based on studies of amphibian and mammalian oocytes as well as somatic cells since it is the cell cycle regulatory factor for both meiotic and mitotic cells [2-4]. The phosphorylation status of CDK1 (and thus its activity) is regulated by protein kinases and phosphatases controlled by signaling molecules produced in the oocyte and surrounding somatic cells. In the arrested state of prophase I in mouse oocytes, MPF is inactive due to phosphorylation of CDK1 through the activity of WEE1/MYT family of kinases including the oocyte-specific WEE2 [5-8]. Evidence indicates that the cAMP dependent protein kinase, PKA maintains meiotic arrest in mouse oocytes by phosphorylating WEE2 (also known as WEE1B) [7]. In addition, PKA is thought to phosphorylate CDC25 proteins [9, 10], which keeps CDC25 proteins in an inactive state that preserves the phosphorylated and inactive status of CDK1.

In mouse oocytes, constitutively active heterotrimeric G protein-coupled receptors, linked to stimulatory G proteins (Gs), activate adenylyl cyclase that maintains a high concentration of cAMP and PKA activity within the oocyte [11-16]. The

concentration of cAMP is controlled by the Gs-adenylyl cyclase responsible for the generation of cAMP and also by the activity of cAMP phosphodiesterases that degrade the phosphodiester bond in cAMP to inactivate it, and thus regulate the duration and amplitude of the cAMP signal. It has been reported that oocytes deficient in phosphodiesterase 3A (PDE3A) do not degrade cAMP and thus cAMP accumulates and meiotic arrest persists [17].

Recent research indicates that the high level of cAMP in the follicle-enclosed oocyte is sustained by cGMP produced in somatic cells which passes through gap junctions and inhibits the hydrolysis of cAMP by PDE3A [18]. Luteinizing hormone (LH) is thought to interrupt the flow of inhibitory cGMP in part by rapidly and completely causing the closure of gap junctions between somatic cells in the follicle [19, 20]. With reduced cAMP levels and PKA activity, MPF is activated by reduced phosphorylation of WEE1/MYT family of kinases and the dephosphorylation of CDK1 by CDC25 proteins [21-23]. Activation of maturation promoting factor (MPF) initiates the resumption of meiosis and the process of oocyte maturation beginning with nuclear envelope breakdown (germinal vesicle breakdown) followed by formation of the first polar body and, in most mammals, arrest at metaphase of the second meiotic division, reviewed in [24, 25]. Failure of oocyte maturation has been documented in animal models and must be considered when human female infertility is examined [26]. Oocyte maturation forms the mature egg and fertilization releases the egg from metaphase II arrest, allowing formation and development of the zygote.

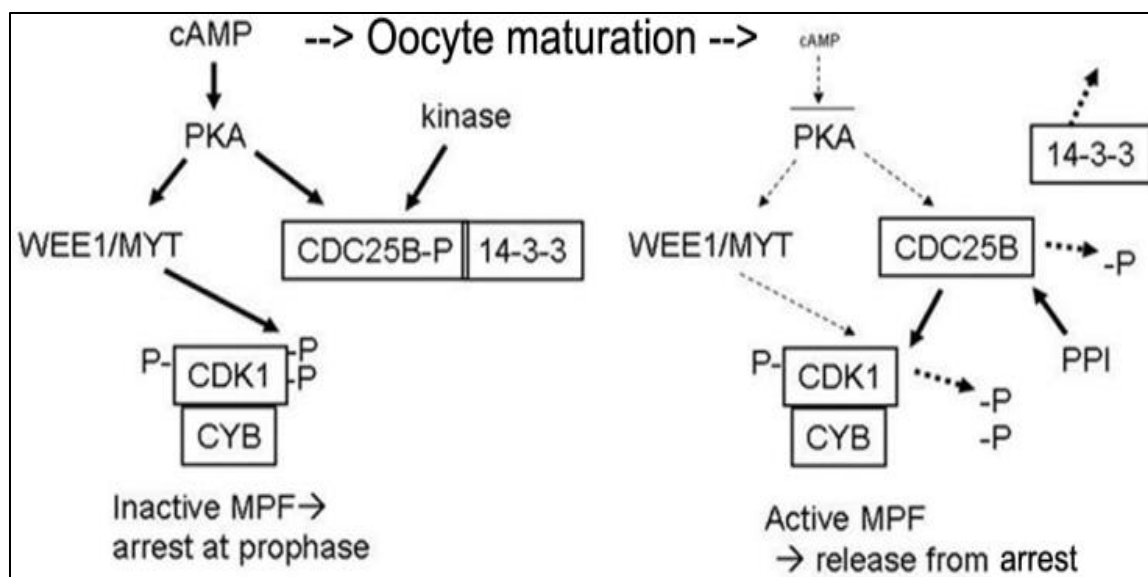


Figure 1. Simplified diagram of the key proteins involved in oocyte arrest at prophase I (left) and the release from meiotic arrest (right). In the arrested state, Mitosis Promoting Factor (MPF), composed of Cyclin-Dependent Kinase 1 (CDK1) and Cyclin B (CYB), is inactive because of phosphorylation on CDK1 (-P). The phosphatase CDC25B is phosphorylated (by PKA or perhaps another kinase dependent on PKA), bound to 14-3-3, and thereby rendered inactive. As cAMP levels fall (triggered by the pre-ovulatory surge in luteinizing hormone *in vivo* or removal of the oocyte from the ovary), CDC25B is dephosphorylated, perhaps by protein phosphatase 1 (PP1), and is released from 14-3-3. Active CDC25B then dephosphorylates CDK1. MPF becomes active and the oocyte is released from meiotic arrest. This model is based in part on studies of frog oocyte maturation.

In mouse oocytes, genetic studies have shown that CDC25B is the primary phosphatase regulating the dephosphorylation of CDK1 and not CDC25C [27, 28]

although CDC25A also appears to play a role in oocyte maturation [29]. CDC25B is inactivated by phosphorylation by PKA and probably is dephosphorylated by protein phosphatase 1 (PP1) and/or protein phosphatase 2 (PP2) reviewed in [30]. Thus, the release from meiotic arrest in the oocyte is dependent on the activation of activation of CDC25B by dephosphorylation. In addition, CDC25B is presumed to be bound to the cell cycle regulatory protein 14-3-3 (YWHA or Tyrosine 3-Monooxygenase/Tryptophan 5-Monooxygenase Activation protein) which is assumed to both maintain the phosphorylated status of CDC25 and sequester CDC25 in the oocyte cytoplasm. Previous studies show that in *Xenopus* oocytes, CDC25 phosphatase is phosphorylated by PKA, and is bound to and sequestered by 14-3-3 in the cytoplasm [31], thus preventing germinal vesicle breakdown and maturation of oocytes. A number of studies implicate 14-3-3 as a critical regulator of the cell cycle in meiotic and mitotic cells [32-39].

Proteins of the 14-3-3 (YWHA) family are now known to be central mediators in a variety of cellular signaling pathways involved in development and growth including cell cycle regulation and apoptosis [40-44]. The 14-3-3 is a highly conserved, homologous family of proteins that have been shown to bind to various cellular proteins where they have been found to complement or supplement intracellular events involving phosphorylation-dependent switching or protein-protein interaction [42, 45]. Generally (but not exclusively), 14-3-3 binds to amino acid motifs in target proteins that contain a phosphorylated serine residue and an arginine residue at positions -3 or -4 (i.e. ArgXXpSer or ArgXXXpSer, where Arg is arginine, pSer is a phosphorylated serine and X is any amino acid) [46, 47]. Most of the binding partners of 14-3-3 are phosphorylated;

however, phosphorylation-dependent sites that differ significantly from these motifs have been reported [48], and some interactions of 14-3-3 do exist independent of phosphorylation. The 14-3-3 proteins exist mainly as homo- or hetero-dimers with a monomeric molecular mass of approximately 30 kDa [40]. There are seven mammalian isoforms of 14-3-3 encoded by separate genes. We previously found that all seven mammalian isoforms of 14-3-3 are expressed in mouse ovaries, immature oocytes and mature eggs [49]. It is known that different isoforms of 14-3-3 can interact with the same ligand and so are somewhat interchangeable, however, although isoforms of 14-3-3 often bind the same protein, there are some indications that homodimers of different types or even heterodimers of 14-3-3 may have different roles in the regulation or sequestering of proteins [48, 50]. Therefore, I explored the interactions of all seven 14-3-3 isoforms with CDC25B to identify which of the 14-3-3 proteins is/are involved in regulating CDC25B and meiotic arrest in mouse oocytes.

This chapter shows the results using the *in situ* proximity ligation assay (PLA; Figure 2) along with co-immunoprecipitation experiments to examine the molecular interactions between each of the 14-3-3 isoforms and CDC25B. The PLA method has been used successfully to not only detect protein-protein interactions at the single molecule level directly in cells, but also to visualize the actual intracellular sites of the interactions in different types of cells and tissues [51-54]. In the PLA method, specific primary antibodies (raised in different species) bind to target proteins. A pair of unique oligonucleotide-conjugated secondary antibodies (PLA probes) bind to the primary antibodies and when the PLA probes are in close proximity (<40 nm), the DNA strands

are joined by enzymatic ligation. A circular DNA molecule is generated and then amplified by rolling circle amplification. The original *in situ* protein-protein interaction is revealed by the amplified DNA through hybridization of a fluorescent probe. The PLA technique is sensitive, specific, and provides a high signal to noise ratio because the signal is amplified and close proximity of the target proteins is required. Thus, the method permits detection of two proteins that interact at the molecular level.

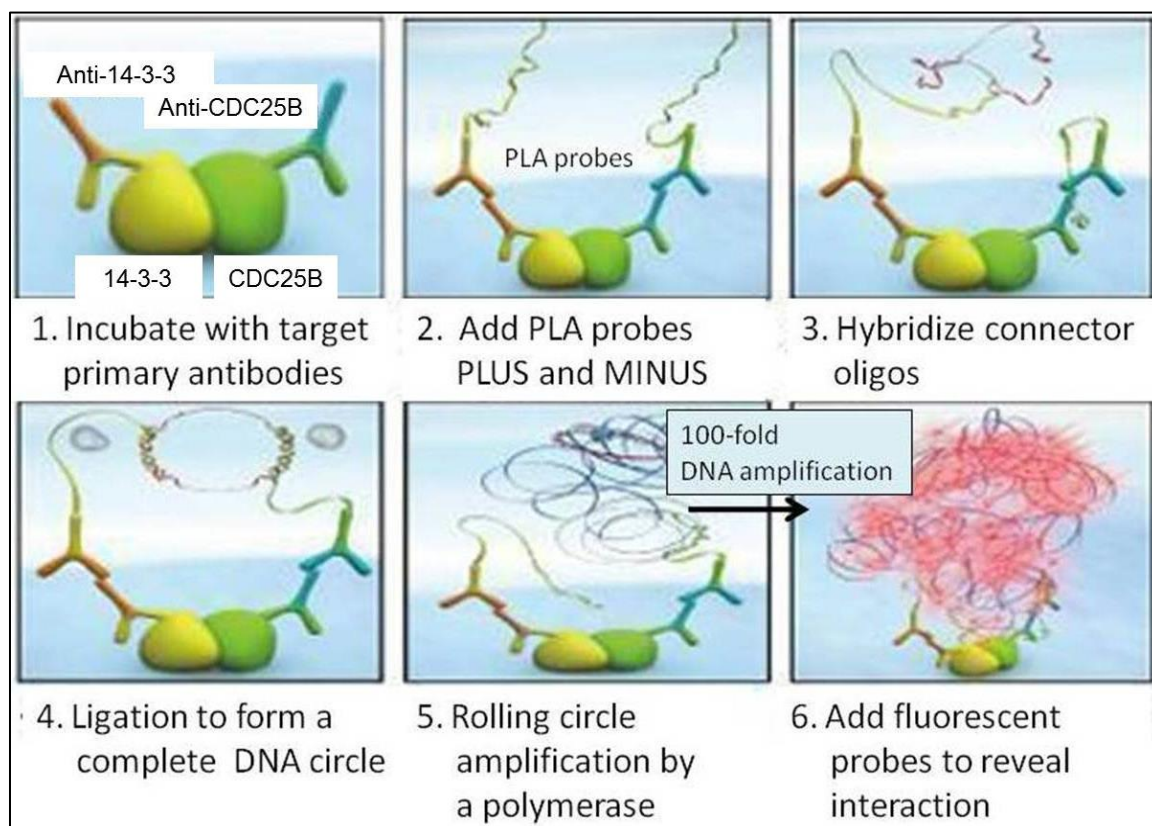


Figure 2. Schematic representation of the process of *in situ* Proximity Ligation

Assay to detect interaction between two proteins. Shown here is the method to identify the sites of interaction of 14-3-3 proteins with CDC25B phosphatase, using respective primary antibodies raised in different species. Figure courtesy: Olink Bioscience.

To investigate which of the 14-3-3 isoforms is/are central in regulating CDC25B-mediated CDK1 activation and oocyte maturation, experiments were performed to reduce the activity or expression of 14-3-3 proteins in mouse oocytes by intracellular microinjection of a translation-blocking morpholino oligonucleotide against each of the 14-3-3 isoform mRNAs. Morpholino oligomers are small sequences of synthetic nucleotides consisting of about 25 standard nucleic acid bases attached to morpholine rings (rather than ribose rings) with a phosphorodiamidate non-ionic linkage instead of a phosphodiester linkage (giving the oligonucleotide a net neutral charge). With the appropriate experimental controls [55], morpholinos have a number of advantages including specificity resistance to nucleases. Morpholinos appear to have few off-target interactions and little non-antisense activity because they are specific (binding to at least 13-14 contiguous bases) and the neutral charge gives little interaction with other RNA species or cellular proteins [56, 57]. Experiments utilizing morpholino antisense oligomers have implicated functions of a number of proteins in mouse oocyte meiotic maturation [58-67].

The experiments outlined in this report give information about the interactions of 14-3-3 isoforms with CDC25B and provide support to the model shown in Figure 1 where release from meiotic arrest with falling cAMP and reduced PKA activity results in dephosphorylation of CDC25B and its uncoupling from 14-3-3, permitting the CDC25B to activate MPF and promote oocyte maturation.

Results and Discussion

CDC25B distribution during mouse oocyte maturation

As shown by other investigators, it was observed that CDC25B translocates into and accumulates in the oocyte nucleus following release from meiotic arrest (Figure 3A-E). In these experiments CDC25B was labeled with an antibody generated in rabbit against human CDC25B, which is known to react with mouse CDC25B. Confocal imaging reveals that CDC25B is distributed throughout the prophase I-arrested oocyte cytoplasm and that some CDC25B is also present within the nucleus (Figure 3A). During the initial stage of oocyte maturation CDC25B accumulates in the nucleus and by 2 hours after release from meiotic arrest the concentration of CDC25B is much greater in the region where the germinal vesicle (nucleus) had broken down, as shown in Figure 3B-D. In all oocytes studied, at each of the time points, the identical distribution of CDC25B was noted. Minimal background staining was observed in all of three control oocytes processed simultaneously and imaged at the same confocal settings, but without the primary antibody (Figure 3E). The following experiments used an antibody raised in goat against a peptide mapping at the N-terminus of CDC25B of human origin, which reacts also with mouse CDC25B in mouse. As shown later, there is some evidence that these two antibodies label the same protein.

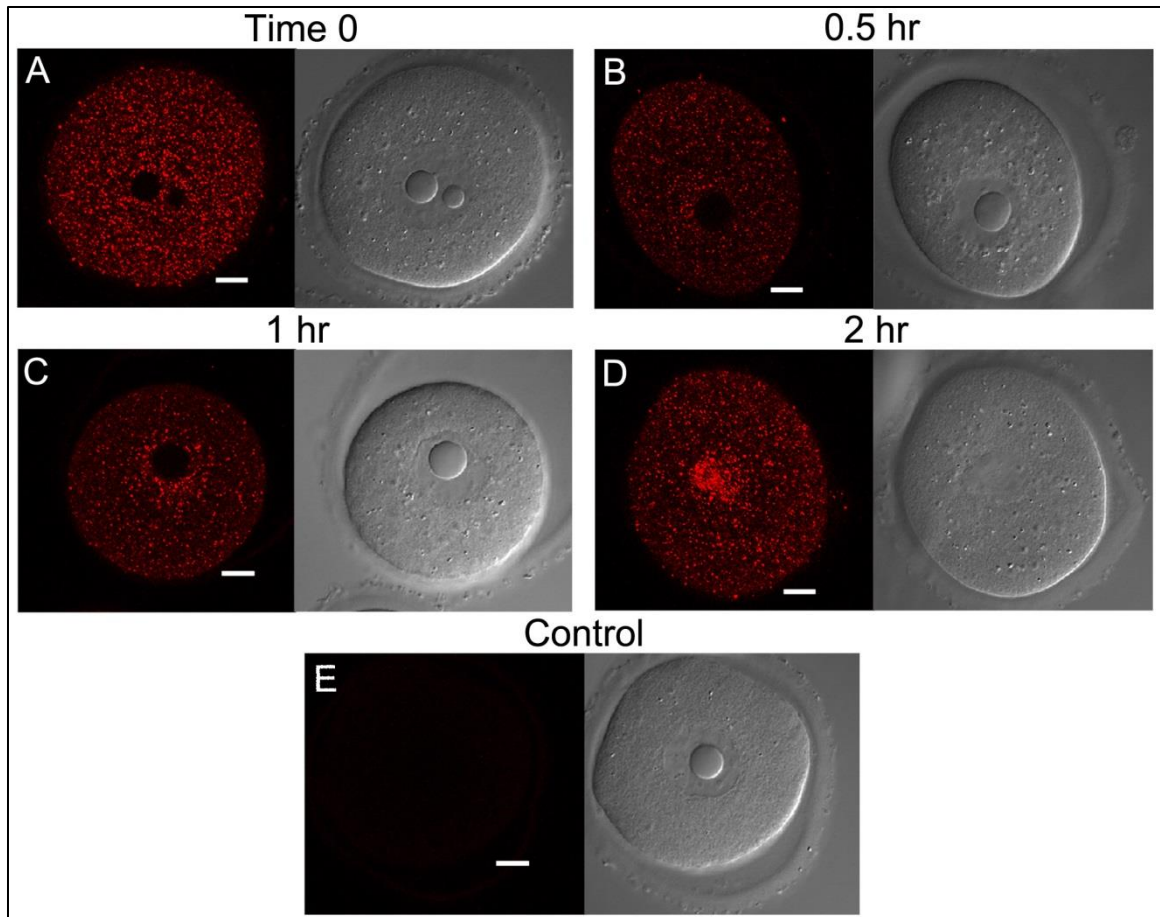


Figure 3. Representative indirect immunofluorescence images showing intracellular distribution of CDC25B during mouse oocyte maturation. Paired confocal images (A-D) of equatorial sections through oocytes (left: immunofluorescence; right: bright field) indicate gradual localization of CDC25B phosphatase into the germinal vesicle along a 2-hour time course assay during *in vitro* maturation of mouse oocytes. Control oocytes processed simultaneously in absence of the primary antibody showed minimal background fluorescence (E). Scale bars represent 10 μm .

***In Situ* Proximity Ligation Assays (PLA) reveal interactions between CDC25B and all 14-3-3 isoforms in mouse oocytes, with reduced interactions in eggs**

To determine the possible binding of each of the 14-3-3 isoforms with CDC25B, a series of *in situ* proximity ligation assays was performed to identify interactions of the two proteins at the molecular level. Following primary antibodies binding to 14-3-3 and to CDC25B, when the PLA secondary probes are in close proximity (<40 nm), as would be expected for two proteins that are interacting with each other, the oligonucleotide DNA chains cross-link with each other when hybridized with connector oligos, forming circular DNA which is amplified and detected by a fluorescent probe highlighting the reaction site as a distinct, bright fluorescent dot when viewed by fluorescence microscopy. We previously examined the 14-3-3 isoforms in oocyte and egg extracts by Western blotting after polyacrylamide gel electrophoresis and by indirect immunofluorescence as well as immunohistochemical staining of cells within ovarian sections [49]. All three approaches relied on a panel of antibodies that has been shown to be specific for the various 14-3-3 isoforms [68-70]. As shown below, the goat CDC25B antibody used in these experiments is specific as evidenced by Western blots, and by its co-localization with a rabbit CDC25B antibody (directed at a different epitope) as well as with a phospho-specific anti-mouse CDC25B antibody.

The PLA assay revealed interactions of all seven 14-3-3 protein isoforms with CDC25B within oocytes and eggs using primary antibodies directed at each of the 14-3-3 isoforms and CDC25B. Representative equatorial as well as compressed z-stack images of oocytes and eggs from PLA assays are provided in Figure 4 and Figure 5. Figure 4A-

C show representative images of the interaction of 14-3-3 β and CDC25B in a mouse oocyte. Interactions are visible in a single equatorial scan (Figure 4A). Each cell was scanned at 3 μ m intervals throughout the cell. An abundance of interaction sites is visualized when these scans are compressed to one image (Figure 4B). The typical number of interaction sites counted in these oocytes in a single experiment, range from 116 to 289, in seven different oocytes examined. It should be noted that the PLA method does not show the complete distribution of all CDC25B and 14-3-3 proteins as would be shown in conventional immunofluorescence but does show protein-protein interactions when a number of criteria have been met that include binding of the two primary antibodies, binding of secondary probes, ligation, amplification and binding of fluorescent detection probes. Each of these steps is concentration- and time- dependent. The number of fluorescent spots represents only a portion of the protein-protein interactions but this method clearly provides more information than simple co-localization studies with immunofluorescence microscopy.

Representative images of the interactions of 14-3-3 β with CDC25B in a mouse egg are shown in Figure 4D-F. The number of interaction sites is reduced in mature eggs compared to immature oocytes. In each of two independent experiments performed to detect interaction of each 14-3-3 β isoform with CDC25B, both oocytes and eggs were examined at the same time under the same conditions of reagent concentration, temperature, incubation times and imaging conditions. The average per cent *in situ* PLA sites of interaction between 14-3-3 β and CDC25B in eggs was reduced by 52% compared to those in oocytes.

Neither of six control oocytes and six control eggs treated simultaneously and under identical conditions, incubated either with no primary antibodies (Figure 4G-L), or with goat anti-CDC25B primary antibody alone, or with rabbit anti-14-3-3 β primary antibody alone, displayed any PLA reaction spot. Background fluorescence from unbound fluorescent DNA probes was minimal. To confirm the effectiveness of the PLA method by another experiment, oocytes were processed for PLA using two different antibodies to CDC25B, one made in the rabbit and the other in goat, each of which bind to CDC25B in mouse oocytes. With these two antibodies, *in situ* PLA reaction spots were detected in all of three different oocytes examined, as shown in Figure 4M-O. Detection of the PLA reaction spots clearly supports the PLA method as these two antibodies bind to the same protein which are certainly within 40 nm to support the process of secondary probe DNA ligation and amplification. In this experiment as well, all of three control oocytes processed simultaneously in the absence of primary antibodies showed no PLA reaction site and minimal background fluorescence from any unhybridized detection probe (Figure 4P-R).

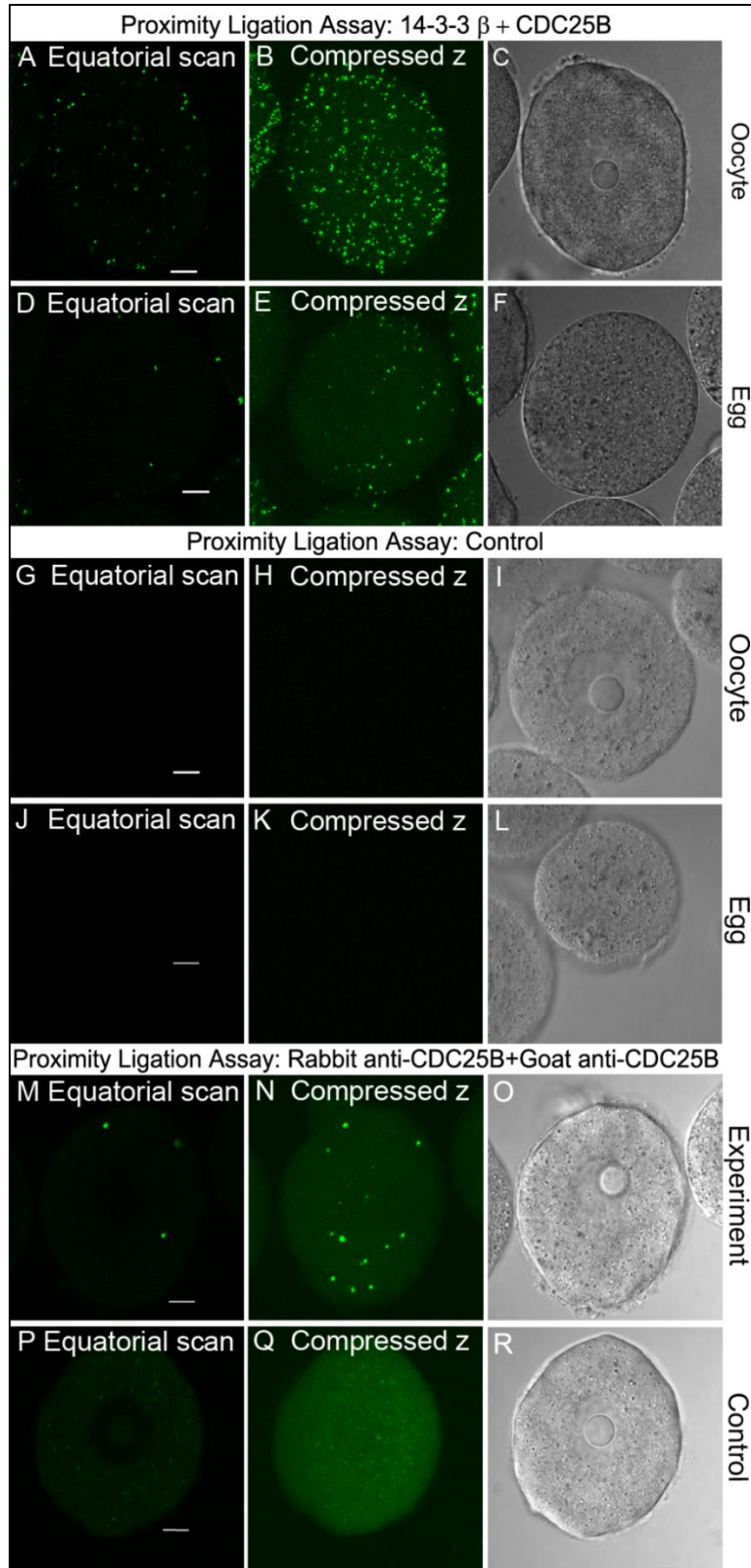


Figure 4. Representative oocytes and eggs showing PLA reaction spots for interaction of 14-3-3 β with CDC25B, compared to controls. Shown are an oocyte (A-C, G-I, M-O, P-R) and an egg (bottom panel; D-F, J-L) imaged at an equatorial plane of a single confocal scan (A, D, G, J, M, P), a compressed z stack of all confocal scans throughout the cells (B, E, H, K, N, Q) and bright field image (C, F, I, L, O, R). Bright, fluorescent PLA reaction spots indicating sites of interaction of 14-3-3 β with CDC25B were noted throughout cytoplasm and germinal vesicle of oocytes (A-C), with reduced interaction sites in eggs (D-F). No PLA reaction spot was observed in control oocytes (G-I) and control eggs (J-L) processed simultaneously in absence of primary antibodies. PLA using two primary antibodies against CDC25B detected the protein in experimental oocytes (M-O), but no PLA reaction spot was noted in control oocytes processed in absence of the primary antibodies, and background fluorescence was minimal (P-R). Scale bars represent 10 μ m.

In addition to interaction of 14-3-3 β with CDC25B as shown above, the PLA method revealed that the other six 14-3-3 isoforms also interact with CDC25B in oocytes, with reduced interactions in eggs (Figure 5).

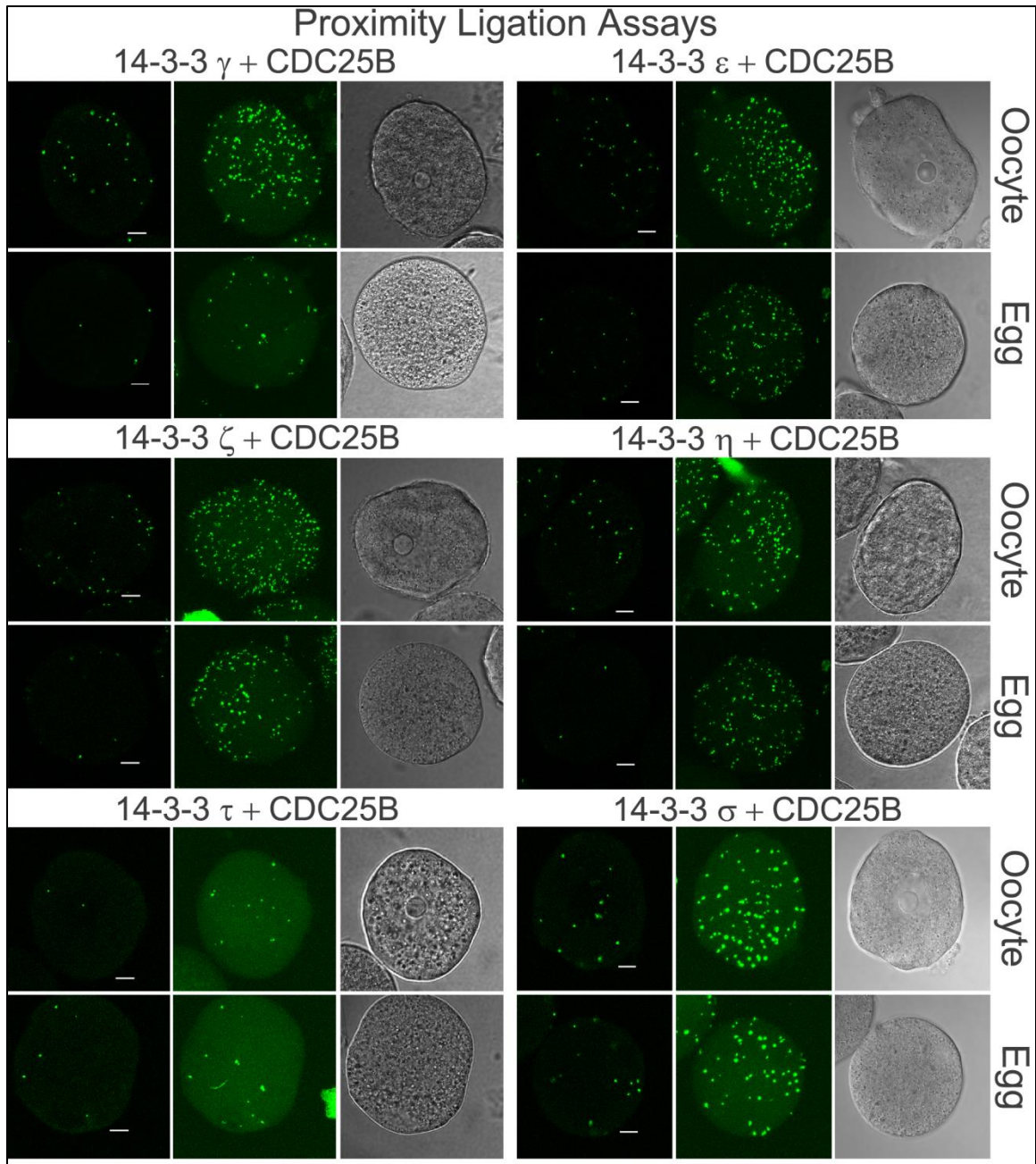


Figure 5. Representative oocytes and eggs showing PLA reaction spots for interaction of CDC25B with 14-3-3 γ , 14-3-3 ϵ , 14-3-3 ζ , 14-3-3 η , 14-3-3 τ and 14-3-3 σ . For interaction of CDC25B with each of the six 14-3-3 isoforms, shown are images of an oocyte (top panel) and an egg (bottom panel) at an equatorial plane of a single confocal

scan (left), a compressed z stack of all confocal scans throughout the cell (middle), and bright field images (right). Interactions of each of the six 14-3-3 isoforms with CDC25B were noted by bright, fluorescent PLA reaction spots throughout cytoplasm and germinal vesicle of oocytes, with reduced interactions in eggs. Scale bars represent 10 μm .

It is not possible to compare the results (the number of interaction sites, for example) among the different 14-3-3 isoforms because of differences in primary antibody binding affinities and the likely variations in the amounts of PLA reagents used between experiments despite using the same protocol; however again, interactions of all isoforms of 14-3-3 with CDC25B appear to be reduced in eggs compared to oocytes, as eggs and oocytes were processed at the same time. The reduction in the average number of *in situ* PLA sites of interaction of 14-3-3 isoforms with CDC25B in eggs compared to oocytes, ranged from 12% for 14-3-3 τ to 78% for 14-3-3 γ as shown in Figure 6.

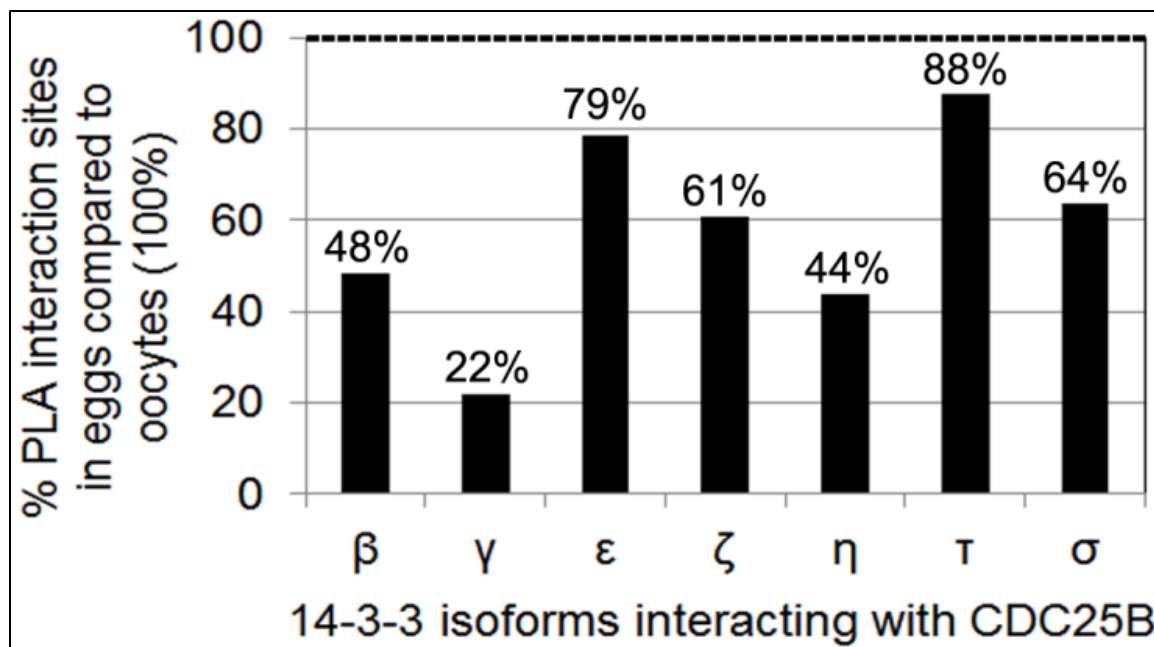


Figure 6. Per cent PLA sites of interaction of seven mammalian 14-3-3 isoforms with CDC25B in mouse eggs compared to oocytes. For interaction of CDC25B with each 14-3-3 isoform, the average number of PLA spots counted in all oocytes examined, was considered 100% (dashed line), relative to which the average number of PLA spots in eggs was represented as a per cent, mentioned on top of the corresponding bar. As shown, the interactions of all 14-3-3 isoforms with CDC25B were found to decrease during maturation of oocytes into eggs.

Co-immunoprecipitation studies indicate interaction of all 14-3-3 isoforms with CDC25B in mouse ovaries and oocytes, with reduced interactions in eggs

CDC25B was successfully pulled down by goat anti-CDC25B antibody from protein extracts of ovaries, oocytes as well as eggs of adult mice (Figure 7A). Protein extract from ovary was used as a positive control (Figure 7A, lane 1). In this whole

ovarian extract, two forms of CDC25B are apparent: one band at about 72 kDa and one band at about 45 kDa. A negative control using normal rabbit serum showed only heavy and light chain of the antibodies, indicating no non-specific protein bound to the beads (Figure 7A lane 2). CDC25B was identified as a 72 kDa band immunoprecipitated from ovarian extracts (Figure 7A lane 3) as well as oocytes (Figure 7A lane 4). In eggs, a 72 kDa band corresponding to CDC25B was not detected. We suspect (as shown in the next section) that CDC25B is present at smaller molecular weight (45 kDa) as a dephosphorylated protein and is masked by the thick band for the antibody heavy chain (50 kDa) (Figure 7A lane 5).

To determine which of the 14-3-3 isoforms might be co-immunoprecipitated with CDC25B, the Western blot membrane was stripped and first re-probed with anti-14-3-3 β (Figure 7B) and then the membrane was stripped and re-probed with the other rabbit anti-14-3-3 isoform-specific antibodies one at a time after stripping off the previously bound antibodies. After each isoform probe, the blot was completely stripped and tested for the presence of residual primary antibody previously bound. At each step, stripping the membrane and incubation in secondary antibody alone displayed no band, confirming complete removal of previously bound antibodies (Figure 7B) at the expected 14-3-3 molecular weight of around 30 kDa, except for 14-3-3 σ . It was previously found that the anti-14-3-3 σ primary antibody does not appear to detect 14-3-3 σ by Western blotting due to possible unsuitability of the antibody used in recognizing a denatured antigen (though the antibody is effective in fixed cells using immunofluorescence [49]). Again, it is not possible to compare the protein amounts for the different isoforms as the isoform-specific

antibodies have different affinities and therefore may exhibit different intensities on a Western blot; however, the co-immunoprecipitation experiment revealed 14-3-3 bands with lesser intensity in eggs as compared to oocytes, for all of the six 14-3-3 isoforms. At the end of the series of re-probing the same membrane for six other isoforms, a prominent band was detected with the same 14-3-3 β antibody (Figure 7C), confirming no significant loss of proteins by repeated membrane stripping.

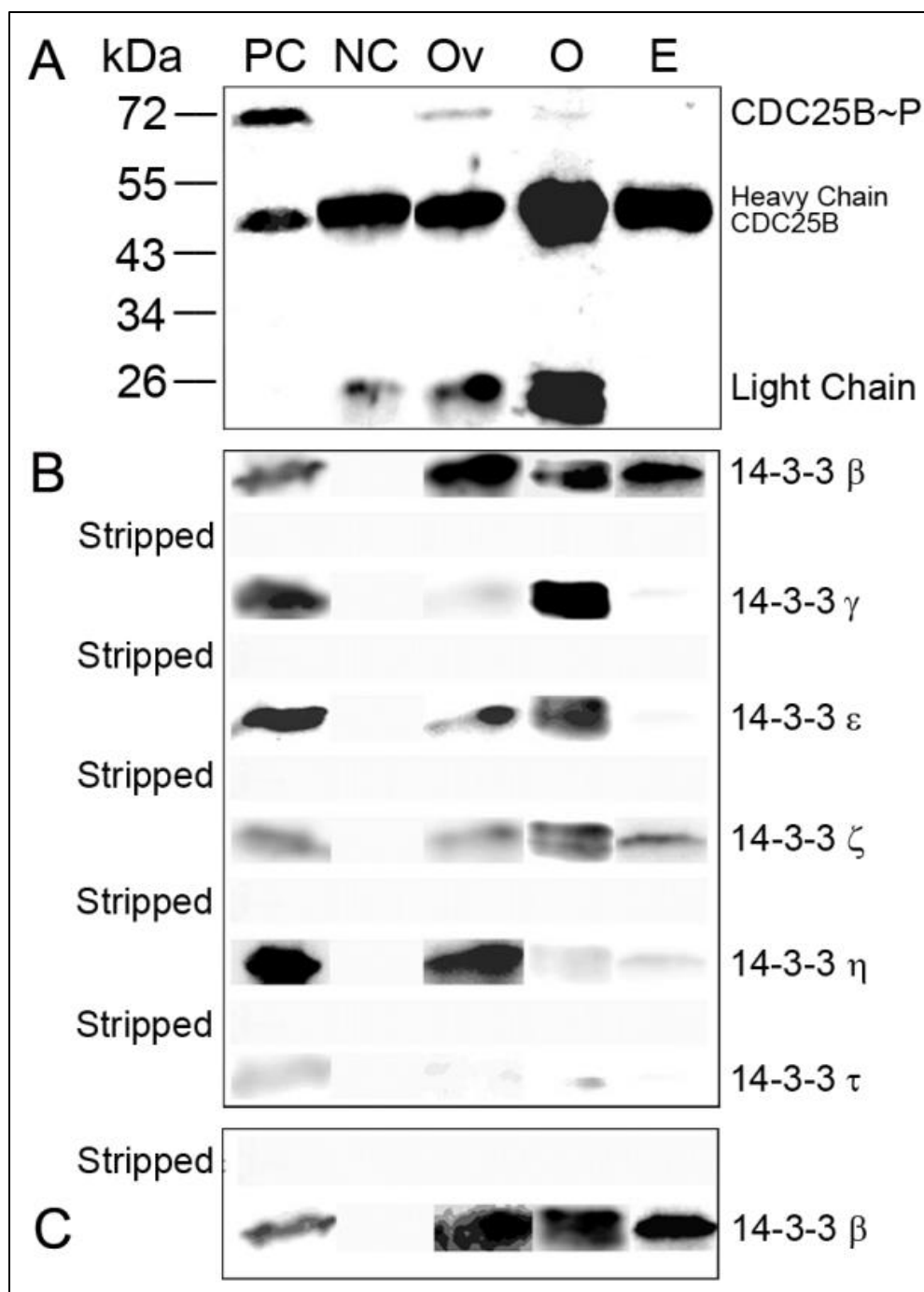


Figure 7. Co-immunoprecipitation of 14-3-3 isoforms with CDC25B phosphatase.

CDC25B was immunoprecipitated from extracts of ovaries, oocytes and eggs (A).

Phosphorylated CDC25B was observed to be pulled down from lysates of ovaries and

oocytes (A), dephosphorylated CDC25B in eggs possibly being masked by the thick band for the antibody's heavy chain. This was followed by repeatedly stripping the blot off the previously bound antibodies and reprobing with each 14-3-3 isoform-specific antibody except 14-3-3 sigma (B). All isoforms of 14-3-3 appear to co-immunoprecipitate with CDC25B in ovaries and oocytes detected by prominent bands, with reduced band intensities in eggs (B). In the end, the blot was reprobbed again for 14-3-3 β to confirm minimal loss of proteins by repeated membrane stripping (C). Ovary lysate was used as positive control (PC) and normal rabbit serum was used as negative control (NC).

The co-immunoprecipitation results indicate that six of the seven mammalian 14-3-3 isoforms are co-immunoprecipitated with CDC25B. Thus, the co-immunoprecipitation experiment confirms the PLA results indicating that all isoforms of 14-3-3 interact with CDC25B in oocytes and to some extent in eggs.

Using *In Situ* Proximity Ligation Assays, it is demonstrated for the first time that all seven mammalian isoforms of 14-3-3 interact with CDC25B in adult mouse oocytes and eggs. Lesser percentages of *In Situ* PLA sites for interactions of CDC25B with all isoforms of 14-3-3 were found in eggs as compared to oocytes. Co-immunoprecipitation studies also showed interaction of six 14-3-3 isoforms with CDC25B in mouse oocytes and eggs, with reduced interactions for all 14-3-3 isoforms in eggs as compared to oocytes.

CDC25B and its phosphorylation in mouse oocytes and eggs

The 14-3-3 proteins are known to generally bind to phosphorylated proteins. Therefore I explored, in part, the phosphorylation status of CDC25B to begin work on the nature of 14-3-3 binding. While comparing extracts of oocytes and eggs, a 72 kDa band was detected in oocytes but not in eggs, by Western blotting (Figure 8). However, a 45 kDa band was observed in eggs. To further explore the difference in molecular weights of CDC25B in oocytes and eggs, extracts of oocytes and eggs were treated with the bacteriophage λ protein phosphatase to dephosphorylate serine, threonine and tyrosine residues in all proteins. A 45 kDa band was found in the λ protein phosphatase-treated oocyte extract. This band at 45kDa matches the band found in untreated or λ phosphatase-treated egg extracts. This suggests a clear and dramatic dephosphorylation of the CDC25B in eggs at multiple sites.

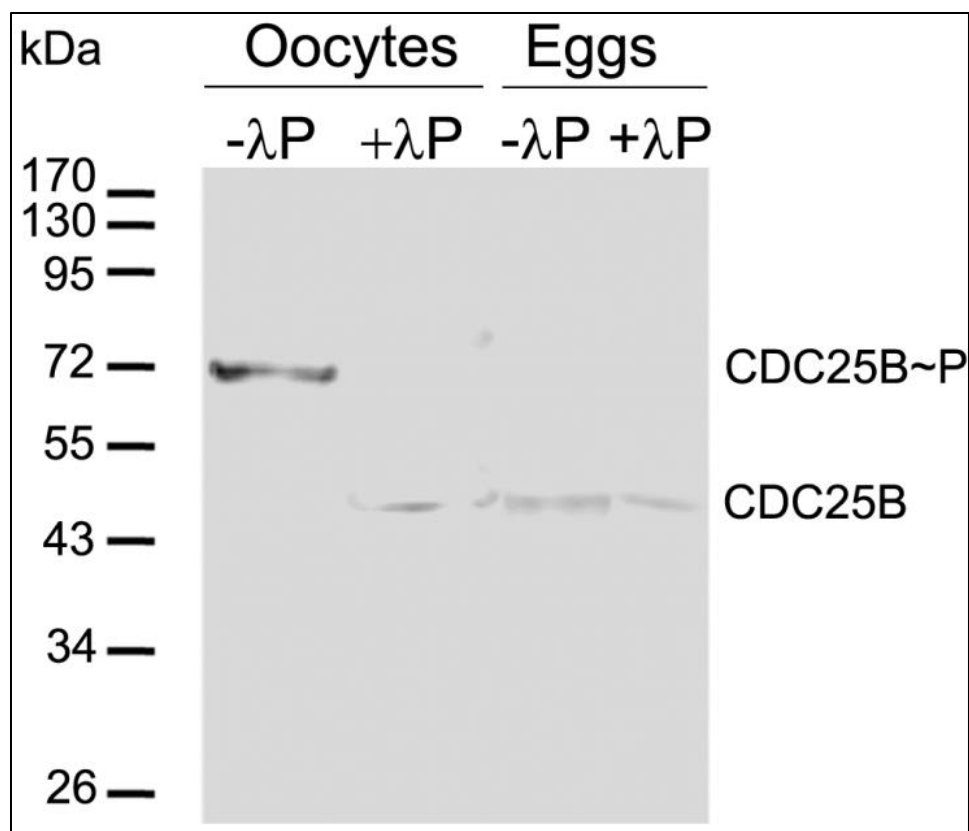


Figure 8. Western blot detecting CDC25B phosphorylation in oocytes versus eggs by λ -phosphatase treatment. CDC25B is phosphorylated in oocytes (72 kDa band; lane 1) and dephosphorylated in eggs (45 kDa band; lane 3). Treatment with λ -phosphatase results in dephosphorylation of the protein in oocytes (45 kDa band; lane 2), and remains dephosphorylated in eggs (45 kDa band; lane 4).

CDC25B phosphorylation status in mouse oocytes and eggs at Ser-149

Previous research has shown that mouse CDC25B can be phosphorylated at Ser-321 by PKA in oocytes [9] and in fertilized eggs [71]. Ser-149 was recently reported to be a second site of phosphorylation on CDC25B in fertilized mouse eggs (zygotes) [72].

While the PKA-dependent phosphorylation of CDC25B in mouse oocytes and fertilized eggs at Ser-321 is fairly well characterized [9, 71], PKA-dependent phosphorylation of CDC25B phosphorylation at Ser-149 is also of interest but has not been examined in oocytes. The Ser-321 residue of CDC25B has been identified as a direct target of PKA in prophase I-arrested oocytes, and phosphorylation at this site results in inhibition of CDC25B and its sequestration by the 14-3-3 protein [10]. Protein 14-3-3 ϵ has been reported to interact with phospho-Ser321-CDC25B, to maintain the prophase I arrest of the mouse oocyte [73]. However, the role of CDC25B phosphorylation at Ser-149 has not yet been investigated in relation to maintenance of prophase I arrest in mouse oocytes. In this project, this phosphorylation in oocytes and unfertilized eggs was examined through Western blotting, immunofluorescence and the PLA method.

A single band at 72 kDa was detected in mouse oocytes with a rabbit anti-phospho-Ser149 antibody; while no bands could be detected in eggs (Figure 9). In immunofluorescence experiments, phosphorylation of CDC25B at Ser-149 was detected abundantly in cytoplasm of oocytes compared to the corresponding germinal vesicles (Figure 9A) but appeared to be reduced in eggs (Figure 9C). To provide some additional evidence for the presence and potential role of Ser149-phosphorylated CDC25B in mouse oocytes an *in situ* proximity ligation assay was conducted using two antibodies, both directed at CDC25B. In this case the interactions of different proteins were not examined; instead, different antibody epitopes on the same protein were utilized. This PLA assay utilized the goat anti-CDC25B and the rabbit anti-phospho-Ser149-CDC25B which binds to the same protein if it is phosphorylated at Ser-149. Prominent PLA

reaction spots were observed throughout all mouse oocytes examined, indicating clearly that CDC25B in oocytes is phosphorylated at Ser-149 (Figure 9G-H). Eight oocytes and eight eggs were studied for the experiment, and fewer reaction sites were identified in eggs compared to oocytes (Figure 9J-K). A 35.5% reduction in the number of PLA interaction sites was observed in eggs compared to oocytes, suggesting some dephosphorylation of CDC25B at Ser-149 during oocyte maturation. Although we have not further quantified this change, the results agree with the reduction of phosphorylated CDC25B as evidenced by Western blotting and immunocytochemistry, which suggest that CDC25B is dephosphorylated in eggs. Such a Western blot may not be sensitive enough to detect any residual phosphorylation that can be observed at the molecular level with the much more sensitive PLA method. All of three control oocytes as well as three control eggs treated simultaneously in absence of primary antibodies, showed no PLA reaction spot (Figure 9M-N and P-Q).

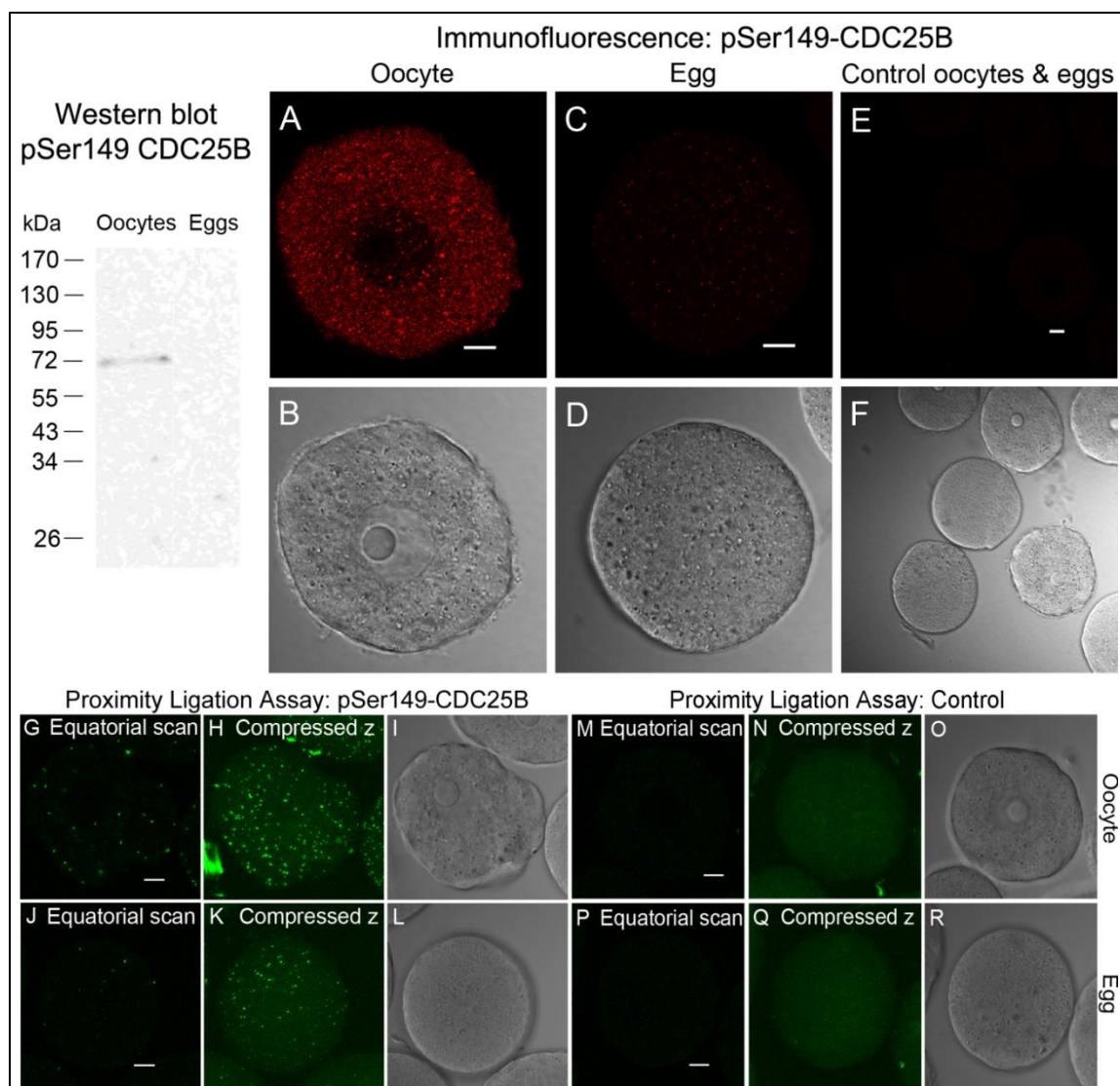


Figure 9. CDC25B is phosphorylated at Ser149 in oocytes, and the phosphorylation is reduced in eggs. Shown on top left is a Western blot detecting phosphoSer149-CDC25B in oocytes but not in eggs. A representative oocyte (A: fluorescence; B: bright field) and a representative egg (C: fluorescence; D: bright field) show immunocytochemistry detecting greater phosphorylation of CDC25B at Ser149 in cytoplasm compared to germinal vesicle of oocytes (A), with reduced phosphorylation in eggs (C). Minimal background staining was noted in control oocytes and eggs processed

simultaneously in absence of the primary antibody (E). Bright, fluorescent PLA reaction spots indicating sites of phosphorylation of CDC25B at Ser-149 were noted in oocytes (G-I), with reduced number of the PLA spots in eggs (J-L). Shown are representative images at an equatorial plane of a single confocal scan (G, J), a compressed z stack of all confocal scans throughout the cell (H, K), and bright field images (I, L). No PLA reaction spot was noted in control oocytes (M-O) and control eggs (P-R) processed simultaneously in absence of primary antibodies. Scale bars represent 10 μm .

The PLA method is highly sensitive and can identify molecular interactions that are below the limit of detection by Western blotting, evident from the Western blot in figure 9 and the PLA data in figure 9H, K. Phosphorylated CDC25B was detected in adult mouse oocytes along with the likely dephosphorylated form of the protein in eggs, by λ -phosphatase treatment and Western blotting, evident from Figure 8. The data correlates with the previously reported result [10] that during maturation of the mouse oocyte by germinal vesicle breakdown, CDC25B translocates and accumulates in the germinal vesicle, inferred from Figure 3.

Microinjection of the 14-3-3-inhibitory peptide R18 and antisense morpholino against 14-3-3 η mRNA induces significant maturation of mouse oocytes

As mentioned before, mouse oocytes are held in prophase I meiotic arrest in the ovary by elevated cAMP (maintained by adenylyl cyclase activity and reduced cAMP phosphodiesterase activity) that sustains PKA activity to activate Wee2 kinase and

inactivate CDC25B, thus keeping CDK1 inactive and maintaining meiotic arrest. Central to this mechanism for meiotic arrest may be the requirement that CDC25B is phosphorylated and that, phosphorylated CDC25B is held in an inactive state by being bound to 14-3-3 proteins. Indeed, evidence from a variety of experiments indicates that a primary role for 14-3-3 proteins may be to sequester and preserve the phosphorylated status of proteins in many cellular processes. Therefore, to demonstrate directly in mouse oocytes that 14-3-3/CDC25B interaction is required for meiotic arrest, a series of experiments was conducted to disrupt the interaction, with the hypothesis that preventing the interaction of CDC25B with 14-3-3 proteins would lead to oocyte maturation, once the CDC25B becomes free to dephosphorylate CDK1, thereby activating MPF.

It is well known that elevated cAMP levels within the oocyte maintains prophase arrest and that, oocytes spontaneously resume meiosis and mature as the cAMP concentration falls when oocytes are removed from the ovarian follicle [17, 74-76]. Maintenance of meiotic arrest in isolated oocytes can be achieved by agents that activate adenylyl cyclase or by application of membrane-permeable cAMP analogs including dibutyryl-cAMP (dbcAMP) [77].

Typically, a concentration of 0.1 mg/mL dbcAMP in the oocyte collection medium is sufficient to maintain meiotic arrest in isolated mouse oocytes. For experiments involving microinjection of R18 or antisense morpholinos against the 14-3-3 isoforms, the threshold or critical concentration of dbcAMP, which is just sufficient to maintain prophase I arrest in at least 75% of oocytes cultured overnight, was determined to be 0.05 mg/mL. Oocyte maturation experiments in this concentration of dbcAMP

permitted us to examine treatments that could promote maturation compared to control cells in which meiotic arrest is maintained, but not dominated by the activation of PKA by dbcAMP.

In a preliminary experiment to examine 14-3-3 protein function, mouse oocytes were microinjected with the synthetic 14-3-3-inhibitory peptide R18. Microinjection of 0.5 $\mu\text{g}/\mu\text{L}$ (final intracellular concentration) of R18 into oocytes, followed by overnight incubation in media containing 0.05 mg/mL dibutyryl cAMP, promoted release from meiotic arrest and GVBD in a larger number of cells compared to uninjected control oocytes or control oocytes injected with deionized water. Ten of 15 (67%) of oocytes underwent GVBD following R-18 injection while only 4/16 (25%) did so when injected with deionized water and only 5 of 18 (28%) control uninjected oocytes (Figures 10A and 11). Statistical analysis of 2X2 contingency tables using Fisher's exact test indicated a significant difference in per cent GVBD among the experimental and control groups of cells. Pairwise comparison of the percentage of GVBD in the uninjected cells and those injected with water revealed no significance difference. Pairwise comparison of the R18 injected and the control water-injected cells revealed a significant difference ($P < 0.05$). The effectiveness of R-18 inhibition is certainly concentration-dependent; however the injection of a more concentrated peptide solution was not possible. In addition, of course, some CDC25B may still be held phosphorylated by residual PKA kept active by the 0.05mg/mL dibutyryl cAMP. Nevertheless, the experiment suggests that inhibiting some interactions of 14-3-3 with its binding partners, here including CDC25B, shifts the balance between phosphorylated and unphosphorylated forms of CDC25B. This may be

true in part, perhaps because some CDC25B is no longer sequestered by 14-3-3 and is likely dephosphorylated, even in the presence of some PKA activity. To further investigate this possibility, the more specific approach of reducing 14-3-3 protein rather than inhibiting its action, was chosen. This would also help to identify which of the 14-3-3 isoforms might be primarily responsible for binding to CDC25B and preventing oocyte maturation.

In a series of experiments for each 14-3-3 isoform, while in prophase I arrest, GV-intact oocytes were microinjected with a translation-blocking morpholino oligonucleotide against each of the 14-3-3 isoforms at a final intracellular concentration of 0.1 mM. The oocytes were held for 24 hours in prophase arrest with media containing 0.1 mg/mL dbAMP to permit a reduction of the existing 14-3-3 protein isoform. The oocytes were then transferred to 0.05 mg/mL dbcAMP and incubated for 13-14 hours, stained with Hoechst and then examined for GVBD.

A high percentage (70%) of oocytes injected with MO against 14-3-3 η were found to have undergone GVBD, in contrast with oocytes injected with MOs targeting other 14-3-3 isoforms (Figures 10B and 12). Under these conditions in this series of experiments, GVBD in control uninjected oocytes was about 7.5% and only about 5% for oocytes injected with a standard, nonsense morpholino oligonucleotide incapable of binding to any of the 14-3-3 mRNAs. Statistical analysis of 2x2 contingency tables using Fisher's exact test indicated no significance difference between GVBD in the uninjected cells and in cells injected with the standard, nonsense morpholino. Pairwise comparison of each of the 14-3-3 isoform morpholino injection conditions with the nonsense

morpholino control revealed no significant difference between the control and the experimental group, with the exception of 14-3-3 η (two-tailed P value of less than 0.0001).

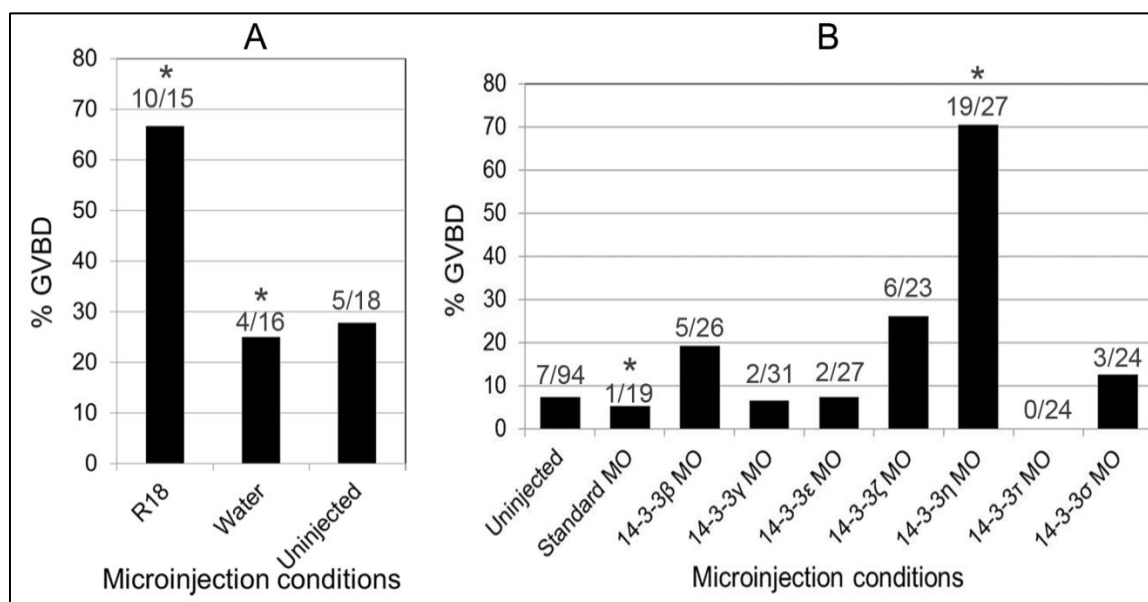


Figure 10. The 14-3-3 proteins, specifically 14-3-3 η , is required for maintaining prophase I arrest of oocytes. Shown are per cent germinal vesicle breakdown (GVBD) following *in vitro* maturation of mouse oocytes microinjected with the 14-3-3-inhibitory peptide R18 (A) and antisense morpholinos against each of the seven mammalian 14-3-3 isoforms (B). At each injection condition, the number of cells with GVBD was represented as a per cent of the total number of cells studied, mentioned on top the corresponding bar. A significantly greater percentage of GVBD was noted for oocytes injected with R18 compared to control (* in A), as well as for oocytes injected with the morpholino targeting 14-3-3 η mRNA compared to control (* in B).

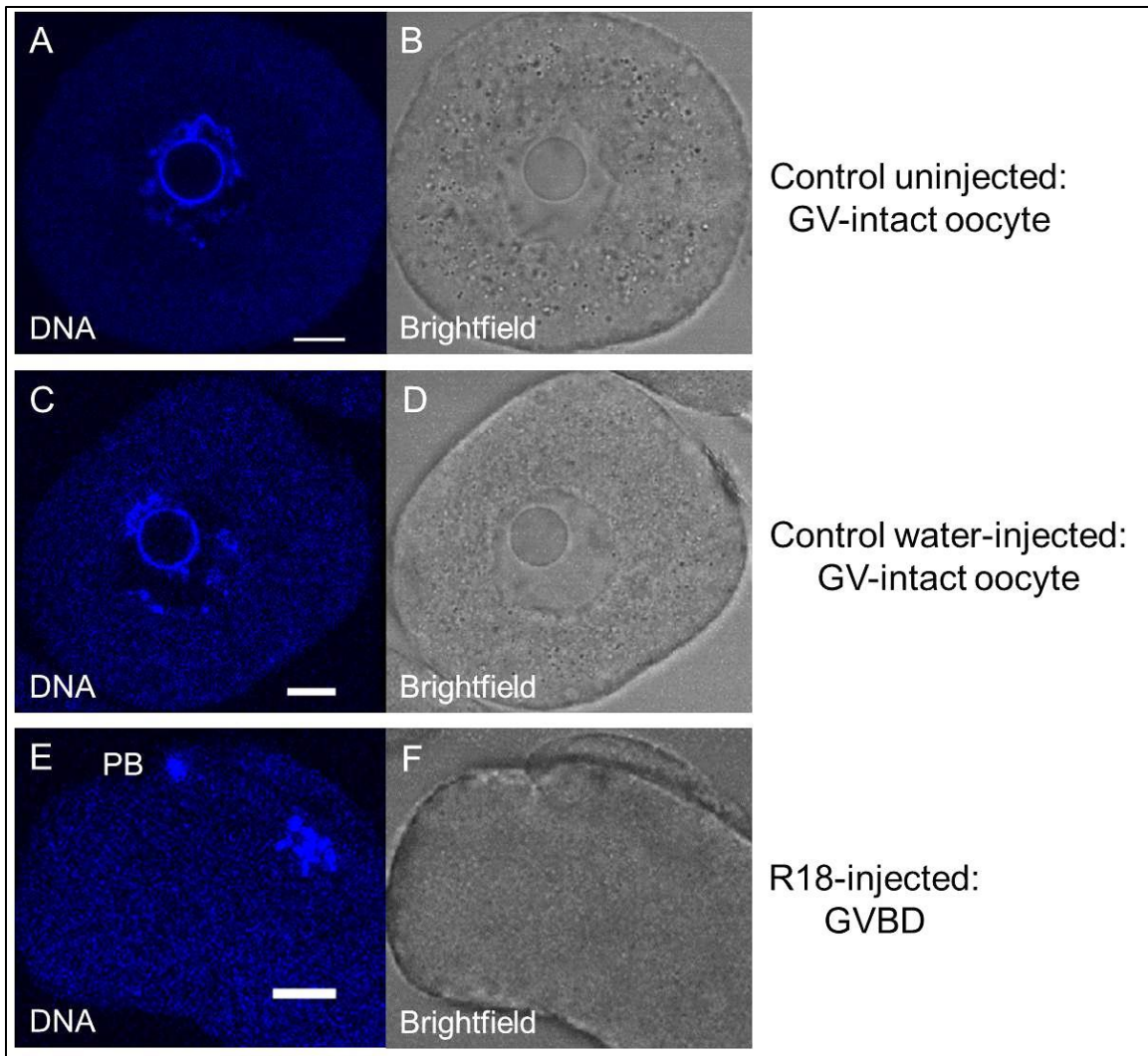


Figure 11. Representative mouse oocytes showing maturation-promoting effect of 14-3-3-inhibitory peptide R18, compared to controls. Intact germinal vesicle (GV) was noted in control uninjected oocytes (A, B) as well as water-injected oocytes (C, D). In contrast, germinal vesicle breakdown (GVBD) was observed along with condensed metaphase chromosomes and first polar body formation from oocytes microinjected with R18 (E, F). DNA was stained blue with Hoechst. PB: First polar body. Scale bars represent 10 μm .

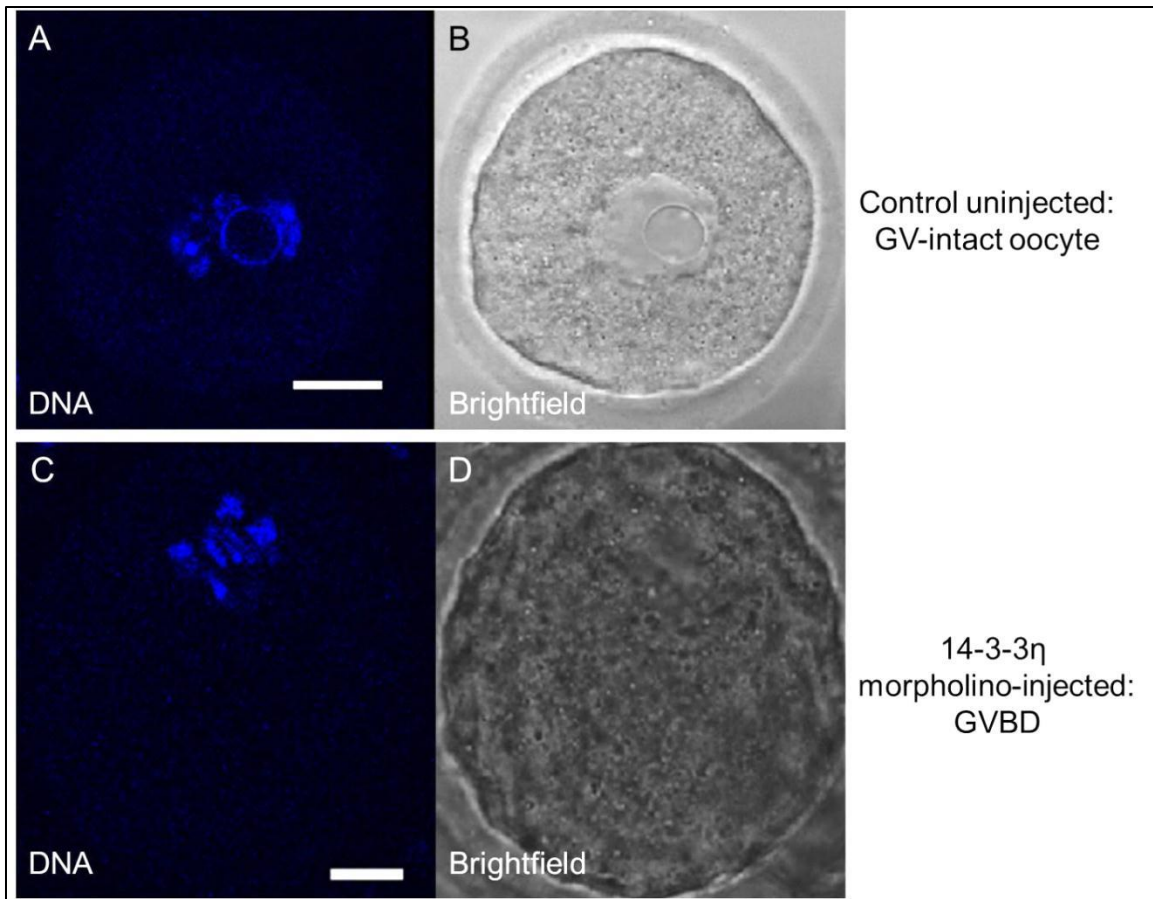


Figure 12. Representative mouse oocytes showing maturation-promoting effect of antisense morpholino against 14-3-3 η , compared to control. Intact germinal vesicle (GV) was noted in control oocytes (A, B). In contrast, germinal vesicle breakdown (GVBD) was observed along with condensed metaphase chromosomes in oocytes microinjected with a translation-blocking morpholino oligonucleotide targeting 14-3-3 η (C, D). DNA was stained blue with Hoechst. Scale bars represent 10 μ m.

These results suggest that among the seven mammalian isoforms of 14-3-3 proteins, all of which were found to bind to CDC25B in mouse oocytes and eggs to

varying extents, 14-3-3 η is functionally important for maintaining the prophase I arrest of mouse oocytes. Reduction of 14-3-3 η protein by morpholino-mediated knockdown of 14-3-3 η protein synthesis is likely to provide fewer binding sites for CDC25B that would maintain it in the inactive state tipping that balance, at least in some cells, to favor the activation of MPF even in presence of residual PKA activity associated with the 0.05 mg/mL dibutyl cAMP in which the MO-injected oocytes were incubated overnight.

The R18 peptide shares a common binding site on 14-3-3 with other 14-3-3 binding partners and peptide R18 competes with 14-3-3 binding partners [78]; thus R18 can displace proteins bound to 14-3-3. The interaction of R18 does not depend on the 14-3-3 isoform and the peptide does not require prior phosphorylation for binding. The utility of the R18 peptide has been demonstrated, for example, to show that 14-3-3 is a critical regulator of anti-apoptotic signaling in various cells [79, 80], including cultured ovarian granulosa cells [81]. Introduction of R18 message in frog eggs produced defects in axial patterning and mesoderm specification [82]. Microinjection of oocytes with the 14-3-3-inhibitory peptide R18 showed about 40% greater maturation compared to uninjected control oocytes or control oocytes injected with sterile, deionized water. Microinjection of GV-intact mouse oocytes with a translation-blocking MO against 14-3-3 η , followed by *in vitro* maturation, showed a majority of oocytes to undergo maturation, unlike oocytes injected with MOs against other 14-3-3 isoforms. This suggests that 14-3-3 η is essential for maintaining meiotic arrest of mouse oocytes.

Dephosphorylation of one or more phosphorylation sites on CDC25B might activate the protein to cause GVBD during mouse oocyte maturation. In mouse oocytes,

the specific 14-3-3 isoform, namely 14-3-3 η , whose knockdown appears to activate GVBD, may be bound to CDC25B phosphorylated at a site different from the site(s) at which CDC25B is phosphorylated and bound to other 14-3-3 isoforms. As reported in chapter 4, by morpholino-mediated knockdown method it was found that the same isoform of 14-3-3 protein, namely 14-3-3 η , is essential for normal meiotic spindle formation during mouse oocyte maturation by interacting with α -tubulin, in part, to regulate the assembly of microtubules [54]. Thus, 14-3-3 η appears to play a key role in not only maintaining the prophase I arrest of mouse oocytes, but also in the regulation of meiotic spindle assembly during maturation of the oocyte.

Materials and Methods

Collection of Oocytes and Eggs and Preparation of Ovarian Tissue Extract

All mice used in the present experiments were housed and used at Kent State University under an approved Institutional Animal Care and Use Committee protocol following the National Research Council's publication Guide for the Care and Use of Laboratory Animals. To obtain oocytes, CF1 mice (2.5 months old) were injected with 7.5 IU eCG and, 44-48 hours later, the ovaries were removed and repeatedly punctured with a 26-gauge needle to rupture follicles. Cumulus cell-enclosed oocytes were isolated and the cumulus cells were removed by repeated pipetting through a small-bore pipette. Fully-grown oocytes with intact nuclei (germinal vesicles) were cultured in MEM α

containing 0.1 mg/ml dibutyryl cAMP to prevent spontaneous oocyte maturation. Mature, metaphase II-arrested eggs were obtained from mice 13-14 hours following superovulation by injection of 7.5 IU hCG which was preceded by a priming injection of 7.5 IU eCG injection 48 hrs earlier. The cumulus cells were removed with 0.3 mg/ml hyaluronidase. *Zonae pellucidae* from oocytes and eggs thus collected were removed by a brief treatment in acid Tyrode's solution (0.14 M NaCl, 3 mM KCl, 1.6 mM CaCl₂·2H₂O, 0.5 mM MgCl₂·6H₂O, 5.5 mM glucose, and 0.1% PVA, pH 2.5). Cells were then used for Western blot, immunofluorescence studies, Duolink *In Situ* Proximity Ligation Assays or co-immunoprecipitation studies as described below. For Western blotting and co-immunoprecipitation experiments, cells collected as above were rinsed in MEM α , counted, and transferred to Tris-buffered saline (TBS; 150 mM NaCl, 25 mM Tris-HCl, pH 7.5) containing 0.1% PVA and the transferred in a small volume to a microcentrifuge tube, lysis buffer was added, and the cell lysates were quick-frozen in ethanol/dry ice and stored at -70°C until use. The lysis buffer contained 10 mM Tris-HCl at pH 7.2, 1 mM EDTA, 1 mM EGTA, 0.1% (v/v) β -mercaptoethanol, 1% (v/v) Triton X-100, protease inhibitors (1 mM PMSF, 0.1 mM TPCK), and phosphatase inhibitors (1 mM Na₃VO₄, 50 mM NaF, 10 mM β -glycerophosphate and 5 mM sodium pyrophosphate).

Ovaries from unprimed adult mice (2.5 months old) were homogenized in a buffer containing (10 mM Tris pH 7.0, 1 mM EDTA, 1 mM EGTA, 0.16% benzamidine hydrochloride, 14 mM β -mercaptoethanol, 1 mM PMSF and 0.1 mM TPCK) pH 7.2, using a mechanical homogenizer. The homogenized cell lysates were then centrifuged at

16,000 g for 30 minutes and the supernatants containing the total soluble protein extracts were used for Western blotting or co-immunoprecipitation studies.

Immunofluorescence

To examine the initial stages of oocyte maturation, oocytes were isolated in MEM containing 0.1 mg/mL dbcAMP and examined by confocal immunofluorescence microscopy using a rabbit anti-CDC25B. Cells were fixed immediately in 3.7% formaldehyde (Time 0; 7 cells), or fixed at 30 minutes (12 cells), 1 hour (8 cells) and 2 hours (6 cells) after transfer to MEM α containing no dbcAMP. After fixation, the oocytes and eggs were washed in PBS-PVA (PBS containing 1% PVA), permeabilized with 1% TritonX-100 to promote antibody penetration, washed in PBS-PVA, treated with blocking buffer (5% normal donkey serum) and incubated overnight with primary antibody. Following washing in blocking buffer (1% donkey serum), the cells were incubated with appropriate secondary antibody for several hours, washed again, and individually imaged with the Olympus Fluoview FV500 confocal microscopy system using a 60X oil immersion lens and various confocal zooms; the scale bars on the images indicate the final magnification. Images were captured and examined at multiple confocal planes. The representative images shown here are primarily images at the plane of the optical equator or the cell or of the nucleus. The primary antibody used in the time course assay was rabbit anti-CDC25B (Proteintech; #10644-1-AP) diluted 1:200, and the secondary antibody used was donkey anti-rabbit (549 nm-conjugated; Jackson ImmunoResearch Laboratories) diluted 1:200. Dilutions were made in 1% donkey serum

blocking buffer. Three control oocytes were processed through identical procedure stated above, but without incubation in the primary antibody. To confirm the detection of CDC25B, a different primary antibody (goat anti-CDC25B, Santa Cruz; sc-6948) and 488 nm-conjugated donkey anti-goat secondary antibody (Jackson Laboratories) were also used in 12 other oocytes (not shown).

***In Situ* Proximity Ligation Assays (PLA) to detect interaction of 14-3-3 isoforms with CDC25B in mouse oocytes versus eggs**

Duolink *in situ* PLA probes, blocking solution, antibody diluents, wash buffers A and B, and detection reagents were obtained from OLink Bioscience. Following fixation and permeabilization, the cells were processed following the manufacturer's instructions for the Duolink *in situ* PLA kit. The cells were transferred to DuoLink *in situ* blocking buffer and then incubated overnight in presence of both the primary antibody for the 14-3-3 isoform (rabbit anti-14-3-3 isoform panel PAN017, AbD Serotec; diluted 1:200 in Duolink *in situ* antibody diluent) and that for CDC25B (goat anti-CDC25B, Santa Cruz, sc-6948; diluted 1:200 in Duolink *in situ* antibody diluent). Following washing in 1X DuoLink Wash Buffer A (diluted from 10X stock with deionised water), the cells were incubated in anti-rabbit DuoLink PLUS PLA probe secondary antibody (diluted 1:5 in DuoLink *in situ* Antibody Diluent) and anti-goat DuoLink MINUS PLA probe secondary antibody (diluted 1:5 in DuoLink *in situ* Antibody Diluent) for two hours in a humidified chamber. Cells were then washed in 1X DuoLink Wash Buffer A, incubated in Ligase-Ligation mixture for 30 minutes at 37°C in a humidified chamber, washed again,

incubated in Polymerase-Amplification mixture for 100 minutes at 37°C in a humidified chamber, then washed in 1X DuoLink Wash Buffer B and 0.01X Duolink wash buffer B (diluted from 10X stock with deionised water). The oocytes and eggs were transferred into a droplet of PBS containing 1% PVA with SlowFade (Invitrogen) under oil for confocal imaging as described for immunofluorescence. Confocal z-stack images of cells were captured at 3µm thickness intervals, at a zoom setting of 2.5, through multiple oocytes and eggs for each isoform tested. The number of interactions of CDC25B with each of the 14-3-3 isoforms was determined by counting the PLA reaction sites in consecutive images taken at 3 µm intervals throughout the oocytes and eggs (using Image J software with visual confirmation). In two such experiments, PLA reaction spots for interaction of CDC25B with each 14-3-3 isoform were imaged in a total of seven to 10 different oocytes and in a total of six to 11 different eggs. A comparison between oocytes and eggs was made for CDC25B interactions with each of the 14-3-3 isoforms. For comparison of the interaction of CDC25B with each 14-3-3 isoform, the average number of PLA spots in oocytes was considered 100%, relative to which the average number of PLA spots in eggs was represented. Six control oocytes and six control eggs were processed simultaneously for *in situ* PLA following identical procedure in absence of the primary antibodies.

To confirm that the PLA method was effective in identifying the close proximity of two different antibodies under the conditions used in these experiments, three oocytes were processed for *in situ* PLA using two different antibodies to CDC25B. In this case the each of the antibodies was targeted to the same protein. The first was an antibody

raised in goat against a peptide mapping at the N-terminus of CDC25B of human origin, which reacts also with mouse CDC25B. This antibody was used in studying 14-3-3 and CDC25B interactions, and the second antibody was made in rabbit against a different epitope of CDC25B of human origin, which is known to react with mouse CDC25B. Three control oocytes were processed simultaneously for *in situ* PLA following identical procedure in absence of the primary antibodies.

The 14-3-3 antibodies used in this report have been used to detect the different 14-3-3 isoforms in mouse ovaries, oocytes and eggs by Western blotting, immunocytochemistry and immunohistochemistry cells within ovarian sections [49]. Martin and his colleagues described the generation of the panel of antibodies and used them to detect the major brain isoforms of 14-3-3. They confirmed, by several methods, the high specificity of each of these antibodies, which is due to the fact that the epitope for each antibody is mainly in the N-acetylated amino terminus of the different peptide immunogens for 14-3-3 isoforms [68-70]. The panel of 14-3-3 isoform-specific antibodies was also used to identify the isoforms of 14-3-3 proteins expressed in human dermal and epidermal layers [83] and in adrenal chromaffin cells [70].

Co-immunoprecipitation studies, membrane stripping and reprobing

Four μ g of goat anti-CDC25B antibody (Santa Cruz) added to Protein G Sepharose (GE Healthcare) was used to bind CDC25B in 1 mg of total protein extracts from ovaries, oocytes and eggs. After incubation with rotation for 1 hour at 4°C, the beads were centrifuged at 4000 rpm for 1 minute, washed twice with 1X TBS containing

0.1% Tween-20, and then once with homogenization buffer containing protease inhibitors and phosphatase inhibitors (homogenization buffer containing 10 mM Tris-HCl [pH 7.2], 1 mM EDTA, 1 mM EGTA, 0.1% (v/v) beta-mercaptoethanol, 1% (v/v) Triton X-100, protease inhibitors [1 mM PMSF, 0.1 mM TPCK] and phosphatase inhibitors [1 mM Na_3VO_4 , 50 mM NaF, 10 mM beta-glycerophosphate, and 5 mM sodium pyrophosphate]) resuspended in homogenization buffer and boiled in sample buffer. The supernatant was used for SDS-PAGE and Western blotting using goat anti-CDC25B primary antibody (Santa Cruz) diluted 1:100 in blocking buffer (5% non-fat milk in TBS, 0.1% Tween-20) and HRP-conjugated donkey anti-goat secondary antibody (Santa Cruz) diluted 1:2000 in blocking buffer. The positive control used normal ovary extract. The negative control used normal rabbit serum IgG (1 $\mu\text{g}/\mu\text{L}$) in place of the CDC25B antibody.

Following Western blot transfer, the membrane containing the proteins co-immunoprecipitated along with CDC25B, was washed in TBS with 0.1% Tween-20, incubated in stripping buffer (Thermo Scientific, #46430), washed again in TBS with 0.1% Tween-20, treated with secondary antibody alone and developed to confirm complete removal of previously bound antibodies. This was followed by incubating the membrane in blocking buffer and re-probing with each of the rabbit anti-14-3-3 isoform-specific primary antibodies (AbD Serotec; PAN017), one at a time, diluted 1:1000 in blocking buffer and HRP-conjugated goat anti-rabbit secondary (Santa Cruz) diluted 1:2000 in blocking buffer. In the end, the membrane was stripped and re-probed with rabbit anti-14-3-3 β (AbD Serotec) primary antibody (since this was the first of all the antibodies used to detect the 14-3-3 isoforms co-immunoprecipitated along with

CDC25B) and HRP-conjugated goat anti-rabbit secondary antibody to confirm that there was minimal loss of proteins by repeated membrane stripping.

SDS-PAGE and Western Blotting

Total protein extracts from 200 oocytes and 200 eggs were prepared in presence of protease inhibitors and phosphatase inhibitors for use in SDS-PAGE and Western blotting, along with extracts from 200 oocytes and 200 eggs treated with lambda protein phosphatase. The lysis buffer comprised 10 mM Tris-HCl [pH 7.2], 1 mM EDTA, 1 mM EGTA, 0.1% (v/v) beta-mercaptoethanol, 1% (v/v) Triton X-100, protease inhibitors [1 mM PMSF, 0.1 mM TPCK] and phosphatase inhibitors [1 mM Na₃VO₄, 50 mM NaF, 10 mM beta-glycerophosphate, and 5 mM sodium pyrophosphate].

For lambda phosphatase treatment, protein extracts from 200 oocytes or 200 eggs were incubated with 2 Units/ μ L of Lambda Protein Phosphatase (New England Biolabs, #P0753S) in 1X NE Buffer (50 mM HEPES, 100 mM NaCl, 2 mM DTT, 0.01% Brij 35, pH 7.5 at 25°C) supplemented with 1 mM MnCl₂ at 30°C for 2 hours. The protein extracts (21 micrograms) were then used for SDS-PAGE and Western blotting by following standard procedures, using rabbit anti-CDC25B primary antibody (Proteintech) diluted 1:200 in blocking buffer, and HRP- conjugated goat anti-rabbit secondary antibody (Genscript) diluted 1:2000 in blocking buffer.

Proteins from the lysates of 200 oocytes and 200 eggs were separated by SDS-PAGE using a 4% stacking, 12% resolving polyacrylamide gel and electrophoretically transferred to Immobilon-P PVDF membrane (Millipore Corp.). The membranes were

incubated in blocking buffer (5% non-fat milk in TBS, 0.1% Tween-20) and then with primary antibodies overnight at 4°C, washed and incubated with secondary antibody and imaged by chemiluminescence with an enhanced chemiluminescence kit according to the manufacturer's instructions (GE Healthcare Life Sciences) using Fujifilm LAS-3000 developer.

The commercial rabbit anti-CDC25B (#10644-1-AP) primary antibody (Proteintech) was utilized for Western blotting to detect CDC25B in mouse oocytes and eggs, raised against the N-terminus of CDC25B of human origin. The antibody was used at a dilution of 1:200 in blocking buffer (5% milk in 1X TBS, 0.1% Tween-20). The secondary antibody used was HRP-conjugated goat anti-rabbit (Genscript; 1 mg/ml stock) used at a dilution of 1:2000 in the blocking buffer.

Detection of phospho-Ser-149-CDC25B by Western blot and immunofluorescence

Protein extracts of 200 oocytes and 200 eggs were used for SDS-PAGE and Western blotting using rabbit anti-pSer149-CDC25B (Signalway; #11553) primary antibody and HRP-conjugated goat anti-rabbit secondary antibody, following standard procedure as stated above. Five oocytes and six eggs were also processed for immunofluorescence staining of pSer149-CDC25B using this antibody following the methods described above. Four control oocytes and four control eggs were processed simultaneously for immunocytochemistry following identical procedure in absence of the primary antibody, to ensure minimal background staining.

***In Situ* PLA to detect phosphorylation of CDC25B at Ser-149 in oocytes versus eggs**

Duolink *In Situ* PLA was performed on eight oocytes and eight eggs, following the manufacturer's protocol and as described above, using rabbit anti-pSer149-CDC25B (Signalway; #11553) and goat anti-CDC25B (Santa Cruz; sc-6948) primary antibodies. Three control oocytes and three control eggs were treated simultaneously following identical protocol in absence of primary antibodies, to confirm that there was minimal non-specific reaction. The *In Situ* PLA spots in each experimental cell studied were counted (using Image J software with visual confirmation) in consecutive 3 μm sections throughout the oocytes and eggs. A comparison between oocytes and eggs was made for the interaction reactions noted for CDC25B and pSer149-CDC25B as a way of examining the phosphorylation status of CDC25B. For comparison, the average number of PLA spots in oocytes was normalized to 100%, relative to which the average number of spots in eggs was expressed as a percentage.

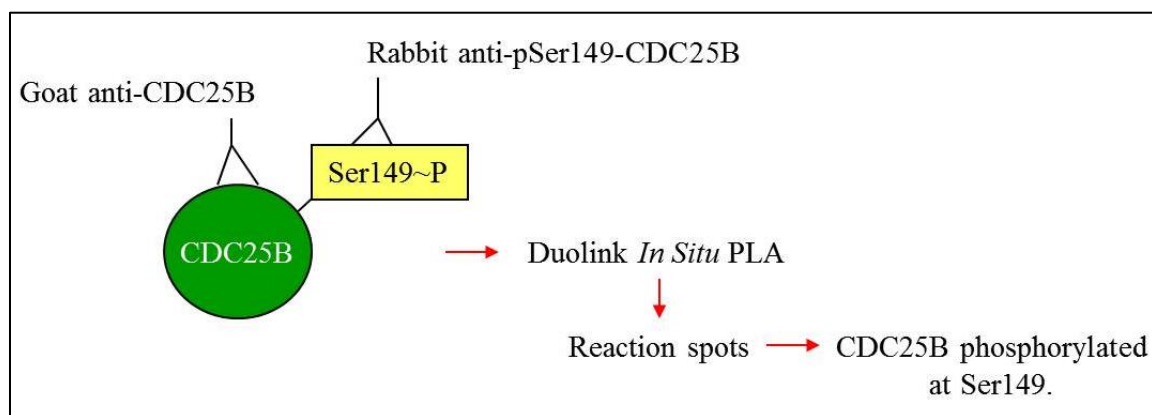


Figure 13. Schematic experimental approach to detect phosphorylation of CDC25B at Ser-149 by *in situ* Proximity Ligation Assay. The assay was performed by standard procedure on fixed mouse oocytes and eggs, using goat anti-CDC25B (Santa Cruz

Biotechnology) and rabbit anti-phospho-Ser149-CDC25B (Signalway) primary antibodies. Detection of bright fluorescent in situ PLA reaction spots would indicate CDC25B phosphorylated at Ser-149.

Microinjection of R18

Ten pL of a 10 mg/mL stock solution of R18 peptide (Enzo Life Sciences) dissolved in sterile deionized water was microinjected by semi-quantitative method into mouse oocytes isolated from adult CF1 mice, to inhibit interactions of all isoforms of 14-3-3 with their binding partners including CDC25B. Following injection the cells were transferred through several washes and incubated in bicarbonate-buffered MEM α containing threshold concentration of dibutyryl cAMP (0.05mg/mL) in presence of 5% CO₂ at 37°C for 13 hours and then examined. Controls included oocytes processed simultaneously through identical procedure, following injection of 10 pL sterile deionized water or no injection. The number of cells with completed GVBD corresponding to injection of R18 was then graphically represented, comparing to water-injected and uninjected control cells.

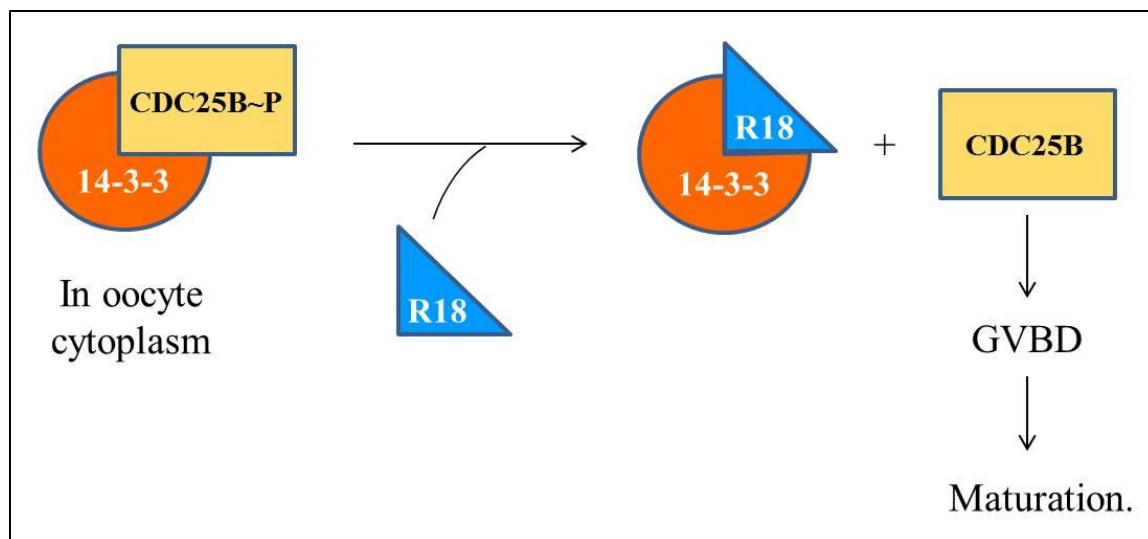


Figure 14. Schematic experimental approach of inhibition of interactions of 14-3-3 proteins with CDC25B by intracytoplasmic microinjection of R18 into mouse oocytes. R18, a known 14-3-3-inhibitory peptide, would competitively block binding interactions of all isoforms of 14-3-3 with CDC25B. Release of CDC25B from 14-3-3 destabilizes its phosphorylation, enabling it to cause germinal vesicle breakdown (GVBD) and maturation of the oocyte.

To determine the threshold or critical concentration of dbcAMP required for maintaining prophase I arrest of oocytes, GV-intact oocytes were isolated from adult CF1 mice by standard procedures as described before. Several dilutions of bicarbonate-buffered MEM α containing stock 0.1 mg/mL dbcAMP were prepared. A number of oocytes were incubated in drop cultures of media with various dilutions of the stock dbcAMP and some in media with no dbcAMP, under mineral oil, at 37°C in presence of

5% carbon dioxide. The cells were examined after 13 hours of incubation and scored under the stereoscope for intact GV or GVBD.

Microinjection of translation-blocking morpholinos against 14-3-3 isoforms

GV-intact oocytes were isolated from adult CF1 mice (as described before) and microinjected with 10 pL of 2 mM stock morpholino oligonucleotide (Gene Tools; final concentration 0.1 mM in each cell) against each of the seven 14-3-3 isoforms and incubated for 24 hours in bicarbonate-buffered minimal essential medium (Sigma) containing full strength stock dbcAMP (0.1 mg/mL) to allow degradation of the existing proteins. A standard picoliter microinjector (Warner Instruments; #PLI-100A) was used for the injections. The cells were then transferred through several washes and incubated in bicarbonate-buffered MEM α containing 0.05 mg/mL dbcAMP in presence of 5% CO₂ at 37°C for 13 hours, stained with Hoechst 33342 (B 226, Sigma) and examined for intact GV or GVBD along with observation of chromosomes. The number of cells with completed GVBD corresponding after injection of morpholino oligonucleotide against each of the 14-3-3 isoforms were compared to the number of cells with GVBD in control uninjected cells and those injected with a standard, nonsense morpholino.

For experiments involving microinjections of R-18 and morpholinos against 14-3-3 isoforms, at each injection condition the cells were classified as having intact GVs or having undergone GVBD, therefore a non-parametric statistical analysis was done using Fisher's exact test (2x2 contingency table). First, uninjected cells and control injected cells (deionized water for R18 experiments and a standard, nonsense morpholino for the morpholino experiments) were compared. Then, each experimental condition was

compared to the control injection condition (water or nonsense morpholino). A P value of less than 0.05 is considered to indicate a significant difference.

Conclusions

All seven mammalian isoforms of 14-3-3 were found interact with CDC25B throughout cytoplasm and nuclei of mouse oocytes, with reduced binding for all isoforms in eggs compared to oocytes. CDC25B appears to be phosphorylated at Ser-149 in mouse oocytes, and the phosphorylation is reduced in eggs. Evidence for a decrease in interaction of 14-3-3 proteins with CDC25B in eggs is in agreement with the hypothesis that 14-3-3 controls mouse oocyte maturation by binding to CDC25B and sequestering it in the cytoplasm, preventing premature germinal vesicle breakdown. Protein 14-3-3 η , among all isoforms of 14-3-3, appears to be essential for maintaining the prophase I arrest in mouse oocytes.

Bibliography

1. Brunet S, Maro K: Cytoskeleton and cell cycle control during meiotic maturation of the mouse oocyte: integrating time and space. *Reproduction* 2005, 130(6):801-811.
2. Masui Y: From oocyte maturation to the in vitro cell cycle: the history of discoveries of Maturation-Promoting Factor (MPF) and Cytostatic Factor (CSF). *Differentiation* 2001, 69(1):1-17.
3. Ma HT, Poon RYC: How protein kinases co-ordinate mitosis in animal cells. *Biochem J* 2011, 435:17-31.
4. Kishimoto T: Cell-cycle control during meiotic maturation. *Current Opinion in Cell Biology* 2003, 15(6):654-663.
5. Mitra J, Schultz R: Regulation of the acquisition of meiotic competence in the mouse: Changes in the subcellular localization of cdc2, cyclin B1, cdc25C and wee1, and in the concentration of these proteins and their transcripts. *J Cell Sci* 1996, 109:2407-2415.
6. Kanatsu-Shinohara M, Schultz R, Kopf G: Acquisition of meiotic competence in mouse oocytes: Absolute amounts of p34(cdc2), cyclin b1, cdc25C, and wee1 in meiotically incompetent and competent oocytes. *Biol Reprod* 2000, 63(6):1610-1616.
7. Han SJ, Chen R, Paronetto MP, Conti M: Wee1B is an oocyte-specific kinase involved in the control of meiotic arrest in the mouse. *Current Biology* 2005, 15(18):1670-1676.
8. Oh JS, Han SJ, Conti M: Wee1B, Myt1, and Cdc25 function in distinct compartments of the mouse oocyte to control meiotic resumption. *J Cell Biol* 2010, 188(2):199-207.
9. Zhang Y, Zhang Z, Xu X, Li X, Yu M, Yu A, Zong Z, Yu B: Protein Kinase A Modulates Cdc25B Activity During Meiotic Resumption of Mouse Oocytes. *Developmental Dynamics* 2008, 237(12):3777-3786.
10. Pirino G, Wescott MP, Donovan PJ: Protein kinase A regulates resumption of meiosis by phosphorylation of Cdc25B in mammalian oocytes. *Cell Cycle* 2009, 8(4):665-670.
11. Mehlmann LM, Jones TLZ, Jaffe LA: Meiotic arrest in the mouse follicle maintained by a G(s) protein in the oocyte. *Science* 2002, 297(5585):1343-1345.

12. Mehlmann LM, Saeki Y, Tanaka S, Brennan TJ, Evsikov AV, Pendola FL, Knowles BB, Eppig JJ, Jaffe LA: The G(s)-linked receptor GPR3 maintains meiotic arrest in mammalian oocytes. *Science* 2004, 306(5703):1947-1950.
13. Freudzon L, Norris RP, Hand AR, Tanaka S, Saeki Y, Jones TLZ, Rasenick MM, Berlot CH, Mehlmann LM, Jaffe LA: Regulation of meiotic prophase arrest in mouse oocytes by GPR3, a constitutive activator of the G(s) G protein. *Journal of Cell Biology* 2005, 171(2):255-265.
14. Mehlmann LM: Oocyte-specific expression of Gpr3 is required for the maintenance of meiotic arrest in mouse oocytes. *Developmental Biology* 2005, 288(2):397-404.
15. Diluigi A, Maier D, Nulsen J, Benadiva C, Schmidt D, Mehlmann LM: Human oocytes express G(s) G-protein and the G-protein-coupled receptor Gpr3, key components in the maintenance of meiotic arrest in mouse oocytes. *Fertility and Sterility* 2006, 86:S394-S394.
16. Kalinowski RR, Berlot CH, Jones TLZ, Ross LF, Jaffe LA, Mehlmann LM: Maintenance of meiotic prophase arrest in vertebrate oocytes by a G(s) protein-mediated pathway. *Developmental Biology* 2004, 267(1):1-13.
17. Vaccari S, Horner K, Mehlmann LM, Conti M: Generation of mouse oocytes defective in cAMP synthesis and degradation: Endogenous cyclic AMP is essential for meiotic arrest. *Dev Biol* 2008, 316(1):124-134.
18. Norris RP, Ratzan WJ, Freudzon M, Mehlmann LM, Krall J, Movsesian MA, Wang H, Ke H, Nikolaev VO, Jaffe LA: Cyclic GMP from the surrounding somatic cells regulates cyclic AMP and meiosis in the mouse oocyte. *Development* 2009, 136(11):1869-1878.
19. Norris RP, Freudzon M, Mehlmann LM, Cowan AE, Simon AM, Paul DL, Lampe PD, Jaffe LA: Luteinizing hormone causes MAP kinase-dependent phosphorylation and closure of connexin 43 gap junctions in mouse ovarian follicles: one of two paths to meiotic resumption. *Development* 2008, 135(19):3229-3238.
20. Norris RP, Freudzon M, Nikolaev VO, Jaffe LA: Epidermal growth factor receptor kinase activity is required for gap junction closure and for part of the decrease in ovarian follicle cGMP in response to LH. *Reproduction* 2010, 140(5):655-662.
21. Nurse P: Universal Control Mechanism Regulating Onset of M-Phase. *Nature* 1990, 344(6266):503-508.
22. Morgan D: Principles of Cdk Regulation. *Nature* 1995, 374(6518):131-134.

23. Malumbres M, Barbacid M: Mammalian cyclin-dependent kinases. *Trends Biochem Sci* 2005, 30(11):630-641.
24. Jones K: Turning it on and off: M-phase promoting factor during meiotic maturation and fertilization. *Mol Hum Reprod* 2004, 10(1):1-5.
25. Mehlmann LM: Stops and starts in mammalian oocytes: recent advances in understanding the regulation of meiotic arrest and oocyte maturation. *Reproduction* 2005, 130(6):791-799.
26. Beall S, Brenner C, Segars J: Oocyte maturation failure: a syndrome of bad eggs. *Fertil Steril* 2010, 94(7):2507-2513.
27. Lincoln AJ, Wickramasinghe D, Stein P, Schultz RM, Palko ME, De Miguel MP, Tessarollo L, Donovan PJ: Cdc25b phosphatase is required for resumption of meiosis during oocyte maturation. *Nature Genetics* 2002, 30(4):446-449.
28. Chen MS, Hurov J, White LS, Woodford-Thomas T, Piwnicka-Worms H: Absence of apparent phenotype in mice lacking Cdc25C protein phosphatase. *Mol Cell Biol* 2001, 21(12):3853-3861.
29. Solc P, Saskova A, Baran V, Kubelka M, Schultz RM, Motlik J: CDC25A phosphatase controls meiosis I progression in mouse oocytes. *Dev Biol* 2008, 317(1):260-269.
30. Solc P, Schultz RM, Motlik J: Prophase I arrest and progression to metaphase I in mouse oocytes: comparison of resumption of meiosis and recovery from G2-arrest in somatic cells. *Mol Hum Reprod* 2010, 16(9):654-664.
31. Duckworth BC, Weaver JS, Ruderman JV: G2 arrest in *Xenopus* oocytes depends on phosphorylation of cdc25 by protein kinase A. *Proceedings of the National Academy of Sciences of the United States of America* 2002, 99(26):16794-16799.
32. Conklin DS, Galaktionov K, Beach D: 14-3-3-Proteins Associate with Cdc25-Phosphatases. *Proc Natl Acad Sci U S A* 1995, 92(17):7892-7896.
33. Uchida S, Kuma A, Ohtsubo M, Shimura M, Hirata M, Nakagama H, Matsunaga T, Ishizaka Y, Yamashita K: Binding of 14-3-3 beta but not 14-3-3 sigma controls the cytoplasmic localization of CDC25B: binding site preferences of 14-3-3 subtypes and the subcellular localization of CDC25B. *J Cell Sci* 2004, 117(14):3011-3020.
34. Giles N, Forrest A, Gabrielli B: 14-3-3 acts as an intramolecular bridge to regulate cdc25B localization and activity. *J Biol Chem* 2003, 278(31):28580-28587.

35. Kumagai A, Yakowec PS, Dunphy WG: 14-3-3 proteins act as negative regulators of the inducer Cdc25 in *Xenopus* egg extracts. *Mol Biol Cell* 1998, 9(2):345-354.
36. Margolis SS, Kornbluth S: When the checkpoints have gone - Insights into Cdc25 functional activation. *Cell Cycle* 2004, 3(4):425-428.
37. Margolis SS, Walsh S, Weiser DC, Yoshida M, Shenolikar S, Kornbluth S: PP1 control of M phase entry exerted through 14-3-3-regulated Cdc25 dephosphorylation. *Embo Journal* 2003, 22(21):5734-5745.
38. Perdiguero E, Nebreda AR: Regulation of Cdc25C activity during the meiotic G(2)/M transition. *Cell Cycle* 2004, 3(6):733-737.
39. Gardino AK, Yaffe MB: 14-3-3 Proteins as Signaling Integration Points for Cell Cycle Control and Apoptosis. *Semin Cell Dev Biol* 2011, 22(7):688-695.
40. Aitken A: 14-3-3 proteins: A historic overview. *Seminars in Cancer Biology* 2006, 16(3):162-172.
41. Morrison DK: The 14-3-3 proteins: integrators of diverse signaling cues that impact cell fate and cancer development. *Trends Cell Biol* 2009, 19(1):16-23.
42. Mackintosh C: Dynamic interactions between 14-3-3 proteins and phosphoproteins regulate diverse cellular processes. *Biochemical Journal* 2004, 381:329-342.
43. Freeman AK, Morrison DK: 14-3-3 Proteins: Diverse functions in cell proliferation and cancer progression. *Semin Cell Dev Biol* 2011, 22(7):681-687.
44. Meek SEM, Lane WS, Piwnica-Worms H: Comprehensive proteomic analysis of interphase and mitotic 14-3-3-binding proteins. *Journal of Biological Chemistry* 2004, 279(31):32046-32054.
45. Dougherty MK, Morrison DK: Unlocking the code of 14-3-3. *J Cell Sci* 2004, 117(10):1875-1884.
46. Rittinger K, Budman J, Xu J, Volinia S, Cantley L, Smerdon S, Gamblin S, Yaffe M: Structural analysis of 14-3-3 phosphopeptide complexes identifies a dual role for the nuclear export signal of 14-3-3 in ligand binding. *Mol Cell* 1999, 4(2):153-166.
47. Yaffe M, Rittinger K, Volinia S, Caron P, Aitken A, Leffers H, Gamblin S, Smerdon S, Cantley L: The structural basis for 14-3-3 : phosphopeptide binding specificity. *Cell* 1997, 91(7):961-971.

48. Aitken A: Functional specificity in 14-3-3 isoform interactions through dimer formation and phosphorylation. Chromosome location of mammalian isoforms and variants. *Plant Mol Biol* 2002, 50(6):993-1010.
49. De S, Marcinkiewicz JL, Vijayaraghavan S, Kline D: Expression of 14-3-3 protein isoforms in mouse oocytes, eggs and ovarian follicular development. *BMC Research Notes* 2012, 5:57.
50. Benzinger A, Muster N, Koch HB, Yates JR, Hermeking H: Targeted proteomic analysis of 14-3-3 sigma, a p53 effector commonly silenced in cancer. *Molecular & Cellular Proteomics* 2005, 4(6):785-795.
51. Fredriksson S, Gullberg M, Jarvius J, Olsson C, Pietras K, Gustafsdottir SM, Ostman A, Landegren U: Protein detection using proximity-dependent DNA ligation assays. *Nat Biotechnol* 2002, 20(5):473-477.
52. Soderberg O, Gullberg M, Jarvius M, Ridderstrale K, Leuchowius K, Jarvius J, Wester K, Hydbring P, Bahram F, Larsson L, Landegren U: Direct observation of individual endogenous protein complexes in situ by proximity ligation. *Nature Methods* 2006, 3(12):995-1000.
53. Weibrecht I, Leuchowius K, Clausson C, Conze T, Jarvius M, Howell WM, Kamali-Moghaddam M, Soderberg O: Proximity ligation assays: a recent addition to the proteomics toolbox. *Expert Review of Proteomics* 2010, 7(3):401-409.
54. De S, Kline D: Evidence for the requirement of 14-3-3eta (YWHAH) in meiotic spindle assembly during mouse oocyte maturation. *Bmc Developmental Biology* 2013, 13:10.
55. Eisen JS, Smith JC: Controlling morpholino experiments: don't stop making antisense. *Development* 2008, 135(10):1735-1743.
56. Summerton J: Morpholino antisense oligomers: the case for an RNase H-independent structural type. *Biochimica Et Biophysica Acta-Genes and Expression* 1999, 1489(1):141-158.
57. Summerton JE: Morpholino, siRNA, and S-DNA compared: Impact of structure and mechanism of action on off-target effects and sequence specificity. *Current Topics in Medicinal Chemistry* 2007, 7(7):651-660.
58. Coonrod SA, Bolling LC, Wright PW, Visconti PE, Herr JC: A morpholino phenocopy of the mouse *mos* mutation. *Genesis* 2001, 30(3):198-200.

59. Homer HA: Mad2 and spindle assembly checkpoint function during meiosis I in mammalian oocytes. *Histol Histopathol* 2006, 21(8):873-886.
60. Madgwick S, Hansen DV, Levasseur M, Jackson PK, Jones KT: Mouse Emi2 is required to enter meiosis II by reestablishing cyclin B1 during interkinesis. *J Cell Biol* 2006, 174(6):791-801.
61. Furuya M, Tanaka M, Teranishi T, Matsumoto K, Hosoi Y, Saeki K, Ishimoto H, Minegishi K, Iritani A, Yoshimura Y: H1foo is indispensable for meiotic maturation of the mouse oocyte. *Journal of Reproduction and Development* 2007, 53(4):895-902.
62. Sun S, Wei L, Li M, Lin S, Xu B, Liang X, Kim N, Schatten H, Lu S, Sun Q: Perturbation of survivin expression affects chromosome alignment and spindle checkpoint in mouse oocyte meiotic maturation. *Cell Cycle* 2009, 8(20):3365-3372.
63. Yuan J, Xu B, Qi S, Tong J, Wei L, Li M, Ouyang Y, Hou Y, Schatten H, Sun Q: MAPK-Activated Protein Kinase 2 Is Required for Mouse Meiotic Spindle Assembly and Kinetochore-Microtubule Attachment. *Plos One* 2010, 5(6):e11247.
64. Ou X, Li S, Xu B, Wang Z, Quan S, Li M, Zhang Q, Ouyang Y, Schatten H, Xing F, Sun Q: p38 alpha MAPK is a MTOC-associated protein regulating spindle assembly, spindle length and accurate chromosome segregation during mouse oocyte meiotic maturation. *Cell Cycle* 2010, 9(20):4130-4143.
65. Zhang C, Wang Z, Quan S, Huang X, Tong J, Ma J, Guo L, Wei Y, Ouyang Y, Hou Y, Xing F, Sun Q: GM130, a cis-Golgi protein, regulates meiotic spindle assembly and asymmetric division in mouse oocyte. *Cell Cycle* 2011, 10(11):1861-1870.
66. Zhu J, Qi S, Wang Y, Wang Z, Ouyang Y, Hou Y, Schatten H, Sun Q: Septin1 Is Required for Spindle Assembly and Chromosome Congression in Mouse Oocytes. *Developmental Dynamics* 2011, 240(10):2281-2289.
67. Homer H, McDougall A, Levasseur M, Yallop K, Murdoch A, Herbert M: Mad2 prevents aneuploidy and premature proteolysis of cyclin B and securin during meiosis I in mouse oocytes. *Genes Dev* 2005, 19(2):202-207.
68. Martin H, Patel Y, Jones D, Howell S, Robinson K, Aitken A: Antibodies Against the Major Brain Isoforms of 14-3-3-Protein - an Antibody Specific for the N-Acetylated Amino-Terminus of a Protein. *FEBS Lett* 1993, 331(3):296-303.
69. Martin H, Rostas J, Patel Y, Aitken A: Subcellular-Localization of 14-3-3-Isoforms in Rat-Brain using Specific Antibodies. *J Neurochem* 1994, 63(6):2259-2265.

70. Roth D, Morgan A, Martin H, Jones D, Martens G, Aitken A, Burgoyne R: Characterization of 14-3-3-Proteins in Adrenal Chromaffin Cells and Demonstration of Isoform-Specific Phospholipid-Binding. *Biochem J* 1994, 301:305-310.
71. Cui C, Zhao H, Zhang Z, Zong Z, Feng C, Zhang Y, Deng X, Xu X, Yu B: CDC25B Acts as a Potential Target of PRKACA in Fertilized Mouse Eggs. *Biol Reprod* 2008, 79(5):991-998.
72. Xiao J, Liu C, Hou J, Cui C, Wu D, Fan H, Sun X, Meng J, Yang F, Wang E, Yu B: Ser(149) Is Another Potential PKA Phosphorylation Target of Cdc25B in G(2)/M Transition of Fertilized Mouse Eggs. *J Biol Chem* 2011, 286(12):10356-10366.
73. Meng J, Cui C, Liu Y, Jin M, Wu D, Liu C, Wang E, Yu B: The Role of 14-3-3 epsilon Interaction with Phosphorylated Cdc25B at Its Ser321 in the Release of the Mouse Oocyte from Prophase I Arrest. *PLoS One* 2013, 8(1):e53633.
74. Pincus G, Enzmann E: The comparative behavior of mammalian eggs in vivo and in vitro. *J Exp Med* 62:665-675.
75. Cho W, Stern S, Biggers J: Inhibitory Effect of Dibutylryl Camp on Mouse Oocyte Maturation In-Vitro. *J Exp Zool* 1974, 187(3):383-386.
76. Masciarelli S, Horner K, Liu C, Park S, Hinckley M, Hockman S, Nedachi T, Jin C, Conti M, Manganiello V: Cyclic nucleotide phosphodiesterase 3A-deficient mice as a model of female infertility. *J Clin Invest* 2004, 114(2):196-205.
77. Schultz RM: Meiotic maturation of mammalian oocytes. In *Elements of mammalian fertilization*. Edited by WASSARMAN P. 1991:77-104.
78. Wang BC, Yang HZ, Liu YC, Jelinek T, Zhang LX, Ruoslahti E, Fu H: Isolation of high-affinity peptide antagonists of 14-3-3 proteins by phage display. *Biochemistry* 1999, 38(38):12499-12504.
79. Masters SC, Fu H: 14-3-3 proteins mediate an essential anti-apoptotic signal. *Journal of Biological Chemistry* 2001, 276(48):45193-45200.
80. Masters SC, Subramanian RR, Truong A, Yang H, Fujii K, Zhang H, Fu H: Survival-promoting functions of 14-3-3 proteins. *Biochemical Society Transactions* 2002, 30:360-365.
81. Peluso JJ, Pappalardo A: Progesterone regulates granulosa cell viability through a protein kinase G-dependent mechanism that may involve 14-3-3 sigma. *Biology of Reproduction* 2004, 71(6):1870-1878.

82. Wu CL, Muslin AJ: Role of 14-3-3 proteins in early *Xenopus* development. *Mechanisms of Development* 2002, 119(1):45-54.
83. Kilani RT, Medina A, Aitken A, Jalili RB, Carr M, Ghahary A: Identification of different isoforms of 14-3-3 protein family in human dermal and epidermal layers. *Mol Cell Biochem* 2008, 314(1-2):161-169.

CHAPTER 4

**Determination of the requirement of
14-3-3 η (YWHAH) in meiotic spindle
assembly during mouse oocyte maturation**

Background

In female mammals, meiosis is initiated prenatally and oocytes remain arrested for long periods in an immature state at prophase of the first meiotic division. Within the ovary, the oocyte is held in arrest by signals from the surrounding granulosa cells. This arrest is released as a result of the preovulatory surge in luteinizing hormone mediated by the granulosa cells and activation of maturation promoting factor (MPF) within the oocyte. MPF triggers the resumption of meiosis leading to a second arrest at metaphase II forming the mature, fertilizable egg [1-4]. In several animals, failure of oocyte maturation has been documented and needs to be considered while investigating human female infertility [5].

Central to this process of oocyte maturation is the correct formation of the metaphase spindles that ensure the accurate alignment and separation of chromosomes at each meiotic division [6-10]. Centrioles are absent in female mouse oocytes and spindle assembly during the two meiotic divisions is therefore independent of centrioles [11]. Examination of spindle assembly in live mouse oocytes revealed that the spindle assembles from many microtubule organizing centers (MTOCs) that are present in the prophase oocyte and that increase in number after nuclear envelope breakdown [12]. It is clear that centrioles are absent in mouse oocytes and the term “acentriolar centrosomes” has been used to describe the MTOCs that ultimately form the spindle; however other researchers refer to mouse oocytes as acentrosomal to denote the formation of a centrosomal equivalent from a clustering of MTOCs [reviewed in 9]. Regardless of the

terminology used, the centrosome or MTOCs (centrosomal equivalent) material associated with the MTOCs contain proteins associated with centrosomes in mitotic cells, including γ -tubulin, pericentrin, Nuclear Mitotic Apparatus (NuMA) protein and other proteins [reviewed in 9]. Aurora kinase A (AURKA) appears to be central in regulating MTOC number during oocyte maturation [13] and microtubule motor proteins aid in the formation and elongation of the bipolar spindle [12].

During oocyte maturation, haploid eggs are produced by two successive divisions that are asymmetric to produce a large egg cell and smaller polar bodies. This process involves both the assembly of the bipolar spindle coordinated by chromatin and spindle positioning at the periphery, which is dependent on the interaction between actin and chromatin. Translocation of the spindle and chromosomes to the periphery also promotes differentiation of the cortex producing a microvilli-free and actin-rich zone that characterizes the site of polar body formation [14, 15].

Proteins of the 14-3-3 (YWHA) family are now known to be central mediators in a variety of cellular signaling pathways involved in development and growth including cell cycle regulation and apoptosis [16-20]. There is strong evidence from studies of the cell cycle in somatic cells that 14-3-3 is involved in signaling systems regulating cell division [21, 22]. There is also recently reported evidence from studies of *Dictyostelium* that 14-3-3 coordinates the interaction between the mitotic spindle and cytokinesis [23, 24] as well as some evidence that 14-3-3 is associated with the mitotic apparatus in mammalian cells [25]. Thus, there is some indication that 14-3-3 proteins have a role in spindle and cytoskeleton function; however, the role of 14-3-3 proteins in mouse meiotic

spindle formation and function is unknown. I previously found that all seven mammalian isoforms of 14-3-3 are expressed in mouse ovaries, oocytes and eggs and showed that 14-3-3 η accumulates and co-localizes with α -tubulin in the region of the meiotic spindle in mouse eggs matured *in vivo* [26] suggesting that 14-3-3 η has a functional role.

In the work presented here, an *in situ* proximity ligation assay (PLA; introduced in chapter 3) was performed to determine if 14-3-3 η interacts directly with α -tubulin in the meiotic spindle. The PLA has been used successfully to not only detect protein-protein interactions at the single molecule level directly in cells, but also to visualize the actual intracellular sites of the interactions in different types of cells and tissues [27-29]. In the PLA method, specific primary antibodies (raised in different species) bind to target proteins. A pair of oligonucleotide-conjugated secondary antibodies (PLA probes) bind to the primary antibodies and when the PLA probes are in close proximity (<40 nm), the DNA strands are joined by enzymatic ligation. A circular DNA molecule is generated and then amplified by rolling circle amplification. The original *in situ* protein-protein interaction is revealed by the amplified DNA detected with a fluorescent probe. The PLA technique is sensitive, specific, and provides a high signal to noise ratio because the signal is amplified and close proximity of the target proteins is required. Thus, the method permits detection of two proteins that interact at the molecular level.

To begin an investigation of the role of 14-3-3 η in spindle formation, experiments were performed to reduce the 14-3-3 η protein in mouse oocytes by interfering with translation of the 14-3-3 η message. A number of techniques that rely on reducing protein expression by RNA interference have been effective in identifying key protein functions

in oocytes, eggs and early embryos of mice and other species. These techniques include RNAi-mediated methods, including RNAi transgenic approaches [30-34]; however, I chose to study the role of 14-3-3 η in meiotic spindle formation during oocyte maturation, by reducing the synthesis of 14-3-3 η protein by intracellular microinjection of a translation-blocking morpholino oligonucleotide against 14-3-3 η .

Morpholino oligomers are small sequences of synthetic nucleotides consisting of about 25 standard nucleic acid bases attached to morpholine rings (rather than ribose rings) with a phosphorodiamidate non-ionic linkage instead of a phosphodiester linkage (giving the oligonucleotide a net neutral charge) [35]. While a number of methods have been developed to block gene expression at the level of the mRNA, including those using the ability of cellular RNAase H-dependent methods and siRNA techniques, the development of morpholinos to knock down proteins by blocking translation has overcome a number of limitations associated with the other techniques. With the appropriate experimental controls [36], morpholinos have a number of advantages including specificity resistance to nucleases. Morpholinos appear to have few off-target interactions and little non-antisense activity because they are specific (binding to at least 13–14 contiguous bases) and the neutral charge gives little interaction with other RNA species or cellular proteins [37, 38]. The feasibility of using morpholino oligomers to block a target gene's function in mouse has been established through a morpholino phenocopy of the easily discernible and well-characterized mouse *mos*^{-/-} phenotype [39]. Morpholino oligonucleotides have been successfully used to inhibit translation of specific genes in embryos of zebrafish [40] and *Xenopus* [41]. Similarly, experiments

utilizing morpholino antisense oligomers have implicated a number of proteins in mouse oocyte meiotic maturation [39, 42-50].

In this study, using several methods, 14-3-3 η is shown to interact with α -tubulin especially in the meiotic spindles in mouse oocytes and eggs. Moreover, morpholino-mediated knockdown of 14-3-3 η provides evidence that 14-3-3 η is required for normal meiotic spindle assembly during mouse oocyte maturation.

Results and Discussion

The protein 14-3-3 η co-localizes with α -tubulin at the metaphase II spindles in mouse eggs

It was previously demonstrated that 14-3-3 η is uniformly distributed in fully grown, immature mouse oocytes with greater distribution in the cytoplasm than in germinal vesicles, and that it accumulates at the metaphase II spindle of eggs matured *in vivo* [26]. In that study, indirect immunofluorescence, utilizing a rabbit antibody directed against the cross-reacting N-terminal sequence of sheep 14-3-3 η , demonstrated that 14-3-3 η , but none of the other 14-3-3 isoforms, is concentrated at the metaphase II spindle and that 14-3-3 η appeared to co-localize with α -tubulin. In the present study, this observation has been confirmed by detecting prominent accumulation of 14-3-3 η at the spindle region in 20 of 23 in eggs matured *in vitro* (Figure 1). These cells, in anticipation of the experiments to follow, were held as oocytes in an arrested state at prophase I for 24 hours

with 0.1 mg/ml dibutyryl cAMP (dbcAMP) in the media. After 24 hours the dbcAMP was removed to allow maturation, and the cells were examined about 13 hours later, a time at which mature eggs are formed. The rabbit antibody targeted against the N-terminal sequence of 14-3-3 η was used for the remaining experiments in this chapter.

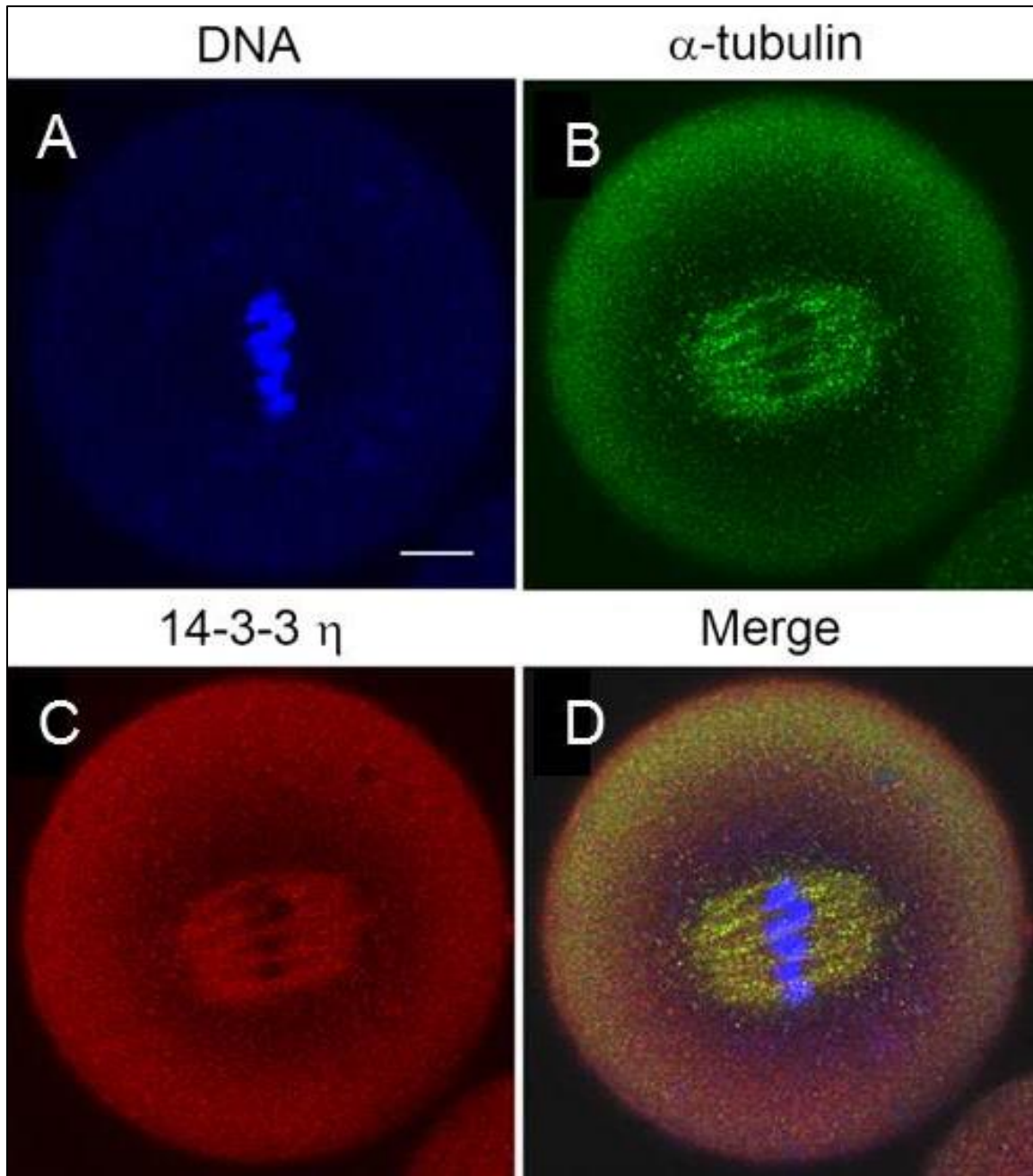


Figure 1. The 14-3-3 η protein accumulates at the metaphase II spindle of the mouse egg matured *in vitro*. Cells were fixed, permeabilized and immunolabeled for confocal double immunofluorescence using a primary antibody against the 14-3-3 η protein (red) and an antibody to α -tubulin (green) and counterstained with Hoechst 33342 (blue) to

visualize DNA. (A-D) A representative *in vitro*-matured egg cell that was held in prophase I arrest for 24 hours, released from the arrest and examined at 13 hours with a rabbit antibody recognizing the N-terminal end of the 14-3-3 η protein (C). The merged image is an overlay of immunofluorescence images from the three channels. Scale bar represents 10 μ m.

There are some differences in the shape and size of the meiotic spindle during *in vivo* maturation compared to *in vitro* maturation, for example, it has been reported that *in vivo*-matured eggs have pointed spindles with compact localization of γ -tubulin at the spindle poles. In contrast, *in vitro*-matured eggs exhibited large more barrel shaped spindles with γ -tubulin distributed over more spindle microtubules [51]. These observations, however, do not represent fundamental differences in spindle function in as much as chromosomes segregate and polar bodies form in both cases. As our studies here rely on *in vitro* maturation, it was first confirmed that 14-3-3 η accumulates in the spindle of *in vitro* matured eggs using the same rabbit antibody used in the previous study of mature, ovulated eggs.

The protein 14-3-3 η accumulates and co-localizes with α -tubulin at both meiosis I and II spindles during *in vitro* mouse oocyte maturation

Given that 14-3-3 η is concentrated at the metaphase II spindle of mouse eggs, the co-localization of 14-3-3 η with α -tubulin was examined during the process of *in vitro* oocyte maturation by additional confocal indirect immunofluorescence studies. Oocytes were collected in HEPES-buffered MEM α containing dbcAMP, and then allowed to

mature *in vitro* by incubation in bicarbonate-buffered MEM α without dbcAMP for 4.5 hours (early spindle formation), 7.5 hours (MI pro-metaphase), 9 hours (MI metaphase) and 12 hours (MI telophase to MII metaphase) before fixation [6]. I examined 15 cells at each stage of maturation and found the following pattern in all cells examined. The 14-3-3 η protein was found to be present throughout the cytoplasm during oocyte maturation at all stages (Figure 2A-J). Accumulation of 14-3-3 η at the meiotic spindle region was detected around prometaphase I at 7.5 hours after release from prophase I arrest (Figure 2C-D). By 9 hours of maturation, a marked co-localization of 14-3-3 η with α -tubulin was observed at the metaphase I spindle with condensed chromosomes aligned at the mid-spindle region (Figure 2E-F). At telophase I, prominent accumulation of 14-3-3 η was found at the broad midbody microtubules during formation of the first polar body (Figure 2G-H). At the end of 12 hours of the maturation, telophase I is followed quickly by the formation of the metaphase II spindle (Figure 2I) and again 14-3-3 η was shown to accumulate in the region of the MII spindle (Figure 2I-J) as well as associated with α -tubulin in the first polar body (Figure 2K-L).

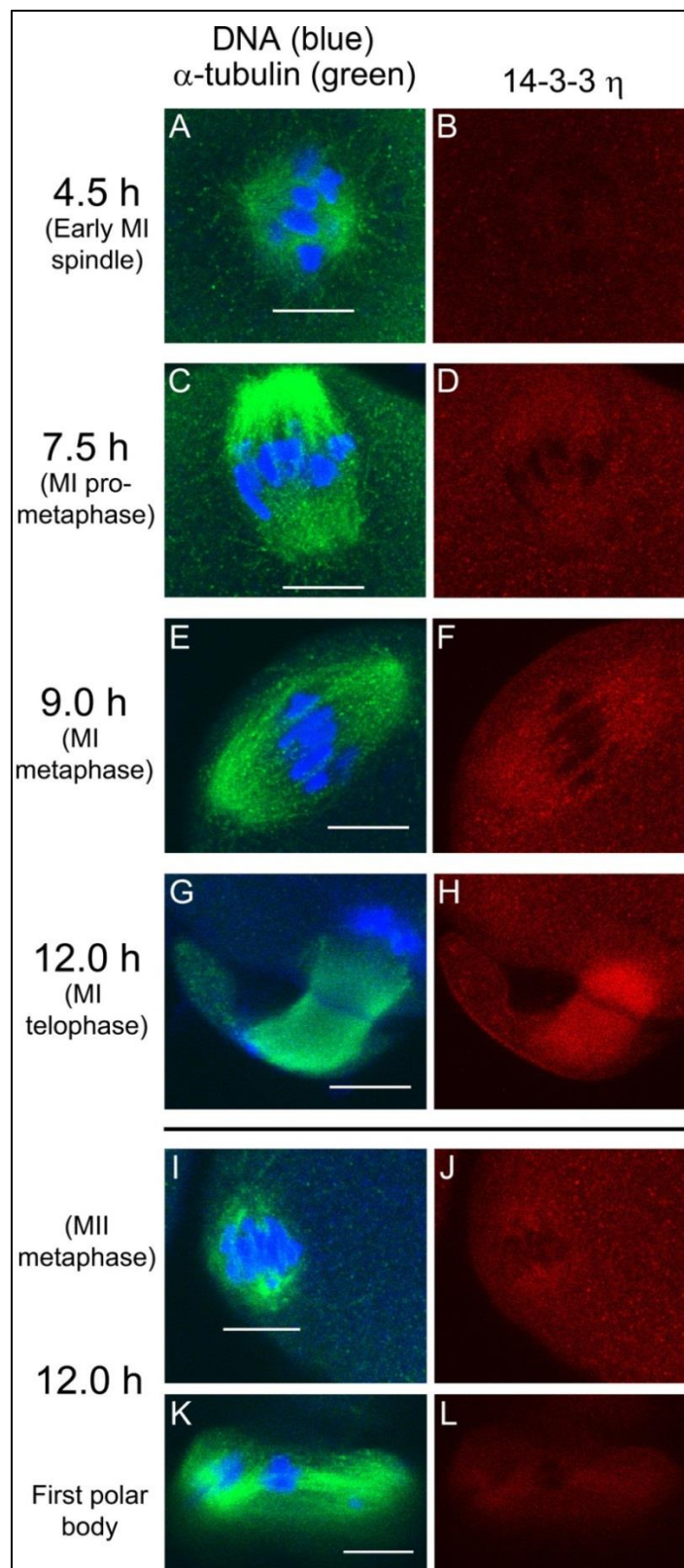


Figure 2. The 14-3-3 η protein accumulates and co-localizes with α -tubulin in MI and MII meiotic spindles during oocyte maturation. Representative cells were fixed, permeabilized and immunolabeled for confocal microscopy during oocyte *in vitro* maturation at the times indicated. The left column shows the merged images of α -tubulin (green) and the counterstain Hoechst 33342 (blue) to visualize the DNA. The right column shows each corresponding image of the 14-3-3 η protein (red). (A-H) Paired confocal images at a single confocal plane of the spindle region of representative cells at the times indicated. (I-L) Representative egg imaged at the plane of metaphase II spindle (I, J) and at a different confocal plane to show the first polar body (K, L) attached to the same egg cell. Scale bars represent 10 μ m.

These experiments suggest a functional role of a specific isoform of 14-3-3 proteins, 14-3-3 η , in the formation of normal meiotic spindles during mouse oocyte maturation. The marked accumulation of 14-3-3 η at the metaphase II meiotic spindles in eggs was observed by immunofluorescence staining of the protein. The gradual accumulation and co-localization of 14-3-3 η at the meiosis I and II spindles observed during mouse oocyte maturation *in vitro*, suggest that the 14-3-3 η protein may be involved with concomitant formation of the spindles by directly or indirectly influencing the assembly of the spindle microtubules.

The 14-3-3 proteins are known to bind to a large number other proteins to regulate many cellular processes [16, 19]; however, the role of 14-3-3 proteins in development of the mammalian meiotic spindle has not yet been examined. Some studies have suggested that isoforms of 14-3-3 are associated with tubulin and may play a role in microtubule assembly and spindle formation in mitosis. Proteomic analysis of interphase and mitotic HeLa cells demonstrated that 14-3-3 proteins interact with α - and β -tubulin in both interphase and mitotic cells [20, 52, 53]. The 14-3-3 γ and 14-3-3 ϵ proteins have been reported to be localized in the centrosomes and mitotic spindle of mouse leukemic FDCP cells and at least one isoform is associated with the centrosomes and spindle of mouse 3T3 cells [25]. The 14-3-3 protein has also been found to interact with ENDOSPERM DEFECTIVE 1 (EDE1), a plant microtubule-associated protein essential for plant cell division and for microtubule organization in endosperm [54]. The potential interaction of 14-3-3 η with α -tubulin was further explored by extending the indirect immunofluorescence co-localization studies to examine the direct interaction of 14-3-3 η with α -tubulin at the molecular level, as described below.

Evidence for direct association of 14-3-3 η with α -tubulin and accumulation of the interactions at the metaphase II spindle

The observation that 14-3-3 η co-localizes with α -tubulin in the double labeling immunofluorescence experiments does not necessarily mean that the 14-3-3 η protein is interacting with α -tubulin directly. Protein-protein interactions at the single molecule level were studied using the *in situ* proximity ligation assay (PLA) and documented the

distribution of intracellular sites of the interactions between 14-3-3 η and α -tubulin in mouse eggs matured *in vitro*. The *in situ* PLA revealed some interactions (noted by distinct bright fluorescent reaction spots) of 14-3-3 η with α -tubulin throughout the cytoplasm of all mouse eggs matured *in vitro*, along with a prominent accumulation of the interaction sites at the meiotic spindles (Figure 3A-E) in 16 out of 18 eggs examined. In addition, an abundance of the interaction sites was noted along the cell cortices next to the spindles of those eggs studied (Figure 3C,E). These observations indicate that 14-3-3 η interacts with α -tubulin in mouse eggs and that such interactions are dramatically more prevalent in the region of the meiotic spindle as would be predicted by the co-localization and enhanced concentration indicated by the immunofluorescence experiments.

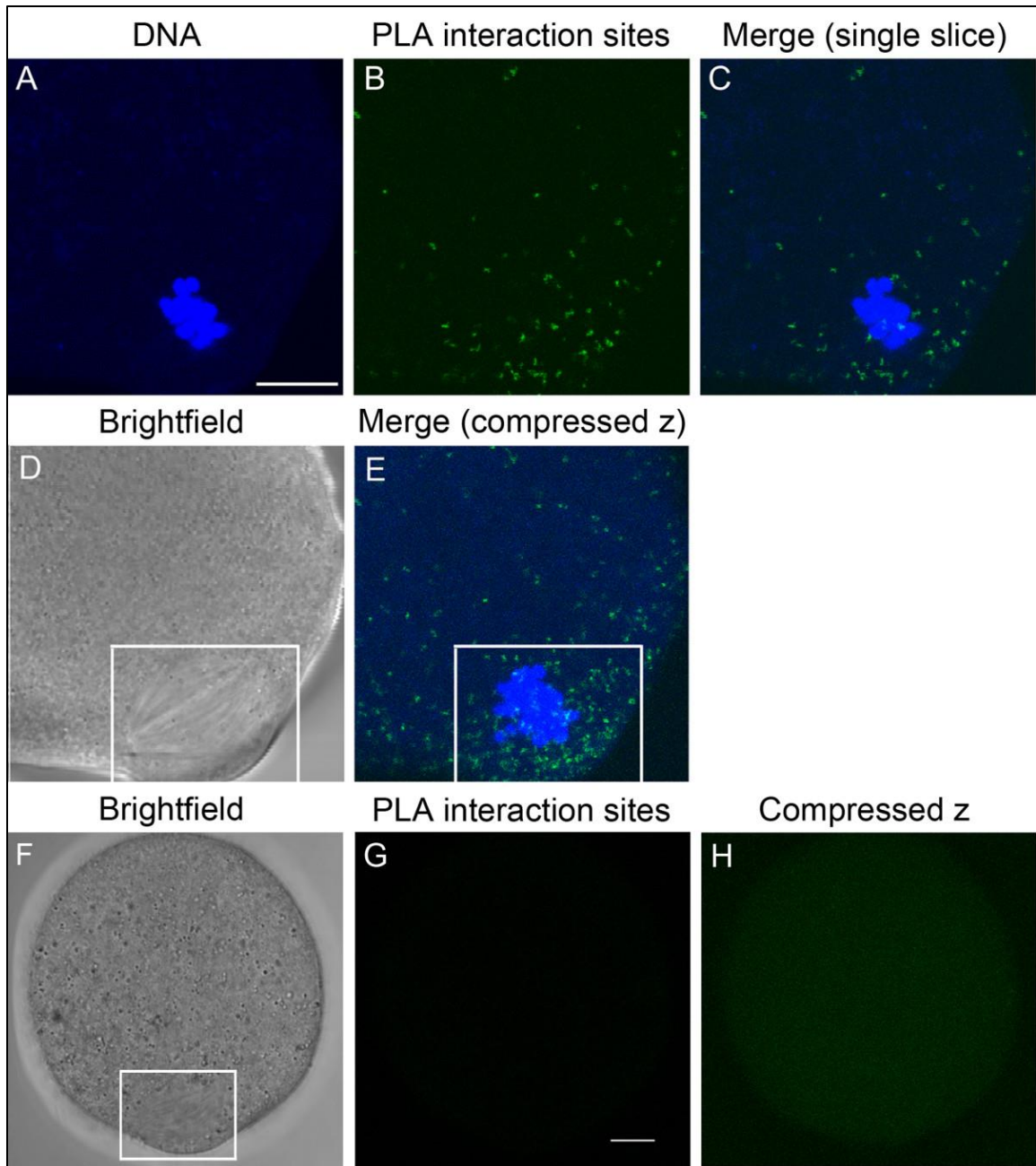


Figure 3. The 14-3-3 η protein interacts directly with α -tubulin. (A-C) A single confocal section through the region of the meiotic spindle of a representative *in vitro*-matured egg. Sites of protein 14-3-3 η and α -tubulin are indicated by the green fluorescent spots (B). The cell was counterstained with Hoechst 33342 (blue) to visualize DNA (A)

and the merged image is shown (C). (D) The non-confocal, brightfield image of this cell and spindle (white box). (E) A compressed stack of seven consecutive confocal scans performed at 2 μm intervals from the bottom of the spindle to its top. A marked accumulation of the *in situ* PLA sites of interaction of 14-3-3 η with α -tubulin was observed at the meiotic spindles in eggs and along the egg cortices about the spindles (highlighted by the white box). (F-H) A representative control egg processed simultaneously for *in situ* PLA by identical procedure, in absence of the primary antibodies for 14-3-3 η and α -tubulin. (F) The non-confocal, brightfield image of the cell and its spindle (white box). (G) A single, confocal fluorescence scan through the spindle region of the egg cell showing no *in situ* PLA fluorescent reaction spot. (H) A compressed stack of all confocal scans from the bottom of the egg cell to its top, showing complete absence of *in situ* PLA fluorescent reaction spots. Background fluorescence was minimal (G, H). Scale bars represent 10 μm .

No *in situ* PLA fluorescent reaction spots were detected throughout control mouse eggs processed simultaneously following the identical procedure but without addition of the primary antibodies (Figure 3F-H). In the absence of primary antibodies there is no ligation and rolling circle amplification of the PLA probes that is necessary for detection. In addition, no background fluorescence from unhybridized probes is detected in confocal sections imaged at the same confocal setting as the experimental cells (Figure 3G) and only a very slight background is apparent in the compressed Z images (Figure 3H).

It is not yet known if 14-3-3 η and tubulin form part of a larger macromolecular complex. Additional studies may indicate if 14-3-3 η also interacts with other proteins at the spindle and elsewhere in the cell. The 14-3-3 protein forms functional homodimers or heterodimers of different isoforms [55, 56]. In some cases, the separate isoforms may have overlapping functions and may be exchangeable in binding to a target protein either as homodimers of isoforms or heterodimers of mixed isoforms. In other cases there may be a specific isoform preference for interaction with some target proteins [57]. There was no evidence for accumulation of any of the other six 14-3-3 isoforms at the meiotic spindle in mature mouse eggs [26], suggesting that the interaction that was observed, is mediated by 14-3-3 η homodimers, and that other isoforms are not specifically associated with the spindle. Moreover, as shown by the following experiments, a reduction in 14-3-3 η protein alone causes defects in spindles, indicating that there is no functional overlap with the other 14-3-3 isoforms.

A 14-3-3 η translation-blocking morpholino causes absence or deformation of the meiosis I spindle during *in vitro* mouse oocyte maturation

The results described above clearly demonstrated that 14-3-3 η is closely associated with α -tubulin during the formation of meiosis I and II and spindles. To begin to understand the functional role of 14-3-3 η in the formation of meiotic spindles during mouse oocyte maturation, a series of experiments were done in which the amount of 14-3-3 η protein in the oocyte was effectively reduced by inhibiting translation of the 14-3-3 η message. While in prophase I arrest, GV-intact oocytes were microinjected with a

translation-blocking morpholino oligonucleotide against 14-3-3 η at a final intracellular concentration of 0.1 mM and held for 24 hours in prophase arrest to permit a reduction of the existing 14-3-3 η protein. The oocytes were then released from the meiotic arrest, allowed to mature *in vitro*, fixed at 13 hours after the release from meiotic arrest and examined by confocal indirect immuno-fluorescence.

Cells underwent germinal vesicle breakdown, but reduction of 14-3-3 η protein caused a substantial decrease in the number of cells that formed a normal bipolar spindle during first meiosis. Only 24% of the cells injected with the morpholino oligonucleotide targeting 14-3-3 η formed an apparently normal bipolar spindle, while in 76% of the cells the spindle was absent or deformed with no polar body formation (Figure 4A).

Immunofluorescence images of two representative morpholino-injected cells that formed no spindle are shown in Figure 5A-H. It can be seen that, in these cases, the DNA is clumped (Figure 5A,E), the spindle microtubules are absent (Figure 5B,F), and there is no accumulation of 14-3-3 η around the chromatin or in the region where the spindle should be forming (Figure 5C,G). The spindle regions of three representative cells with deformed meiotic spindle are shown in Figure 5I-T. In these cases, the DNA is partially clumped (Figure 5I,M,Q) and the spindle is unipolar, disorganized, or apolar and incompletely formed (Figure 5J,N,R). Again, there is little or no accumulation of 14-3-3 η detected in these incompletely formed spindle regions (Figure 5K,O,S). None of these cells injected with the 14-3-3 η morpholino formed polar bodies, indicating that such cells, with absent or deformed meiosis I spindles, do not progress to cytokinesis and first polar body formation.

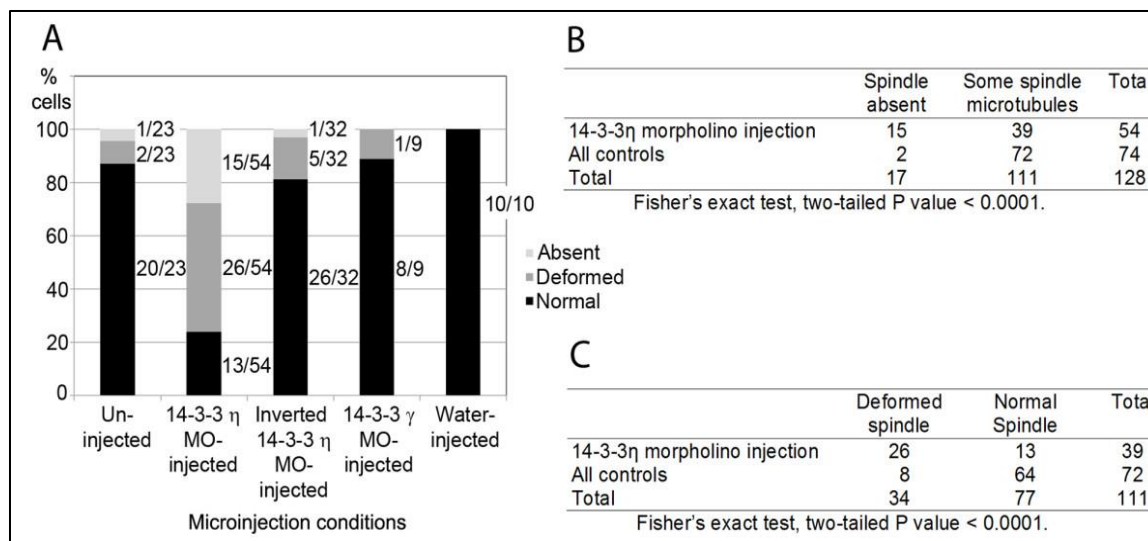


Figure 4. Summary of experimental results on meiotic spindle structure following injection of the 14-3-3 η morpholino and control conditions. As described in Methods, oocytes were held in prophase I meiotic arrest for 24 hours, allowed to mature *in vitro* for 13 hours and then processed for immunofluorescence and confocal microscopy to examine the spindle structure. (A) For each condition, the number of cells with a normal spindle, deformed spindle or no spindle is represented graphically as a percentage of the total number of cells examined. Light grey, spindle absent; dark grey, deformed spindle; black, normal spindle. The number of cells with absent, deformed or normal spindles out of the total number of cells studied for each injection condition is indicated alongside the corresponding percentage bars. Representative images of cells displaying the three categories are presented in Figure 5 and 6. (B) Fisher's Exact test comparing the experimental group (14-3-3 η morpholino injection) and combined controls for the absence of spindles or presence of at least some spindle. (C) Fisher's Exact test

comparing the experimental group (14-3-3 η morpholino injection) and combined controls for deformed or normal spindle. MO, morpholino oligonucleotide.

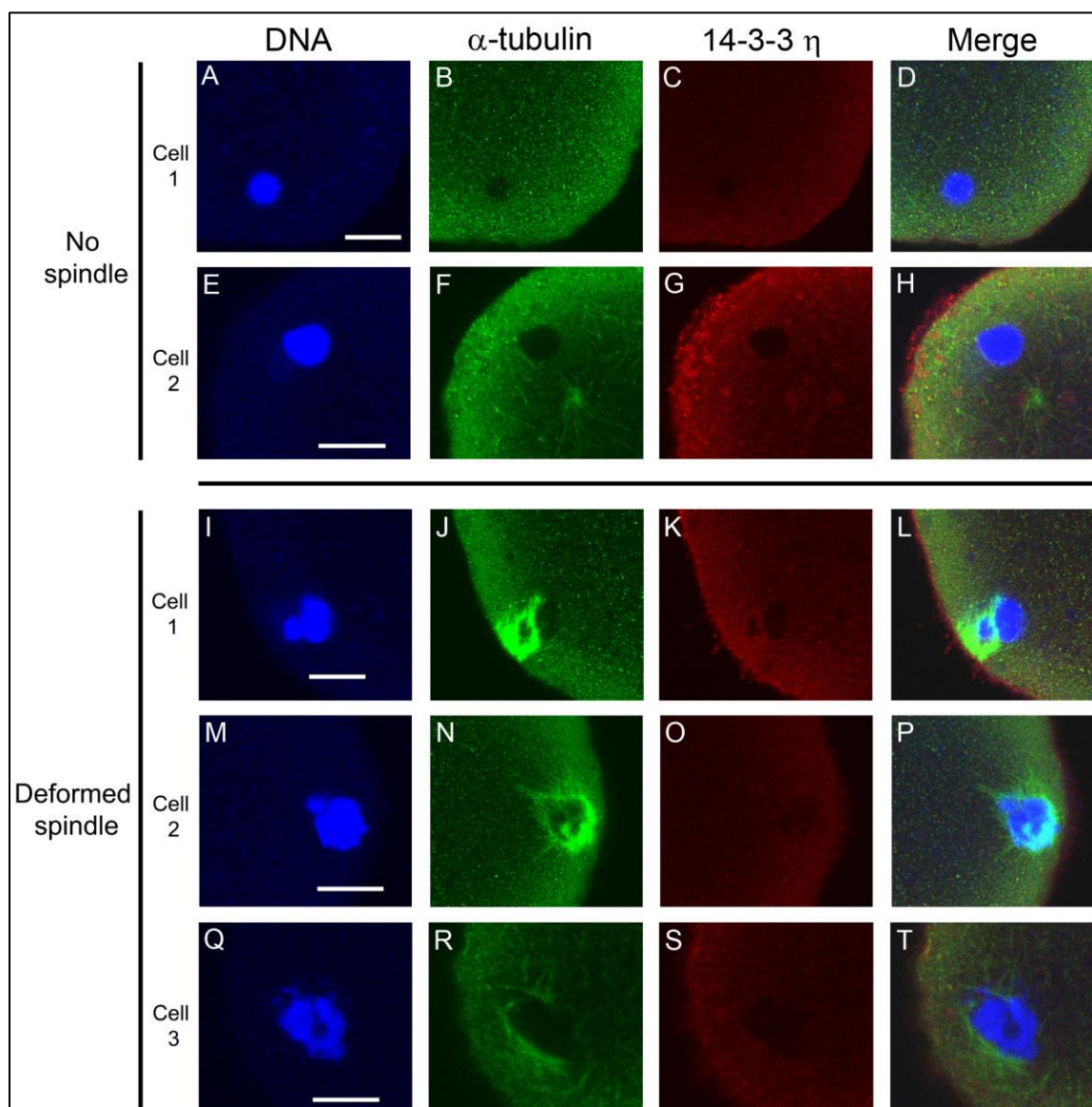


Figure 5. Microinjection of a morpholino against 14-3-3 η causes absence or deformation of meiotic spindles in cells matured *in vitro*. Oocytes were injected with

0.1 mM 14-3-3 η morpholino, held for 24 hours in prophase I arrest, released from the arrest for 13 hours, fixed, permeabilized and immunolabeled for confocal immunofluorescence with an antibody to α -tubulin (green), the antibody to 14-3-3 η protein (red), and counterstained with Hoechst 33342 (blue) to visualize the DNA. The panel on the far right is the merged overlay of immunofluorescence images from all three channels. (A-D and E-H) The upper two rows (cells 1 and 2) are images of two representative cells that have clumped DNA, no spindle and no 14-3-3 η accumulation. (I-L, M-P, and Q-T) The lower 3 rows (cells 1–3) are representative images of cells that have deformed spindles, disorganized DNA and no accumulation of 14-3-3 η at the spindle region. None of these cells injected with the 14-3-3 η morpholino formed a first polar body, indicating that the disrupted spindles shown here are MI spindles. Scale bars represent 10 μ m.

As indicated by indirect immunofluorescence, some 14-3-3 η protein was detected throughout the cytoplasm of eggs matured from oocytes microinjected with the morpholino against 14-3-3 η mRNA (Figure 5C, G, K, O and S). This may be residual protein produced before the morpholino injection as well as some protein translated from 14-3-3 η mRNA not completely blocked by the morpholino. It is not possible to make a quantitative comparison of 14-3-3 η protein content using fluorescence microscopy because, while controls were imaged along with the experimental cells, there will be small inherent differences in primary and secondary antibody concentration and binding and the confocal optics may be slightly different. Clearly however, though some of the

protein might be present in the cytoplasm, the absence of 14-3-3 η accumulation at the meiotic spindle is striking, indicating a reduction in the protein that is targeted to the spindle. Moreover, the reduction in the 14-3-3 η protein around the DNA correlates with the absence or abnormal formation of the spindle.

There will be some variability in the 14-3-3 η protein concentration and knock-down effects. The amount of 14-3-3 η protein may have been sufficient to permit spindle formation in the 24% of 14-3-3 η morpholino-injected cells categorized as having a spindle that appeared normal. Polar bodies were observed to be associated with about half (7/13) of these cells indicating the cells proceeded to metaphase II. Other cells had no adhering polar body. This suggests that these cells formed an apparently normal metaphase I spindle, but did not continue with cytokinesis, which could be the case. However, the polar body sometimes breaks within the zona pellucida surrounding mature eggs and the polar body often becomes dissociated when zona-free eggs are pipetted through processing media drops, so that by the time these cells are examined carefully with confocal microscopy the polar body of a mature metaphase II egg may be absent. Therefore the small percentage of cells with a normal spindle may have proceeded to metaphase II or stopped at metaphase I. In any event, the 14-3-3 η morpholino injection prevents spindle formation or caused abnormal spindles in about 76% of cells injected. The limitation in the knockdown procedure to completely eliminate the 14-3-3 η protein can be overcome by gene knockout experiments and our lab is currently developing a conditional 14-3-3 η knockout mouse.

For comparison with the 54 experimental cells injected with the morpholino against 14-3-3 η , a total of 51 eggs matured *in vitro* from oocytes injected with several control solutions, were examined. Like the experimental cells, these oocytes were injected, held in arrest for 24 hours and then allowed to mature. I also examined 23 uninjected cells treated in the same manner. The results are summarized in Figure 4 and representative images are shown in Figure 6. For the series of injected control cells, 86% had normal metaphase II spindles and, for the uninjected cells, 87% had normal metaphase II spindles (compared to only 24% of cells injected with the 14-3-3 η morpholino, as indicated before).

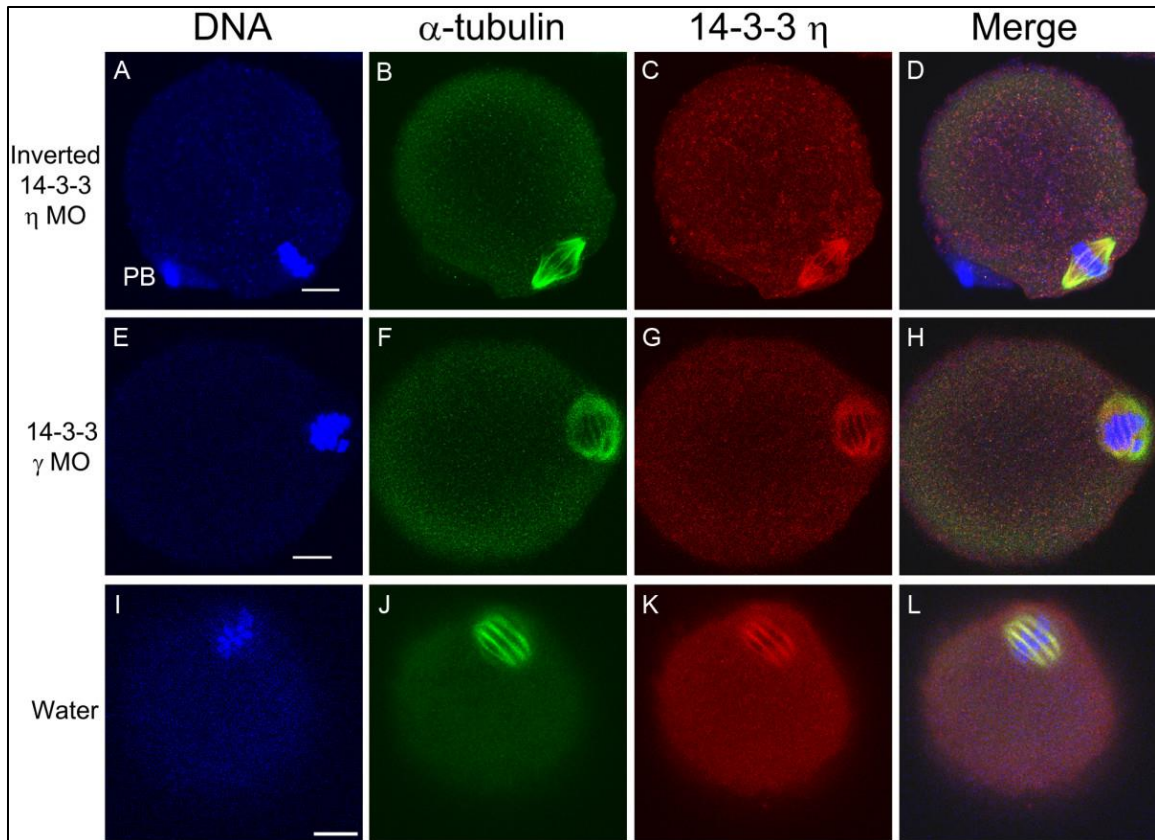


Figure 6. Representative control eggs matured *in vitro* from injected oocytes, showing normal, bipolar meiotic spindles. (A-D) Images of an oocyte injected with 0.01 mM of the inverted 14-3-3 η morpholino. (E-H) Images of an oocyte injected with 0.01 mM the 14-3-3 γ morpholino. (I-L) Images of an oocyte injected with 10 pL of deionized water. In all cases these oocytes, representative of others (see Figure 4) both injected and uninjected, were held for 24 hours in prophase arrest, released from arrest for 13 hours, fixed, permeabilized and immunolabeled for confocal immunofluorescence with an antibody to α -tubulin (green), the antibody to 14-3-3 η protein (red), and counterstained with Hoechst 3342 (blue) to visualize DNA. The panel at the far right is the merged overlay of immunofluorescence images from all three channels. In all cases,

the spindle appears normal and 14-3-3 η accumulates at the spindle. PB, first polar body. MO, morpholino oligonucleotide. Scale bars represent 10 μ m.

One series of control experiments utilized the inverted form of the morpholino oligonucleotide against 14-3-3 η mRNA; a panel of immunofluorescence images of a representative egg cell is shown in Figure 6A-D. The inverted morpholino cannot bind to the 14-3-3 η mRNA and should not knockdown protein synthesis. In such cells, the metaphase II spindle formed, 14-3-3 η accumulated at the metaphase II spindle and the cell completed first polar body formation. Some cells were also injected with a translation-blocking morpholino targeting 14-3-3 γ (YWHAG). This 14-3-3 isoform is known to be present in the mouse oocyte and mature egg, though it does not accumulate in the egg spindle region [26]. Injection of an equivalent amount of this morpholino did not disrupt spindle formation nor seemed to affect oocyte maturation; a representative egg cell is shown in Figure 6E-H. Finally, since the morpholinos were dissolved in deionized water, some mouse oocytes were microinjected with an equivalent amount of deionized water alone. When treated in the same manner as the experimental cells, these cells formed normal metaphase II spindles (Figure 6I-L).

Statistical analysis of 2 \times 2 contingency tables using Fisher's Exact test validated the significant differences between the experimental and control groups (Figure 4B, C). Pairwise comparison across the four control groups revealed no significant difference among them; as a result, all control groups were combined. When the absence of spindles is compared to the presence of at least some spindle microtubules between the

experimental group and combined controls, the two-tailed P value is less than 0.0001. When the presence of deformed spindles is compared to the presence of normal spindles between the experimental group and the combined controls, the two-tailed P value is less than 0.0001. The analysis reveals a very strong statistical difference between the 14-3-3 η morpholino injection group and controls when the number of absent spindles is scored (Figure 4B) and a very strong statistical difference between the 14-3-3 η morpholino injection group and controls when the number of deformed spindles is scored (Figure 4C). Each analysis indicates that injection of 14-3-3 η morpholino blocks or disrupts spindle formation.

The results of microinjection of the translation-blocking morpholino oligonucleotide against 14-3-3 η confirms that this particular isoform of 14-3-3 is essential for meiosis I spindle formation. Except for some cells in which the 14-3-3 η morpholino may have been less effective, the majority of cells form no spindle or a deformed spindle when examined 13 hours after release from meiotic arrest. In those cases, the spindle and chromosomes do not resemble any of the transition stages we would expect to see if the spindle formation were merely delayed. Based on live cell imaging of spindle formation in mouse eggs, the spindle forms from a collection and expansion of microtubule organizing centers that aggregate in a ball just after germinal vesicle breakdown. A bipolar spindle forms with progressive clustering of MTOCs and activity of motor proteins. During this process, individual condensed bivalent chromosomes form during the initial contacts with microtubules. Thus the chromosomes remain individualized throughout the process of spindle formation [12]. The absent or

deformed spindles observed in 14-3-3 η morpholino-injected cells do not represent transitional states. Aggregating MTOCs and individualized condensed chromosomes should be present continuously after germinal vesicle breakdown. Instead, the 14-3-3 η morpholino injections show that spindle formation is prevented and that the DNA forms a clump in the absence of a spindle or if the spindle is abnormally formed. When maturing oocytes are treated with colchicine [14] or nocodazole [12] to depolymerize microtubules, the spindle doesn't form and the chromosomes collapse into a single mass very similar to the appearance of the DNA that were seen in oocytes injected with 14-3-3 η morpholino. Interestingly, one or several chromosome masses move to the cortex in oocytes treated with colchicine during oocyte maturation [14] as were also observed in my experiments (Figure 5A-H). Thus our results are somewhat analogous to the inhibition of spindle formation by microtubule depolymerizing agents, but we do see in some cases a partial, imperfect spindle associated with a chromatin mass of indistinct chromosomes (Figure 5I-T). These results suggest that 14-3-3 η is required at a sufficient concentration to enable the aggregation of MTOCs to form a complete bipolar spindle.

In the absence of spindle formation and first polar body formation, the oocyte would not proceed to metaphase II. We do not yet know if reducing 14-3-3 η protein alters other cytoplasmic maturation events that would affect the ability of the cell to be fertilized or develop a polyspermy block characteristic of a normal metaphase II-arrested egg. Nor do we know if more subtle changes in 14-3-3 activity and spindle structure might be associated with aneuploidy. There may be some changes in the spindles of 14-3-3 η morpholino-injected cells in which we see an apparently normal looking spindle that

could lead to aneuploidy or other developmental defects after fertilization. It is known for mammalian eggs that maintenance of spindle integrity is important in preventing aneuploidy and that aneuploidy in meiosis I is common and increases with maternal age in humans [reviewed in 9, 10].

With the morpholino-mediated knockdown of the 14-3-3 η isoform, other isoforms, though present, do not appear to substitute or compensate for the absence of 14-3-3 η , indicating that 14-3-3 η is the central 14-3-3 protein required for normal spindle formation. The 14-3-3 proteins have been implicated in controlling mitosis in somatic cells; however the exact correspondence of regulatory mechanisms by 14-3-3 in somatic cells or oocytes of other species with the mouse oocyte will need to be explored further in the light of our findings. For example, in somatic (HeLa) cells, 14-3-3 η depletion appears to disrupt chromosome segregation and disrupt mitosis, leading to cell death. The identity of the 14-3-3 η target proteins in these cells was not examined, but depletion of 14-3-3 η also sensitizes the cells to several microtubule inhibitors, suggesting an interaction with tubulin [58].

Our results indicate a specific interaction of 14-3-3 η with α -tubulin in the meiotic spindle and that this interaction is required for normal spindle formation. It may be that 14-3-3 η interacts with other proteins individually or in a complex with tubulin. In addition to playing a role in spindle formation, 14-3-3 η could also function in other maturation events apart from a direct interaction with tubulin and formation of the spindle. The 14-3-3 proteins are known to be important in regulating mitosis through interactions with CDC25 (cell division cycle 25) proteins [22, 59-62] and some evidence

implicates 14-3-3 proteins in serving to maintain meiotic arrest at prophase I in mouse oocytes [63,64]. The experiments reported here indicate that reduction of 14-3-3 η or 14-3-3 γ protein synthesis by morpholino injection, under the conditions used, does not interfere with the resumption of meiosis following the removal of dbcAMP since oocyte nuclear envelope breakdown occurs normally. As described before, I also investigated which of the 14-3-3 proteins is involved in the regulation of cell cycle control proteins, particularly CDC25B (cell division cycle 25B) phosphatase.

The 14-3-3 proteins have also been found to regulate cell mechanics and cytokinesis in somatic cells by integrating key cytoskeletal components. In *Dictyostelium*, for example, where only one 14-3-3 isoform is known to be present, partial knockdown of 14-3-3 protein does not appear to alter spindle formation during mitosis, though it does cause cytokinesis defects resulting in multi-nucleated cells [23]. Similar mechanical events in meiosis would suggest a role for 14-3-3 as well [65]. It has been suggested that the central spindle found in anaphase of animal cells during mitosis is required for formation of the contractile ring. A number of microtubule-bundling and stabilizing factors are required for formation of the central spindle; among them is centralspindlin which is regulated by Aurora B and 14-3-3. In this case, 14-3-3 apparently acts to sequester centralspindlin, maintaining it in an inactivate state until it is phosphorylated by Aurora B, and is released from 14-3-3 to form centralspindlin clusters in the central spindle [66]. The characteristic asymmetric cell division in meiosis apparently requires different organization and regulation though, for example, the Aurora kinases are involved with the regulation of cytokinesis in oocytes [67, 68]. Additional

studies may reveal possible interactions of 14-3-3 with target proteins associated with cytokinesis.

Materials and Methods

Collection of oocytes and eggs

All mice were housed and used at Kent State University under an approved Institutional Animal Care and Use Committee protocol following the National Research Council's publication Guide for the Care and Use of Laboratory Animals. Oocytes and eggs were collected as previously described [69]. Adult (2–3 months old) CF1 mice were injected with 7.5 IU eCG (G4877, Sigma) and, 44–48 hours later, the ovaries were removed and repeatedly punctured with a 26-gauge needle to rupture follicles. Cumulus cell-enclosed oocytes were isolated and the cumulus cells were removed by repeated pipetting through a small-bore pipette. Fully-grown oocytes with intact nuclei (germinal vesicles) were collected and cultured in Minimum Essential Medium α modification (MEM α) (12000–014, Invitrogen) containing 120 U/ml penicillin G (P4687, Sigma), 50 μ g/ml streptomycin sulfate (S1277, Sigma), 0.24 mM sodium pyruvate (P-4562, Sigma), 0.1% polyvinyl alcohol (P-8136, Sigma), and buffered with 20 mM HEPES to pH 7.2. Throughout these experiments with oocytes, except where indicated, 0.1 mg/ml dibutyryl cAMP (D0627, Sigma) was added to prevent spontaneous oocyte maturation. Mature, metaphase-II arrested eggs were obtained from adult CF1 mice 13 hours after injection of

7.5 IU hCG (CG10, Sigma) which was preceded by a priming injection of 7.5 IU eCG injection 48 hours earlier. Cumulus cells were removed with 0.3 mg/ml hyaluronidase (H4272, Sigma). Cumulus-free eggs were collected in MEM α .

Immunofluorescence and confocal microscopy

Cells were briefly treated in acid Tyrode's solution solution (0.14 M NaCl, 3 mM KCl, 1.6 mM CaCl₂·2H₂O, 0.5 mM MgCl₂·6H₂O, 5.5 mM glucose, and 0.1% PVA, pH 2.5) to remove zonae pellucidae. Cells were then fixed in freshly prepared 3.7% paraformaldehyde for 30–60 minutes, washed in 0.1% PVA in PBS, permeabilized with 1% triton X-100 (X100, Sigma), washed in 0.1% PVA in PBS and in blocking buffer containing 5% normal donkey serum (017-000-121, Jackson ImmunoResearch), and incubated at 4°C overnight simultaneously with rabbit anti-14-3-3 η (AHP1046, AbD Serotec) and rat anti- α -tubulin (sc-69970, Santa Cruz Biotechnology), each diluted 1:200 in blocking buffer containing 1% normal donkey serum. This rabbit anti-14-3-3 η was made against a synthetic peptide corresponding to acetylated N-terminal sequence of sheep 14-3-3 η and was used to detect 14-3-3 η in mouse oocytes and eggs by Western blotting and immunofluorescence [26] and has been used effectively in other cells to detect 14-3-3 η [70]. The cells were then washed in 1% blocking buffer and incubated simultaneously in DyLight™ 549 donkey anti-rabbit (711-505-152, Jackson ImmunoResearch) and FITC-conjugated goat anti-rat (711-505-152, Jackson ImmunoResearch), each diluted 1:200 in blocking buffer containing 1% donkey serum for several hours, washed again in blocking buffer, counter stained with the DNA-

staining Hoechst 33342 (B 226, Sigma) at a final concentration of 1.0 $\mu\text{g/ml}$ and transferred into an anti-fade solution (SlowFade®, S-2828, Invitrogen) diluted 1:1 in PBS with 0.1% PVA. All cells were imaged with the Olympus FluoView FV1000 confocal microscopy system (60X oil immersion lens with various confocal zooms; the scale bar on the images indicates the final magnification). Images were captured at multiple confocal planes. The representative images shown here are primarily images at the plane of the meiotic spindles in the cells examined.

For this experiment and all of the following immunocytochemical staining experiments, some cells were processed through the identical procedure, but omitted the primary antibodies (not shown). Minimal or no background fluorescence was noted, indicating no nonspecific binding of the secondary antibodies when cells were imaged at the confocal settings used with the experimental cells.

Time course assay of oocyte maturation *in vitro* to detect accumulation of 14-3-3 η at meiotic spindles

Oocytes were isolated from adult (2–3 months old) CF1 mice as outlined above. All oocytes were then removed from the HEPES-buffered MEM α containing dibutyryl AMP and allowed to mature *in vitro* by incubation in bicarbonate-buffered MEM α (M4526, Sigma) containing 1X Antibiotic-Antimycotic (15240–062, Invitrogen) and 0.001 g/ml polyvinyl alcohol (P-8136, Sigma) and containing no dbcAMP. Groups of cells from the same batch of oocytes were allowed to mature *in vitro* and then were fixed at 4.5 hours, 7.5 hours, 9 hours and 12 hours. The cells were then processed for double

immunofluorescence staining with rabbit anti-14-3-3 η and rat anti- α -tubulin along with staining of chromosomes with Hoechst dye and imaged by confocal microscopy, as described before. At each time point, 15 different cells were examined.

***In situ* proximity ligation assay**

The Duolink *In Situ* PLA process (Olink Bioscience) allows visualization of sites of interaction between two proteins within cells *in situ*. Oocytes were collected and then maintained in bicarbonate-buffered MEM α containing 0.1 mg/ml dbcAMP in a humidified chamber with 5% carbon dioxide at 37°C. After 24 hours the media was replaced with bicarbonate-buffered MEM α without dbcAMP releasing the oocyte from meiotic arrest. At 13 hours the *in vivo* matured eggs were fixed, permeabilized and processed for *in situ* PLA using the manufacturer's protocol and solutions modified to accommodate the standard method of manipulating eggs in media drops under oil. Cells were incubated overnight at 4°C simultaneously in rabbit anti-14-3-3 η (AHP1046, AbD Serotec) and goat polyclonal antibody to human α -tubulin (03-15500, American Research Products), each diluted 1:200 in Duolink antibody diluent. Following four washes in the Duolink wash buffer A, the cells were incubated in Duolink PLUS, anti-rabbit and Duolink MINUS, anti-goat PLA probes (1:5 dilution in Duolink antibody diluent) for two hours in a humidified chamber at 37°C. Cells were then washed twice in Duolink wash buffer A, incubated with ligase-ligation solution for 30 minutes in a humidified chamber at 37°C, washed two more times in Duolink wash buffer A, incubated in polymerase-amplification solution (for rolling circle amplification of the

DNA strands attached to the PLA probes) for 100 minutes in humidified chamber at 37°C, washed twice in 1X Duolink wash buffer B and once for 10 min in 0.01X Duolink wash buffer B containing Hoechst 33342 dye (1 µg/mL). The eggs were then transferred to a solution of SlowFade® (S-2828, Invitrogen) diluted 1:1 in PBS with 0.1% PVA for imaging for confocal imaging. Z-stack images of cells were collected at 2 µm intervals from one side of the spindle to the other. Images are presented here as a single slice or as a compressed Z-stack of the spindle region. The *in situ* PLA sites of interaction between 14-3-3 η and α -tubulin were examined in this manner in 18 different egg cells. Seven control eggs processed were for *in situ* PLA following the identical procedure, but in the absence of the primary antibodies; these cells had no PLA reaction spots indicating that there is no rolling circle amplification in the absence of the primary antibodies.

Microinjections

A translation-blocking morpholino oligonucleotide was designed to block translation of the mouse 14-3-3 η mRNA (5'-CTGCTCTCGATCCCCCATGTCGCTC-3', Gene Tools) and it was solubilized in sterile deionized water to prepare a 2 mM solution. The injection pipettes were beveled [71], backfilled with the injection solution and connected to a semi-quantitative injection system utilizing pneumatic pressure injection (PLI-100A Pico-Injector, Harvard Apparatus). The injection pressure and the injection duration were adjusted to match calibrated injection volumes determined by measuring the diameter and calculating the volume of the sphere of the injection solution injected into inert dimethylpolysiloxane (viscosity 12,500 cSt; DMPS12M, Sigma) which covered

a drop of HEPES-buffered MEM α containing the oocytes. Ten pL (approximately 5% of the oocyte cell volume) of the morpholino solution was injected into the cytoplasm of mouse oocytes to give a final concentration of approximately 0.1 mM within each oocyte.

To show that the injection alone did not have an effect on oocyte maturation and to show that the morpholino was specifically blocking the 14-3-3 η mRNA, a number of control experiments were done. Some mouse oocytes were injected with 10 pL of deionized water (the vehicle for morpholino injections). In addition, two morpholino controls were used that should have no effect on 14-3-3 η mRNA. Of these, the first consisted of 10 pL of a 2 mM stock non-sense morpholino that should not bind to 14-3-3 η (5'-CTCGCTGTACCCCCTAGCTCTCGTC-3', Gene Tools; the invert of the morpholino against 14-3-3 η). Also, some oocytes were injected with 10 pL of a 2 mM solution of a translation-blocking morpholino against mouse 14-3-3 γ mRNA (5'-GGTCCACCATCTTCACAGGGCTGAA-3', Gene Tools). This morpholino should not bind to 14-3-3 η mRNA and serves as an additional control for the morpholino injection. All injections were performed in HEPES-buffered MEM α with 0.1 mg/ml dbcAMP.

The injected oocytes and some additional control uninjected oocytes were held in prophase I meiotic arrest for 24 hours. The oocytes were maintained in a bicarbonate-buffered MEM α containing 0.1 mg/ml dbcAMP in a humidified chamber with 5% carbon dioxide at 37°C. After 24 hours the media was replaced with bicarbonate-buffered MEM α without dbcAMP. The oocytes allowed to mature *in vitro* for 13 hours and then processed for immunofluorescence and confocal microscopy, as described before with staining for 14-3-3 η , α -tubulin and DNA. Images were captured at multiple confocal

planes. The representative images shown are primarily images at the plane of the meiotic spindles or DNA in the cells examined. For each injection condition, the cells were classified into three categories depending on whether the meiotic spindle was absent, deformed or normal in appearance. Nonparametric statistical analysis was done using Fisher's exact test. First, pairwise orthogonal comparisons were made across the four control groups; because they were not different, they were combined for further analysis. The combined control group and the experimental group were compared for the absence of a spindle versus the presence of at least some spindle microtubules, and for presence of deformed spindles versus the presence of normal spindles.

Conclusions

The study reveals the functional importance of a specific isoform of 14-3-3, namely 14-3-3 η , in regulating meiotic spindle formation during mouse oocyte maturation *in vitro*, by morpholino-mediated knock-down of the protein. The results of the study indicate that 14-3-3 η regulates the organization or stabilization of meiosis I spindle assembly and may be required for first polar body formation, thereby allowing normal progression to metaphase II spindle formation as well. *In situ* proximity ligation assays and confocal indirect immunofluorescence experiments demonstrate that 14-3-3 η interacts with α -tubulin in eggs, with an accumulation of the interactions at the meiotic spindle. These results suggest that 14-3-3 η is essential for formation of the normal meiotic spindle apparatus during mouse oocyte maturation *in vitro* by interacting, in part with α -tubulin to regulate the assembly of microtubules.

Bibliography

1. Jones K: Turning it on and off: M-phase promoting factor during meiotic maturation and fertilization. *Mol Hum Reprod* 2004, 10(1):1–5.
2. Mehlmann LM: Stops and starts in mammalian oocytes: recent advances in understanding the regulation of meiotic arrest and oocyte maturation. *Reproduction* 2005, 130(6):791–799.
3. Von Stetina JR, Orr-Weaver TL: Developmental control of oocyte maturation and egg activation in metazoan models. *Cold Spring Harbor Perspect Biol* 2011, 3(10):a005553.
4. Conti M, Hsieh M, Zamah AM, Oh JS: Novel signaling mechanisms in the ovary during oocyte maturation and ovulation. *Mol Cell Endocrinol* 2012, 356(1–2):65–73.
5. Beall S, Brenner C, Segars J: Oocyte maturation failure: a syndrome of bad eggs. *Fertil Steril* 2010, 94(7):2507–2513.
6. Wassarman P, Fujiwara K: Immunofluorescent anti-tubulin staining of spindles during meiotic maturation of mouse oocytes in vitro. *J Cell Sci* 1978, 29(FEB):171–188.
7. Vogt E, Kirsich-Volders M, Parry J, Eichenlaub-Ritter U: Spindle formation, chromosome segregation and the spindle checkpoint in mammalian oocytes and susceptibility to meiotic error. *Mutat Res Genet Toxicol Environ Mutag* 2008, 651(1–2):14–29.

8. Yin S, Sun X, Schatten H, Sun Q: Molecular insights into mechanisms regulating faithful chromosome separation in female meiosis. *Cell Cycle* 2008, 7(19):2997–3005.
9. Schatten H, Sun Q: Centrosome dynamics during mammalian oocyte maturation with a focus on meiotic spindle formation. *Mol Reprod Dev* 2011, 78(10–11):757–768.
10. Jones KT, Lane SIR: Chromosomal, metabolic, environmental, and hormonal origins of aneuploidy in mammalian oocytes. *Exp Cell Res* 2012, 318(12):1394–1399.
11. Szollosi D, Calarco P, Donahue R: Absence of centrioles in first and second meiotic spindles of mouse oocytes. *J Cell Sci* 1972, 11(2):521.
12. Schuh M, Ellenberg J: Self-organization of MTOCs replaces centrosome function during acentrosomal spindle assembly in live mouse oocytes. *Cell* 2007, 130(3):484–498.
13. Solc P, Baran V, Mayer A, Bohmova T, Panenkova-Havlova G, Saskova A, Schultz RM, Motlik J: Aurora kinase A drives MTOC biogenesis but does not trigger resumption of meiosis in mouse oocytes matured in vivo. *Biol Reprod* 2012, 87(4):85–85.
14. Longo F, Chen D: Development of cortical polarity in mouse eggs - involvement of the meiotic apparatus. *Dev Biol* 1985, 107(2):382–394.
15. Brunet S, Maro K: Cytoskeleton and cell cycle control during meiotic maturation of the mouse oocyte: integrating time and space. *Reproduction* 2005, 130(6):801–811.
16. Aitken A: 14-3-3 proteins: A historic overview. *Semin Cancer Biol* 2006, 16(3):162–172.

17. Morrison DK: The 14-3-3 proteins: integrators of diverse signaling cues that impact cell fate and cancer development. *Trends Cell Biol* 2009, 19(1):16–23.
18. Mackintosh C: Dynamic interactions between 14-3-3 proteins and phosphoproteins regulate diverse cellular processes. *Biochem J* 2004, 381:329–342.
19. Freeman AK, Morrison DK: 14-3-3 Proteins: Diverse functions in cell proliferation and cancer progression. *Semin Cell Dev Biol* 2011, 22(7):681–687.
20. Meek SEM, Lane WS, Piwnica-Worms H: Comprehensive proteomic analysis of interphase and mitotic 14-3-3-binding proteins. *J Biol Chem* 2004, 279(31):32046–32054.
21. Hermeking H, Benzinger A: 14-3-3 Proteins in Cell Cycle Regulation. *Semin Cancer Biol* 2006, 16(3):183–192.
22. Gardino AK, Yaffe MB: 14-3-3 Proteins as Signaling Integration Points for Cell Cycle Control and Apoptosis. *Semin Cell Dev Biol* 2011, 22(7):688–695.
23. Zhou Q, Kee Y, Poirier CC, Jelinek C, Osborne J, Divi S, Surcel A, Will ME, Eggert US, Mueller-Taubenberger A, Iglesias PA, Cotter RJ, Robinson DN: 14-3-3 coordinates microtubules, rac, and myosin II to control cell mechanics and cytokinesis. *Curr Biol* 2010, 20(21):1881–1889.
24. Robinson DN: 14-3-3, an integrator of cell mechanics and cytokinesis. *Small GTPases* 2010, 1(3):165–169.
25. Pietromonaco S, Seluja G, Aitken A, Elias L: Association of 14-3-3 proteins with centrosomes. *Blood Cells Mol Dis* 1996, 22(19):225–237.

26. De S, Marcinkiewicz JL, Vijayaraghavan S, Kline D: Expression of 14-3-3 protein isoforms in mouse oocytes, eggs and ovarian follicular development. *BMC Res Notes* 2012, 5:57.
27. Fredriksson S, Gullberg M, Jarvius J, Olsson C, Pietras K, Gustafsdottir SM, Ostman A, Landegren U: Protein detection using proximity-dependent DNA ligation assays. *Nat Biotechnol* 2002, 20(5):473–477.
28. Soderberg O, Gullberg M, Jarvius M, Ridderstrale K, Leuchowius K, Jarvius J, Wester K, Hydbring P, Bahram F, Larsson L, Landegren U: Direct observation of individual endogenous protein complexes in situ by proximity ligation. *Nat Methods* 2006, 3(12):995–1000.
29. Weibrecht I, Leuchowius K, Clausson C, Conze T, Jarvius M, Howell WM, KamaliMoghaddam M, Soderberg O: Proximity ligation assays: a recent addition to the proteomics toolbox. *Expert Rev Proteomics* 2010, 7(3):401–409.
30. Stein P, Svoboda P, Schultz RM: Transgenic RNAi in mouse oocytes: a simple and fast approach to study gene function. *Dev Biol* 2003, 256(1):187–193.
31. Xu Z, Williams CJ, Kopf GS, Schultz RM: Maturation-associated increase in IP3 receptor type 1: Role in conferring increased IP3 sensitivity and Ca²⁺ oscillatory behavior in mouse eggs. *Dev Biol* 2003, 254(2):163–171.
32. Svoboda P: Long dsRNA and silent genes strike back: RNAi in mouse oocytes and early embryos. *Cytogenet Genome Res* 2004, 105(2–4):422–434.

33. Yu JY, Deng MQ, Medvedev S, Yang JX, Hecht NB, Schultz RM: Transgenic RNAi-mediated reduction of MSY2 in mouse oocytes results in reduced fertility. *Dev Biol* 2004, 268(1):195–206.
34. Knott J, Kurokawa M, Fissore R, Schultz R, Williams C: Transgenic RNA interference reveals role for mouse sperm phospholipase C in triggering Ca²⁺ oscillations during fertilization. *Biol Reprod* 2005, 72(4):992–996.
35. Summerton J, Weller D: Morpholino antisense oligomers: Design, preparation, and properties. *Antisense Nucleic Acid Drug Dev* 1997, 7(3):187–195.
36. Eisen JS, Smith JC: Controlling morpholino experiments: don't stop making antisense. *Development* 2008, 135(10):1735–1743.
37. Summerton J: Morpholino antisense oligomers: the case for an RNase H-independent structural type. *Biochim Biophys Acta Gene Struct Expr* 1999, 1489(1):141–158.
38. Summerton JE: Morpholino, siRNA, and S-DNA compared: Impact of structure and mechanism of action on off-target effects and sequence specificity. *Curr Top Med Chem* 2007, 7(7):651–660.
39. Coonrod SA, Bolling LC, Wright PW, Visconti PE, Herr JC: A morpholino phenocopy of the mouse *mos* mutation. *Genesis* 2001, 30(3):198–200.
40. Nasevicius A, Ekker SC: Effective targeted gene 'knockdown' in zebrafish. *Nat Genet* 2000, 26(2):216–220.
41. Heasman J, Kofron M, Wylie C: beta-catenin signaling activity dissected in the early *Xenopus* embryo: A novel antisense approach. *Dev Biol* 2000, 222(1):124–134.

42. Homer HA: Mad2 and spindle assembly checkpoint function during meiosis I in mammalian oocytes. *Histol Histopathol* 2006, 21(8):873–886.
43. Madgwick S, Hansen DV, Levasseur M, Jackson PK, Jones KT: Mouse Emi2 is required to enter meiosis II by reestablishing cyclin B1 during interkinesis. *J Cell Biol* 2006, 174(6):791–801.
44. Furuya M, Tanaka M, Teranishi T, Matsumoto K, Hosoi Y, Saeki K, Ishimoto H, Minegishi K, Iritani A, Yoshimura Y: H1foo is indispensable for meiotic maturation of the mouse oocyte. *J Reprod Dev* 2007, 53(4):895–902.
45. Sun S, Wei L, Li M, Lin S, Xu B, Liang X, Kim N, Schatten H, Lu S, Sun Q: Perturbation of survivin expression affects chromosome alignment and spindle checkpoint in mouse oocyte meiotic maturation. *Cell Cycle* 2009, 8(20):3365–3372.
46. Yuan J, Xu B, Qi S, Tong J, Wei L, Li M, Ouyang Y, Hou Y, Schatten H, Sun Q: MAPK-activated protein kinase 2 is required for mouse meiotic spindle assembly and kinetochore-microtubule attachment. *PLoS One* 2010, 5(6):e11247.
47. Ou X, Li S, Xu B, Wang Z, Quan S, Li M, Zhang Q, Ouyang Y, Schatten H, Xing F, Sun Q: p38 alpha MAPK is a MTOC-associated protein regulating spindle assembly, spindle length and accurate chromosome segregation during mouse oocyte meiotic maturation. *Cell Cycle* 2010, 9(20):4130–4143.
48. Zhang C, Wang Z, Quan S, Huang X, Tong J, Ma J, Guo L, Wei Y, Ouyang Y, Hou Y, Xing F, Sun Q: GM130, a cis-Golgi protein, regulates meiotic spindle assembly and asymmetric division in mouse oocyte. *Cell Cycle* 2011, 10(11):1861–1870.

49. Zhu J, Qi S, Wang Y, Wang Z, Ouyang Y, Hou Y, Schatten H, Sun Q: Septin1 is required for spindle assembly and chromosome congression in mouse oocytes. *Dev Dyn* 2011, 240(10):2281–2289.
50. Homer H, McDougall A, Levasseur M, Yallop K, Murdoch A, Herbert M: Mad2 prevents aneuploidy and premature proteolysis of cyclin B and securin during meiosis I in mouse oocytes. *Genes Dev* 2005, 19(2):202–207.
51. Sanfins A, Lee G, Plancha C, Overstrom E, Albertini D: Distinctions in meiotic spindle structure and assembly during in vitro and in vivo maturation of mouse oocytes. *Biol Reprod* 2003, 69(6):2059–2067.
52. Rubio MP, Peggie M, Wong BHC, Morrice N, MacKintosh C: 14-3-3s regulate fructose-2,6-bisphosphate levels by binding to PKB-phosphorylated cardiac fructose-2,6-bisphosphate kinase/phosphatase. *EMBO J* 2003, 22(14):3514–3523.
53. Rubio MP, Geraghty KM, Wong BHC, Wood NT, Campbell DG, Morrice N, Mackintosh C: 14-3-3-affinity purification of over 200 human phosphoproteins reveals new links to regulation of cellular metabolism, proliferation and trafficking. *Biochem J* 2004, 379:395–408.
54. Pignocchi C, Doonan JH: Interaction of a 14-3-3 protein with the plant microtubule-associated protein EDE1. *Ann Bot* 2011, 107(7):1103–1109.
55. Chaudhri M, Scarabel M, Aitken A: Mammalian and yeast 14-3-3 isoforms form distinct patterns of dimers in vivo. *Biochem Biophys Res Commun* 2003, 300(3):679–685.

56. Jones DH, Ley S, Aitken A: Isoforms of 14-3-3-protein can form homodimers and heterodimers in-vivo and in-vitro - implications for function as adapter proteins. *FEBS Lett* 1995, 368(1):55–58.
57. Aitken A: Post-translational modification of 14-3-3 isoforms and regulation of cellular function. *Semin Cell Dev Biol* 2011, 22(7):673–680.
58. Lee CG, Park GY, Han YK, Lee JH, Chun SH, Park HY, Kim KH, Kim EG, Choi Y-J, Yang K, Lee CW: Roles of 14-3-3 eta in mitotic progression and its potential use as a therapeutic target for cancers. *Oncogene* 2013, 32:1560–1569.
59. Kumagai A, Dunphy W: Binding of 14-3-3 proteins and nuclear export control the intracellular localization of the mitotic inducer Cdc25. *Genes Dev* 1999, 13(9):1067–1072.
60. Conklin DS, Galaktionov K, Beach D: 14-3-3-proteins associate with cdc25-phosphatases. *Proc Natl Acad Sci USA* 1995, 92(17):7892–7896.
61. Uchida S, Kuma A, Ohtsubo M, Shimura M, Hirata M, Nakagama H, Matsunaga T, Ishizaka Y, Yamashita K: Binding of 14-3-3 beta but not 14-3-3 sigma controls the cytoplasmic localization of CDC25B: binding site preferences of 14-3-3 subtypes and the subcellular localization of CDC25B. *J Cell Sci* 2004, 117(14):3011–3020.
62. Giles N, Forrest A, Gabrielli B: 14-3-3 acts as an intramolecular bridge to regulate cdc25B localization and activity RID A-6597-2008. *J Biol Chem* 2003, 278(31):28580–28587.

63. Zhang Y, Zhang Z, Xu X, Li X, Yu M, Yu A, Zong Z, Yu B: Protein Kinase A modulates Cdc25B activity during meiotic resumption of mouse oocytes. *Dev Dyn* 2008, 237(12):3777–3786.
64. Pirino G, Wescott MP, Donovan PJ: Protein kinase A regulates resumption of meiosis by phosphorylation of Cdc25B in mammalian oocytes. *Cell Cycle* 2009, 8(4):665–670.
65. Evans JP, Robinson DN: The spatial and mechanical challenges of female meiosis. *Mol Reprod Dev* 2011, 78(10–11):769–777.
66. Douglas ME, Davies T, Joseph N, Mishima M: Aurora B and 14-3-3 coordinately regulate clustering of centralspindlin during cytokinesis. *Curr Biol* 2010, 20(10):927–933.
67. Ding J, Swain JE, Smith GD: Aurora Kinase-A regulates microtubule organizing center (MTOC) localization, chromosome dynamics, and histone-H3 phosphorylation in mouse oocytes. *Mol Reprod Dev* 2011, 78(2):80–90.
68. Yang K, Li S, Chang C, Tang CC, Lin Y, Lee S, Tang TK: Aurora-C kinase deficiency causes cytokinesis failure in meiosis I and production of large polyploid oocytes in mice. *Mol Biol Cell* 2010, 21(14):2371–2383.
69. Snow AJ, Puri P, Acker-Palmer A, Bouwmeester T, Vijayaraghavan S, Kline D: Phosphorylation-dependent interaction of tyrosine 3-monooxygenase /tryptophan 5-monooxygenase activation protein (YWHA) with PAD16 following oocyte maturation in mice. *Biol Reprod* 2008, 79(2):337–347.

70. Martin H, Rostas J, Patel Y, Aitken A: Subcellular-localization of 14-3-3-isoforms in rat-brain using specific antibodies. *J Neurochem* 1994, 63(6):2259–2265.
71. Kline D: Quantitative microinjection of mouse oocytes and eggs. In *Microinjection: Methods and Applications, Methods in Molecular Biology, Volume 518*. Edited by Carroll DJ. New York: Humana Press, Inc; 2009:135–156.

CHAPTER 5

Summary and Significance

Appendix of Abbreviations

Summary and Significance

The work is the first to reveal that all seven mammalian 14-3-3 protein isoforms are expressed in mouse eggs and ovarian follicular cells including oocytes.

Immunofluorescence confocal microscopy of isolated oocytes and eggs confirmed the presence of all of the isoforms with characteristic differences in some of their intracellular localizations. For example, some 14-3-3 isoforms (β , ϵ , γ , and ζ) are expressed more prominently in peripheral cytoplasm compared to the germinal vesicles in oocytes, but are uniformly dispersed within eggs. On the other hand, 14-3-3 η is diffusely dispersed in the oocyte, but attains a uniform punctate distribution in the egg with marked accumulation in the region of the meiotic spindle apparatus.

Immunohistochemical staining detected all isoforms within ovarian follicles, with some similarities as well as notable differences in relative amounts, localizations and patterns of expression in multiple cell types at various stages of follicular development. The study of the differential expression of 14-3-3 isoforms in female germ cells and ovarian follicles provides a foundation for further investigating 14-3-3 isoform-specific interactions with key proteins involved in ovarian development, meiosis and oocyte maturation.

To examine the interactions of 14-3-3 isoforms with CDC25B in oocytes and eggs, an *in situ* Proximity Ligation Assay was performed, that can detect protein-protein interactions at the single molecule level and allows visualization of the actual intracellular sites of the interactions. Prominent interactions of all seven 14-3-3 isoforms

with CDC25B were observed throughout cytoplasm and nuclei of mouse oocytes, along with reduced interactions for each individual isoform in eggs compared to oocytes. Co-immunoprecipitation studies with extracts of mouse oocytes also demonstrated interaction of CDC25B with six 14-3-3 isoforms. Phosphorylation of CDC25B at Ser-149 is reduced in eggs compared to oocytes. These results suggest that any of the 14-3-3 isoforms may have the potential to hold CDC25B inactive in oocytes to maintain the meiotic arrest. In preliminary experiments to explore if interactions of 14-3-3 with other proteins are important for maintaining meiosis I arrest, oocytes were microinjected with 0.5 μ g/ μ L R18, a synthetic non-isoform specific 14-3-3-blocking peptide. Injected oocytes were incubated overnight in media containing threshold concentration (0.05mg/mL) of dbcAMP (dibutyryl cAMP) which normally holds oocytes arrested through activation of PKA and phosphorylation of CDC25B and CDK1. A significant increase in germinal vesicle breakdown (GVBD) was observed in cells injected with R18, compared to control oocytes. To investigate which specific isoform(s) of 14-3-3 is/are responsible for maintaining the meiotic arrest, the synthesis of each 14-3-3 isoform in mouse oocytes was reduced by intracytoplasmic microinjection of 0.1mM translation-blocking morpholino oligonucleotide against the corresponding isoform mRNA. Injected oocytes were held arrested at prophase I for 24 hours, and then incubated overnight in media containing the threshold concentration of dbcAMP. GVBD was observed in a significant percentage (70%) of oocytes microinjected with morpholino against 14-3-3 η , despite the presence of dbcAMP. Injection of morpholinos targeting other 14-3-3 isoforms caused little or no GVBD. Thus, reduction in 14-3-3 η /CDC25B interaction releases the mouse

oocyte from meiotic arrest. These results suggest that, while all 14-3-3 isoforms interact with CDC25B in mouse oocytes, 14-3-3 η is essential for maintaining the prophase I meiotic arrest.

Immunofluorescence staining and examination of oocytes matured *in vitro* demonstrated that 14-3-3 η accumulates in both meiosis I and II spindles. To explore if 14-3-3 η interacts directly with α -tubulin in meiotic spindles during mouse oocyte maturation, *in situ* proximity ligation assay was performed. This assay revealed a marked interaction between 14-3-3 η and α -tubulin at the metaphase II spindle. To demonstrate a functional role for 14-3-3 η in oocyte maturation, mouse oocytes were microinjected with a translation-blocking morpholino oligonucleotide against 14-3-3 η mRNA to reduce 14-3-3 η protein synthesis during oocyte maturation. Meiotic spindles in those cells were studied by immunofluorescence staining of 14-3-3 η and α -tubulin along with observation of DNA. In 76% of cells injected with the morpholino, meiotic spindles were noted to be deformed or absent and there was reduced or no accumulation of 14-3-3 η in the spindle region. Those cells contained clumped chromosomes, with no polar body formation. Immunofluorescence staining of 14-3-3 η and α -tubulin in control eggs matured *in vitro* from uninjected oocytes and oocytes microinjected with the ineffective, inverted form of a morpholino against 14-3-3 η , a morpholino against 14-3-3 γ , or deionized water showed normal, bipolar spindles. These findings indicate that 14-3-3 η is essential for normal meiotic spindle formation during *in vitro* maturation of mouse oocytes, in part by interacting with α -tubulin, to regulate the assembly of microtubules.

Taken together, these studies elucidate significant roles of 14-3-3 proteins and their isoform-specific interactions with other key proteins such as CDC25B and α -tubulin, in regulating mouse oocyte maturation. The results add to our understanding of the importance of 14-3-3 protein isoforms in mouse oocyte maturation and mammalian reproductive development.

Appendix of Abbreviations

ABC: Avidin-Biotin Complex

Arg: Arginine

cAMP: Cyclic Adenosine Monophosphate

CCNB1: Cyclin B1

CDC25B: Cell Division Cycle 25 homolog B

CDK1: Cyclin-Dependent Kinase 1

cGMP: Cyclic Guanosine Monophosphate

Cy3: Cyanin3

DAB: 3,3' Diaminobenzidine

dbcAMP: Dibutryl Cyclic Adenosine Monophosphate

DEAE: diethylaminoethanol

eCG: Equine Chorionic Gonadotropin

FITC: Fluorescein Isothiocyanate

GV: Germinal Vesicle

GVBD: Germinal Vesicle Breakdown

hCG: Human Chorionic Gonadotropin

HEPES: 4-(2-hydroxyethyl)-1-piperazineethanesulfonic acid

HRP: Horse Radish Peroxidase

MI: Meiosis I

MII: Meiosis II

MEM: Minimal Essential Medium

MO: Morpholino Oligonucleotide

MPF: Mitosis Promoting Factor

Na₃VO₄: Sodium Ortho-Vanadate

NaF: Sodium Fluoride

PADI6: Peptidyl Arginine Deiminase 6

PBS: Phosphate Buffered Saline

PDE3A: Phosphodiesterase 3A

PKA: Protein Kinase A

PLA: Proximity Ligation Assay

PMSF: Phenylmethylsulfonyl Fluoride

PP1: Protein Phosphatase 1

pSer: Phospho-Serine

PVA: Polyvinyl Alcohol

PVDF: Polyvinylidene Fluoride

SDS-PAGE: Sodium Dodecyl Sulfate Polyacrylamide Gel Electrophoresis

Ser: Serine

TBS: Tris Buffered Saline

TPCK: Tosyl Phenylalanyl Chloromethyl Ketone

Tris-HCl: Tris-hydrochloride

YWHA: Tyrosine 3-monooxygenase/tryptophan 5-monooxygenase activation protein.